Title
XMEN disease reveals novel regulatory roles for magnesium in the immune system

Author
Li, Feng-Yen

Publication Date
2012

Peer reviewed|Thesis/dissertation

XMEN disease reveals novel regulatory roles for magnesium in the immune system

by

Feng-Yen Li

DISSERTATION

Submitted in partial satisfaction of the requirements for the degree of

DOCTOR OF PHILOSOPHY

in

Biomedical Sciences

in the

GRADUATE DIVISION

of the

UNIVERSITY OF CALIFORNIA, SAN FRANCISCO

Dedication

I dedicate this thesis to my loving mother, whose perpetual energy and continual support in whatever I choose to do inspired me to persist through anything, to never give up, and to pick myself up high no matter how badly I fall.

Acknowledgments

I am only one part of a very large team of scientists, clinicians, patients and their families, and normal blood donor volunteers who made this thesis possible. Everyone who has been part of this project deserves credit for this story and a big THANK YOU; these include but not limited to:

From the Lenardo Lab (NIAID, NIH):

Mike LENARDO: Thank you for taking huge leap of faith on me 4 years ago and for your dedicated mentorship through all these years. I greatly appreciate you taking your time to correct my broken English and pushing me to achieve more than I ever thought I could have achieved.

Benjamin CHAIGNE-DELALANDE: You are my right hand (and I'm right-handed) and my left brain. This story definitely would have taken another year to unfold if it were not for your unparalleled set of talented hands and your keen intellectual insights. I cannot thank you enough for backing me whenever I needed and helping me complete all those flux assays, confocal microscopy, immunoblots, ELISAs, and the spectacular Mg^{2+} supplementation studies. You are well deserved to inherit this project.

Lixin ZHENG: Thank you for your advice on subcloning and making the additional MagT1 constructs. Your guidance and advice have helped me matured tremendously as a scientist through all these years.

Marshall LUKACS: You are my first, last, and best post-bac student in the Lenardo lab. Thank you for your ultra-high enthusiasm in the project, your continual

persistence with Western blots, helping me process cells on those long nights, and picking up the DNA sequencing and real-time assays.

Chryssa KANELLOPOULOU: Thank you for joining my efforts in this project before I even found the gene. I greatly appreciated your help and advice during those long days of blood draws and with knockdown and overexpression studies. Thank you for performing the initial MagT1 real-time assays.

Andy SNOW: Thank you for working with me and Huie on the library preps for the Next-Gen sequencing and sharing your data on the additional XMEN patients I found.

Wei LU: I couldn't have chosen a better person to share my bench with. Thank you for taking care of my cells and make viruses during the holidays as well as putting up with all my teasing.

Pearl CHEN: Thank you for doing all the Maxipreps and making all the LB media. Your yields on those Maxi's are unbeatable.

Nicole YUNG: Thank you for processing all those sequencing shipments.

Carol TRAGESER: Thank you for processing all my orders in such a timely fashion.

Kimberly SCHAFER-WEAVER: Thank you for sharing your expertise on NK cells and helping me process all those tech transfer paperwork and chasing down those mouse ES clones.

Ping JIANG: Thank you for offering me help whenever I needed, whether it was emergency orders or experiments. I greatly appreciate your friendship and moral support.

Maria HESSIE: Thank you for all your secretarial assistance and moral support.

Nick BECKLOFF: Thank you for searching for a list of X-chromosome genes highly expressed in T cells or hematopoietic cells.

From the Su Lab (NIAID, NIH):

Helen SU: This thesis would have never existed if you had not referred the proband family to me to work on in the first place. Thank you for all your input and assembly of the clinical data.

Jeremiah DAVIS: Thank you for performing the first lyonization assay on my patients and teaching me the technique. Your result made my mutation search 23 times easier.

Helen MATTHEWS: You are the woman who makes all the blood draws happen. Thank you for coordinating all the patient samples and gathering all the patient data.

Thomas DIMAGGIO: Thank you for delivering all those blood draws.

Yu ZHANG: Thank you for helping me upload the data to dbGaP.

Huie JING: Thank you for making the HVS lines and LCLs for some of my patients and teaching me how to do it.

Qian ZHANG: Thank you for processing blood samples and purifying some cells for the lyonization assays. Your advice and suggestions have always been insightful.

Ian LAMBORN: Thank you for sharing your DNA sequencing protocols.

Other members of the Lenardo and Su labs: Pushpa PANDIYAN, Bernice LO, Zhihua LIU, Rebecca BAKER, Carrie LUCAS, Fengyi WAN, Tony BARNITZ, Austin SWAFFORD, Matt BIANCALANA, Sonia MAJRI, Jaewon LEE, Jinwoo LEE, Dara STRAUSS-ALBEE, Chris DOVE, Jordan GARCIA, Rachael GRODICK, and Tim

LENARDO. Thank you for sharing your reagents and suggestions during group meetings and Saturday student meetings.

From the Douek Lab (VRC, NIAID, NIH):

Danny DOUEK: Thank you for letting me use your lab resources to perform state of the art flow cytometry and sequencing. Your brilliant insights into my project were always appreciated.

Netanya SANDLER: Thank you for teaching me how to do more than 4 color flow cytometry, designing and guiding me to perform extensive flow cytometry panels, and just being there whenever I needed help navigating through the Douek lab.

David AMBROZAK: Thank you for helping me sort the cells for the microarray studies.

Maire QUIGLEY: Thank you for designing the flow cytometry panel and doing the tetramer conjugations for my tetramer staining

Jorge ALMEIDA: Thank for your assistance in setting up the Solexa runs.

From the Holland lab (NIAID, NIH):

Steve HOLLAND: Thank you for sharing your clinical expertise on the proband family and the clinical trial.

Gulbu UZEL: Thank you for your clinical assessments on the XMEN patients and pointing out the unusual susceptibility to EBV infections early on.

From the Cohen lab (NIAID, NIH):

Jeff COHEN: Thank you for sharing your patient samples and data.

Kennichi DOWDELL: Thank you for sharing your EBV virus stocks, EBV cell lines, and your expertise in this area.

From the Malech lab (NIAID, NIH):

Narda THEOBALD: Thank you for expanding, purifying, and characterizing the CD34+ hematopoietic stem cells for the lyonization studies

Randy MERLING: Thank you for expanding, purifying, and characterizing the CD34+ hematopoietic stem cells for the lyonization studies, sharing you antibodies, and showing me how to use new ABI Gene Analyzer.

From the NIH:

Jennifer HEIMALL, Alex FREEMAN and Irini SERETI *(NIAID)*: Thank you for letting me screen through all your male ICL patients.

Geraldine O'CONNOR *(NCI-frederick)*: Thank you for assessing the expression of a large panel of NK receptors, sending me cell lines and reagents, and giving me advice and protocols for the NK cell experiments.

Eric LONG and Sumati RAJAGOPALAN *(NCI)*: Thank you sharing your antibodies and cell lines (particularly the P815+ULBP1) as well as your expertise on NK cells.

Bernard LAFONT *(NIAID)*: Thank you for giving me a sample of your NKG2D antibody and sharing your experience on NK cell cultures.

Rimas ORENTAS *(NCI-CCR)*: Thank you for giving me your rhIL7 and sharing your expertise on EBV, NK cells, and CTLs.

Mary CARRINGTON and Richard APPS *(NCI-frederick):* Thank you for sharing your expertise on NK cells.

Members of the Laboratory of Immunology *(NIAID)* and the Immunology Interest Group at the NIH: Thank you all for sharing reagents and equipment or just for your friendly collegiality.

From outside NIH:

Jack BLEESING and Rebecca MARSH *(Cincinnati Children's Hospital)*: Thank you for sending me a panel of chronic EBV patients to screen and providing the clinical data on the affected patients.

Taco KUIJPERS, E.M.M. van LEEUWEN, P.A. BAARS *(Emma Childen's Hospital, Netherlands):* Thank you for sending me a panel of chronic EBV patients to screen and sharing the clinical and flow cytometry data on your patient.

Rafick-Pierre SEKALY, Elias HADDAD, and Rebeka BORDI *(Vaccine and Gene Therapy Institute)*: Thank you for performing gene expression microarrays and TREC analyses on our proband family.

David KILLILEA *(Children's Hospital Oakland Research Institute)*: Thank you for performing the inductively coupled plasma mass spectrometry measurements and helping us interpret the data.

Federica WOLF *(Università Cattolica del Sacro Cuore, Italy):* Thank you for sharing your expertise on magnesium.

Cliff LOWELL and Art WEISS *(UCSF):* Thank you for your highly insightful questions, comments, and suggestions during all those committee meetings. Thank you, Art, for sending us those ZAP-70-AS cell lines.

Kevin SHANNON and Jana TOUTOLMIN *(UCSF):* Thank you for allowing me to stay at the NIH to complete my thesis and supporting me through thick and thin.

All my family and friends: Thank you for your moral support in all these years.

And last but not least, I would like to thank all the **patients, families, and normal volunteers** for donating their own biological specimens to make this study possible.

Abstract

The etiologies of human primary immunodeficiencies (PIDs) often yield novel insights about the immune system. This thesis revealed an unexpected regulatory role for magnesium in the immune system from the characterization of a novel PID now named X-linked immunodeficiency with Mg^{2+} defect, Epstein-Barr Virus (EBV) infection and neoplasia (XMEN) disease. This story stemmed from the characterization of two young brothers of a non-consanguineous family exhibiting recurrent viral infections and decreased thymic output of $CD4^+$ T cells. The mother of these two boys was found to have completely skewed lyonization in her T cells, suggesting that she carried a defective X-linked gene that confers decreased fitness relative to the wildtype allele. Using X-chromosome exon capture next-generation sequencing, a 10 base pair deletion ablating a splicing junction of *Magnesium Transporter 1* (*MAGT1)* was found by identifying genes with missing coverage in the two boys but not in the mother. This mutation led to altered splicing, frameshift, early termination, and absent protein expression. Five additional unrelated patients with deleterious mutations in *MAGT1* were later identified, and they all suffered from chronic EBV infections and a propensity to develop lymphomas. MagT1 is a Mg^{2+}-selective transporter required for zebrafish development that had unknown roles in human biology. We found that MagT1 mediates a transient Mg^{2+} flux required for the function of inducible T cell kinase (ITK) upon T cell antigen receptor (TCR) stimulation, implicating Mg^{2+} as a novel second messenger. Moreover, we also found that MagT1 deficiency leads to decreased basal free Mg^{2+} and downmodulation of NKG2D, a receptor mediating antiviral and antitumor

cytotoxicity, and both of these defects can be restored by Mg^{2+} supplementation. These findings not only explain the disease manifestation of XMEN patients but also provide diagnostic and/or therapeutic insights for this disease and disorders requiring immunomodulation such as autoimmunity and allograft rejections.

Table of Contents

List of abbreviations

ADA: *Adenosine Deaminase*

ADCC: *Antibody Dependent Cellular Cytotoxicity*

AIDS: *Acquired Immunodeficiency Syndrome*

ALPS: *Autoimmune Lymphoproliferative Syndrome*

BAPTA-AM: *1,2- Bis(o-aminophenoxy)ethane-N,N,N',N'-Tetraacetic Acid Acetoxymethyl ester*

BCR: *B Cell Receptor*

BLS: *Bare Lymphocyte Syndrome*

CAEBV: *Chronic Active EBV*

CASK: *Ca2+/calmodulin-activated Ser-Thr kinase*

CDC: *Centers for Disease Control*

cDNA: *complementary DNA*

CFSE: ***Carboxyfluorescein Succinimidyl Ester***

CGD: *Chronic Granulomatous Disease*

CGH: *Comparative Genomic Hybridization*

CMC: *Chronic Mucocutaneous Candidiasis*

CMV: *Cytomegalovirus*

CTL: *Cytotoxic T Lymphocytes*

CVID: *Common Variable Immune Deficiency*

DAG: *Diacylglycerol*

DIDS: *Dock8 Immunodeficiency Syndrome*

DIP: *Deletion Insertion Polymorphisms*

DNA: *Deoxyribonucleic Acid*

EBNA-1: *EBV Nuclear Antigen 1*

EBV: *Epstein-Barr Virus*

ECL: *Enhanced Chemiluminescence*

EDTA: *Ethylenediaminetetraacetic Acid*

Erk1/2: *Extracellular signal regulated kinase 1/2*

FBS: *Fetal Bovine Serum*

FIM: *Fulminant Infectious Mononucleosis*

gDNA: *genomic DNA*

HIV: *Human Immunodeficiency Virus*

HLH: *Hemophagocytic Lymphohistiocytosis*

HPRT: *Hypoxanthine-guanine PhosphoribosylTransferase*

HRP: *Horseradish Peroxidase*

HSC: *Hematopoietic Stem Cell*

HSCT: *Hematopoietic Stem Cell Transplantation*

HSV: *Herpes Simplex Virus*

IAP: *Implantation Associated Protein*

ICL: *Idiopathic CD4 Lymphopenia*

IFNγ: *Interferon γ*

IMDM: *Iscove modified Dulbecco medium*

IP_3: *Inositol Triphosphate*

ITAM: *Immunoreceptor Tyrosine-based Activation Motifs*

ITK: *Inducible T cell Kinase*

KIR: *Killer cell Inhibitory Receptor*

KSHV: *Kaposi's Sarcoma-associated Herpesvirus*

Lck: *Leukocyte-specific protein tyrosine Kinase*

LCL: *Lymphoblastoid Cell Line*

MAGT1: *Magnesium Transporter 1*

MAPK: *Mitogen Activated Protein Kinase*

MHC: *Major Histocompatibility Complex*

NGS: *Next Generation Sequencing*

NK: *Natural Killer*

PBS: ..... *Phosphate Buffered Saline*

PCR: ..... *Polymerase Chain Reaction*

PHA: ..... *Phytohemagglutinin*

PID: ..... *Primary Immunodeficiencies*

PKCθ: ..... *Protein Kinase C θ*

PLCγ1: ..... *Phospholipase Cγ1*

PMA: ..... *Phorbol 12-Myristate 13-Acetate*

PTK: ..... *Protein Tyrosine Kinase*

pTα: ..... *pre-TCRα chain*

RICD: ..... *Restimulation-Induced Cell Death*

Rlk: ..... *Resting lymphocyte kinase*

SAC: ..... *Staphylococcus aureus Cowan*

SAP: ..... *SLAM-Associated Protein*

SCID: ..... *Severe Combined Immunodeficiency*

siRNA: ..... *small interfering RNA*

SLAM: ..... *Signaling Lymphocytic Activation Molecule*

SLC: ..... *Secondary Lymphoid tissue Chemokine*

SLP76: . *SH2 domain-containing leukocyte protein of 76 kDa*

SNP: ..... *Single Nucleotide Polymorphism*

TCR: ..... *T Cell antigen Receptor*

T_{FH}: ..... *T Follicular Helper*

TLR: ..... *Toll-Like Receptor*

TNFα: ..... *Tumor Necrosis Factor-α*

TTD: ..... *Trichothiodystrophy*

ULBP: ..... *UL16 Binding Protein*

VZV: ..... *Varicella Zoster Virus*

WES: ..... *Whole Exome Sequencing*

XIAP: ..... *X-linked Inhibitor of Apoptosis Protein*

XLA: ..... *X-linked agammaglobulinemia*

XLP: ..... *X-linked Lymphoproliferative disease*

XMEN: *X-linked immunodeficiency with Mg2+ defect, EBV infection and Neoplasia*

XP: ..... *Xeroderma Pigmentosum*

ZAP-70: .. *Zeta-chain-Associated Protein kinase of 70 kDa*

List of tables

List of figures

Chapter 1 Human primary immunodeficiencies: shedding light on immunology

"human immunodeficiency disease is still the best source of insight into normal pathways of host defense against infectious diseases in humans."

--Charles Janeway Jr.

1.1 Introduction

The immune system is a network of highly specialized organs, tissues, cells, and soluble proteins interconnected by the lymphatic and circulatory system and evolved to fight "danger", such as infectious microorganisms and cancer, and to tolerate non-threatening antigens from self or the external environment[1,2]. When components of this complex system are compromised as a result of congenital mutations (primary) or acquired environmental exposures (secondary), immunodeficiency disease is manifested by increased susceptibility to infections, autoimmunity, and malignancy[2]. While secondary immunodeficiencies such acquired immunodeficiency syndrome (AIDS) can be sometimes widespread, primary immunodeficiencies (PIDs) are usually rare diseases (~1/10,000 live births) caused by a single genetic lesions transmitted by inheritance. Nevertheless, the prevalence of PIDs as a heterogenous group of diseases can be quite high (~1/2000) and often higher in consanguineous or genetically isolated populations[3,4].

The birth of the study of PIDs is often traced back to Olden Bruton's 1952 description of a X-linked agammaglobulinemia (XLA) patient who exhibited no gammaglobulin peak on serum electrophoresis and responded well to serum globulin replacement therapy. Although descriptions of ataxia-telangiectasia and chronic mucocutaneous candidiasis (CMC) were noted as early as the 1920's, the field expanded in the 1950's with the characterizations of many new PIDs. The first genetic etiology of a PID was established in 1972 with the identification of adenosine deaminase (ADA) deficiency in two boys suffering from severe combined

immunodeficiency (SCID)[5,6]. To date, more than 150 genetic etiologies of PIDs have been identified, and the International Union of Immunological Societies Expert Committee for Primary Immunodeficiency updates the classification of these disorders every two years. Currently, PIDs are classified into the following categories: (1) combined immunodeficiencies, (2) well-defined syndromes with immunodeficiency, (3) predominantly antibody deficiencies, (4) diseases of immune dysregulation, (5) congenital defects of phagocyte number and/or function, (6) defects in innate immunity, (7) autoinflammatory disorders, and (8) complement deficiencies[7]**.** Comprehensive descriptions of all currently known PIDs have been documented in excellent reviews and books in the literature[2,3,8].

Since the 1950's, PIDs have proven to be highly fruitful genetic experiments of nature to investigate. We have gained many novel insights into the development and/or function of the immune system from such studies. For instance, recent identification of chronic mucocutaneous candidiasis disease patients with mutations in Interleukin-17 receptor A and Interleukin-17F revealed the importance of the Th17 helper T cell subset for defense against *Candida albicans* in humans[9]. Research on PIDs can uncover important differences between humans and experimental mammalian models. Identification of ZAP-70 (Zeta-chain-associated protein kinase of 70 kDa) mutations in SCID patients established a critical role for this protein tyrosine kinase not only in the activation of T cells in the periphery but also in the thymic development of $CD8^+$ but not $CD4^+$ T cells, unlike the ZAP-70 deficient mice[10–13]. Moreover, identifying the etiology of these inborn errors of immunity have often led to development of new diagnostic or therapeutic tools for treatment

of such diseases or other more common disorders. For instance, ADA-inhibitors and deoxyadenosine analogs were developed for the treatment of hairy cell leukemia after the discovery of SCID patients with adenosine deaminase (ADA) deficiency[5].

This thesis will demonstrate once again that we can learn new aspects of immunology from characterizing a novel PID. From studying a family of two boys affected by idiopathic CD4 lymphopenia (ICL), we uncovered a new PID with increased susceptibility to chronic EBV infection and associated lymphomas due to the loss of MagT1 required for optimal T cell activation and cytotoxicity of natural killer (NK) cells and cytotoxic T lymphocytes (CTLs). Given these findings, I will now introduce the study of ICL as a PID as well as other PIDs with an increased susceptibility to EBV infections and cancer.

1.2 Idiopathic CD4 Lymphopenia: a heterozygenous syndrome with unknown genetic causes

$CD4^+$ T lymphocytes can have many functions in the immune system ranging from suppression to killing. The largest subset of these cells serves as helper cells to empower other parts of the immune system, such as cytotoxic $CD8^+$ T cells and B cells, to fight infections. Mice deficient in $CD4^+$ T cells have significantly decreased antibody responses and impaired cytotoxic T cell activity[14]. The significance of $CD4^+$ T cells is greatly underscored by the emergence of human immunodeficiency virus (HIV), which has taken millions of lives by specifically depleting this subset and thereby increasing the susceptibility to many unusual opportunistic infections.

While most cases of CD4 lymphopenia, or abnormally low $CD4^+$ T cell counts, in humans have been found to be caused by HIV infection, a number of cases

without evidence of HIV infection have been reported since 1989[15–17]. Subsequently, the U.S. Centers for Disease Control (CDC) and Prevention defined a syndrome called ICL by a stable absolute circulating $CD4^+$ T cell count <300 cells/mm^3 or <20% of total T cells without HIV infection or any known causes of lymphopenia[18,19]. Unlike CD4 lymphopenia induced by HIV or other external causes, the $CD4^+$ T cell loss in ICL is not gradual or transient. Moreover, the immunoglobulin levels are usually normal in contrast to the elevated or decreased levels seen in HIV or common variable immune deficiency (CVID), respectively [20]. Although some cases of ICL (6%) can be asymptomatic, most of the cases have led to AIDS-defining (40%) or non-AIDS-defining illnesses (53%) and severe morbidity and mortality[20–22]. While there are antiretroviral drugs available to treat HIV, there is currently no standard treatment for ICL as the underlying cause(s) is still unknown.

The prevalence of ICL is low with 47 cases identified among 230,179 cases reviewed by the original CDC ICL task force[20]. Though some cases of ICL are not diagnosed until late adulthood, pediatric cases occur and have been diagnosed at birth. Given that ICL is a rare immunodeficiency with all secondary causes such as infection, malignancy, and drug reaction excluded[20,23], a leading hypothesis is that there is a primary or genetic cause. Importantly, several familial cases of ICL (including one consanguineous case) have been reported[24–26].

Even though no genetic mutation has yet been specifically attributed to ICL, CD4 lymphopenia is observed in several other known genetic diseases. Nevertheless, they all have features that differ from ICL. A decreased $CD4^+$ T cell count is found in Bare Lymphocyte Syndrome (BLS) exhibiting major

histocompatibility complex (MHC) class II deficiency due to mutations in genes regulating MHC class II expression: RFXANK, RFX5, RFXAP, and CIITA[27]. The loss in $CD4^+$ T cells in this syndrome is caused by defective thymic positive selection of $CD4^+$ T cells, which requires TCR:MHC class II interactions. CD4 lymphopenia is also observed in about 25% of cases of CVID, a congenital disorder characterized by hypogammaglobulinemia with recurrent bacterial infections. About 10-15% of cases of CVID have been associated with mutations in ICOS, CD19, BAFF-R and TACI, but CVID is believed to be a heterogeneous disease that needs further classification[28,29]. CD4 lymphopenia is also associated with a small number of cases of xeroderma pigmentosum (XP) and trichothiodystrophy (TTD), two skin diseases with unusual UV-light sensitivity due to defects in nucleotide excision repair as a result of mutations in the XPB or XPD gene[30,31]. While these diseases should be considered in the differential diagnosis for ICL patients, they can be excluded by distinctive features. For instance, XP and TTD patients have dermatologic manifestations, and BLS and CVID patients, unlike ICL patients, have decreased immunoglobulin levels.

Despite no T cell intrinsic genetic etiology for ICL has yet been identified, the mechanism of pathogenesis of some ICL cases may involve a deficiency in TCR signaling, which is not only critical for activating peripheral mature T cells but also crucial for T cell development in the thymus. T cell development is a well-orchestrated process involving distinct stages marked by T cell specification, T cell commitment, $\alpha\beta/\gamma\delta$ lineage commitment, and positive and negative selection. Upon successful rearrangement of the TCRβ locus, signaling through the pre-TCR formed by pairing of this β chain with the surrogate α chain (pTα) induces allelic exclusion

of the β locus, rapid cell proliferation, and expression of the co-receptors CD4 and CD8. This is followed by repeated rearrangements of the TCRα locus to produce the αβ TCR until positive or negative selection ensues. Intact signaling through pre-TCR and TCR requires the Src-family protein tyrosine kinase (PTK) Lck (leukocyte-specific protein tyrosine kinase) or Fyn to phosphorylate immunoreceptor tyrosine-based activation motifs (ITAMs) on the CD3ε/γ/δ/ζ chain and activate the subsequently recruited ZAP-70 to promote downstream signaling. Constitutive signaling through Lck at the pre-TCR after β chain gene rearrangement ensures allelic exclusion of the β locus and proper progression to the double positive ($CD4^+CD8^+$) stage where Lck associates with CD4 and CD8 coreceptors[32–34]. During subsequent positive selection, Lck directs commitment to the CD4 lineage by a stronger or more sustained signal when CD4 is engaged by MHC class II than by MHC class I[35]. Hence, Lck deficiency in mice leads to decreased double-positive thymocytes and greatly reduced mature lymphocytes particularly of the CD4 lineage[36]. Restoration of Lck in these mice enhances positive selection for $CD4^+$ T cells more than CD8+ T cells[37]. Lck deficiency and/or decreased TCR signaling has been found in several patients with CD4 lymphopenia, although no mutation in Lck has been found[38–40]. Nevertheless, mutations in TCR signaling could be a possible mechanism in ICL as mutations in many components of the TCR signaling pathway have led to PIDs with defective T cell development[41]. Alternatively, increased expression of apoptotic proteins such as the Fas receptor has also been proposed to increase death of $CD4^+$ T cells in some ICL cases[42,43].

1.3 Epstein-Barr Virus: a common virus with rare malignant outcomes

Not only did the patients I characterized in this thesis exhibit ICL, they also had uncontrolled EBV infections. EBV is named after Michael Epstein and Yvonne Barr who discovered the virus in a sample from a Burkitt's lymphoma patient from Uganda[44,45]. EBV is a gammaherpesvirus present in more than 90% of adults worldwide. While infection in childhood is often asymptomatic, adult infection leads to infectious mononucleosis 30-50% of the time, manifested by fever, fatigue, sore throat, inflamed tonsils, and enlarged lymph nodes. Infectious mononucleosis is rarely fatal and usually resolves in 1-2 months. EBV will remain latent in all infected hosts and reactivate intermittently without symptoms or cytopathic effects. However, chronic active EBV (CAEBV) infection persists in some people and is characterized by: (1) mononucleosis-like symptoms or abnormal EBV antibody titers lasting more than 6 months, (2) major organ involvement such as interstitial pneumonia, bone marrow hypoplasia, uveitis, lymphadenitis, persistent hepatitis, and/or splenomegaly; and (3) elevated EBV particles in affected tissues. There are currently no vaccines or antiviral drugs to treat EBV[44,45].

The natural life cycle of EBV mainly takes advantage of the proliferative cycle of B cells to persist in its host (Figure 1-1). EBV is transmitted between hosts through the saliva (hence nicknamed the "kissing disease"), and primary infection usually infects epithelial or naïve B cells in the oropharynx. EBV subsequently uses one of its several gene expression programs to persist in B cells. First, it uses its growth program (latency III) to activate infected naïve B cell into proliferating blasts in secondary lymphoid tissues of the pharynx, the so-called Waldeyer's ring. Cells in

this growth program will be susceptible to detection and elimination by EBV-specific CTLs, but this adaptive immune response will be slow initially. Some EBV-infected blasts will escape and turn on a default program (latency II) to drive these blasts to form germinal centers and differentiate into a long-lived resting memory B cells without T cell help, antigen, or cytokine signals. These latently infected memory B cells will enter the periphery and express no EBV genes (latency 0). Occasionally, they begin homeostatic proliferation, and the EBV in these cells will start to express only EBV nuclear antigen 1 (EBNA-1) to allow the viral genome to propagate with the cells (latency I). Because CTLs are incapable of detecting the latently infected resting memory B cells, EBV persists throughout the life of the host. Finally, when these memory cells differentiate into plasma cells, EBV will turn on its lytic program to make infectious viral particles to infect other B cells, epithelial cells, T cells, NK cells, or smooth muscle cells. In a high viremia state such as during infectious mononucleosis, EBV may also infect proliferating germinal center and memory B cells and express the growth program to cause them to expand. However, CTLs from immunocompetent hosts will eliminate all cells in the growth or lytic program to restrict persisting EBV in resting memory B cells in healthy individuals. Interferon γ (IFNγ) production by NK cells and EBV-specific antibodies by B cells also play roles in limiting the infection[45,46].

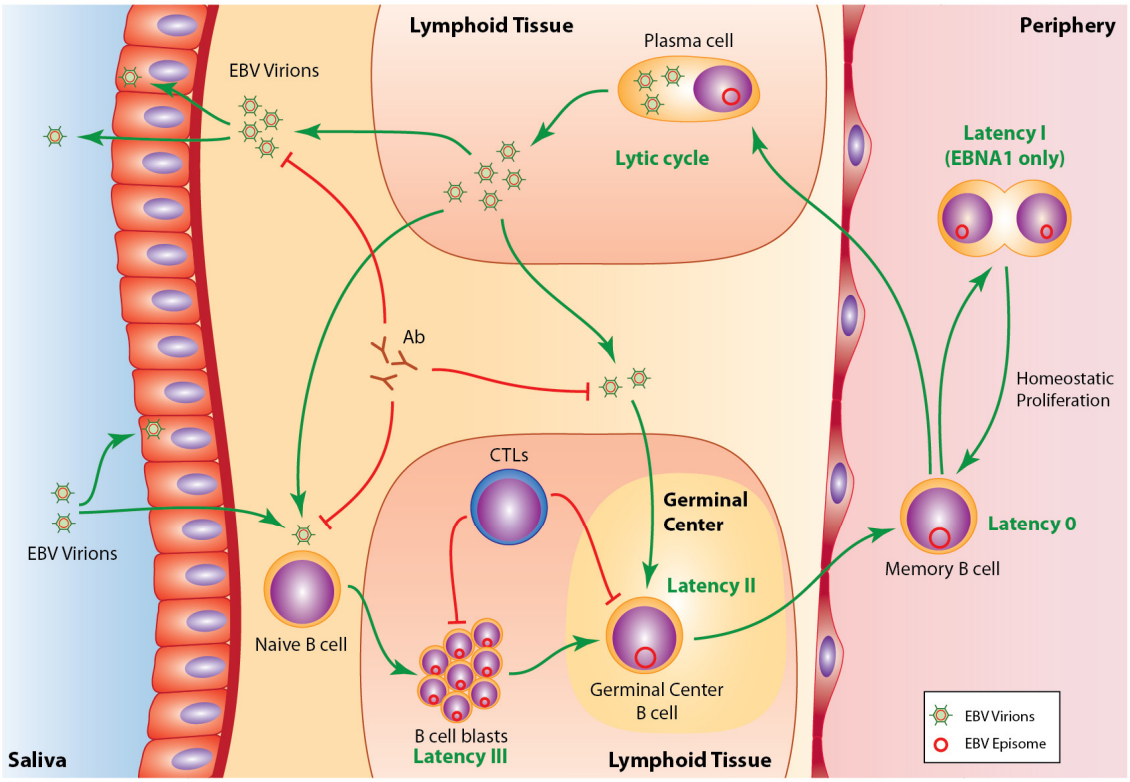

Figure 1-1: Persistence of EBV in human B cells.

Schematic of EBV life cycle in the human host. Transmitted in the saliva, EBV enters host by infecting epithelial and naïve B cells in the oropharynx and persists through all B cell types using various gene expression programs. The growth program (latency III) activates B cells to proliferate, while the default program (latency II) promotes memory B cell differentiation. Gene expression is shut off in latency 0, and only EBNA-1 is expressed in latency I to replicate viral genome. The lytic program produces more infectious viral particles. Immune responses such as activated CTLs and EBV-specific antibodies (Ab) can only detect naked virions or non-latently infected cells. Created with graphical assistance from Benjamin Chaigne-Delalande

In vitro infection of B lymphocytes can cause transformation of B cells to generate lymphoblastoid cell lines (LCLs). This is a common technique used to immortalize patient B lymphocytes for experimental studies. *In vivo,* CAEBV has been associated with the development of a number of lymphoid, epithelial, and

mesenchymal malignancies, particularly in the context of some form of immunodeficiency in the host such as HIV infection, transplantation, malnutrition, malaria infection, or PIDs. EBV can be detected in tumor tissues from nearly 100% of the Burkitt's lymphoma cases from malaria-endemic regions. Also, almost all cases of endemic nasopharyngeal carcinoma in southern China have detectable EBV in tumor tissues[45–47]. The association suggests EBV may have a direct causative role in the development of such cancers, but it is certainly not the only factor. Unrestricted growth of infected cells probably results from the cells exclusively in the proliferative state due to growth-promoting mutations and/or loss of immune surveillance. In many cases of Burkitt's lymphoma, for example, some EBNA-1 expressing memory B cells undergoing homeostatic proliferation acquire a genetic lesion that activates the c-Myc oncogene and prevents their exit from the cell cycle. Given that the viral load of immunocompromised patients is ~50x higher than that in immunocompetent hosts, germinal center and memory B cells are more likely in the former to become infected directly by EBV expressing the growth program and proliferate without CTL restriction[45,46]. The increased susceptibility to EBV-associated lymphomas is also notably increased in several well-characterized PIDs: X-linked lymphoproliferative disease (XLP) and ITK-deficiency syndrome.

1.4 PIDs with increased susceptibility to chronic EBV infections

XLP is a disease of immune dysregulation characterized by fulminant infectious mononucleosis (FIM), dysgammaglobulinemia, and lymphoproliferation[48–50]. Almost 60% of XLP cases have exhibited FIM, which is an over-reactive, often fatal immune response against EBV. The disease is

characterized by liver failure, hepatosplenomegaly, cytopenias, expansion of EBV-infected B cells, over-reactive CTLs, and/or hyperactivated macrophages leading to hemophagocytic lymphohistiocytosis (HLH) and systemic lymphocytic infiltration. Dysgammaglobulinemia (usually with elevated IgA and IgM and decreased IgG subclasses or generalized hypogammaglobulinemia) is observed in ~30% of XLP cases. Likewise, lymphoproliferative disorders, most commonly Burkitt's lymphoma, is observed in only about a third of XLP cases. Although EBV infection is associated with the mortality of this disease (70% die by age 10), dysgammaglobulinemia and lymphoproliferation have been observed in XLP patients without EBV, and some EBV$^+$ XLP patients do not develop FIM[48–50].

The first etiology described for XLP was a genetic deficiency in the SLAM (signaling lymphocytic activation molecule)-associated protein (SAP), an adaptor molecule that binds to the SLAM family of cell surface receptors: SLAM, LY9, 2B4, CD84, NTB-A, and CRACC. The second etiology described for XLP is a loss of function mutation in the X-linked inhibitor of apoptosis protein (XIAP), an inhibitor of caspases during apoptosis with no specific function in the immune system. While SAP is expressed in T cells, NK cells, and NKT cells, XIAP is ubiquitously expressed in all tissues. Thus, it has been an enigma why two such different proteins cause a similar disease. Careful analysis of the XIAP-deficient XLP patients' clinical phenotypes suggests that these patient may be better classified with the familial HLH syndromes (defects in the perforin cytotoxicity pathway) since their main consistent phenotype is HLH with or without EBV and none develop

lymphoma[48,50,51]. Nevertheless, XIAP-knockout mice, like the SAP-deficient mice, are more susceptible to infection by MHV-68 virus, a gammaherpesvirus like EBV[52].

Many cellular and functional defects in SAP deficiency have been described to account for the disease phenotypes in XLP, including lack of germinal center formation due to defects in T follicular helper (T_{FH}) cells, abnormal T:B cell conjugation, aberrant memory B cell development and class switching, loss of NKT cells, impaired Th2 cytokine production, decreased OKT3 restimulation-induced cell death (RICD) in T cells, and reduced NK and CTL cytotoxicity[48,50]. All these defects contribute to ineffective clearance of EBV-infected B cells and prolong the stimulation of CTLs, which secrete proinflammatory cytokines that chronically activate macrophages[48,50]. However, many of these pathogenic mechanisms are not observed in XIAP deficiency. In particular, the latter do not have NK cytotoxicity defects nor absent NKT cells, and contrary to SAP deficient patients, they have increased RICD[53]. Although it is unclear how XIAP deficiency leads to an HLH-like phenotype, it has been suggested that it may decrease the viability of the infected cells or activate immune cells that might enhance the persistence of the pathogens and the chronic production of proinflammatory cytokines[48,50].

Besides XLP, another recently identified PID with increase susceptibility to EBV infections is ITK deficiency. ITK is a non-receptor tyrosine kinase expressed in T cells, NK cells, iNKT cells, and mast cells that gets recruited to the plasma membrane upon TCR activation and phosphorylates PLCγ1 (Phospholipase Cγ1) Although ITK is not clearly connected to the SAP signaling pathways, like XLP patients, these patients exhibit EBV-induced lymphoproliferation and FIM with HLH

and a tendency to develop Hodgkin's lymphoma. Other clinical features include hypogammaglobulinemia, decreased naïve $CD4^+$ T cells and invariant NKT (iNKT) cells, impaired CTL and Fc receptor mediated NK cytotoxicity as well as decreased responses to primary TCR stimulation or RICD. Similarities between the clinical phenotypes of the diseases suggest that ITK deficiency falls within the XLP spectrum of diseases[54–58].

1.5 Concluding Remarks

The study of PIDs has taught us many fundamental principles about immunology, such as the importance of T cell function for antiviral immunity whereas antibody defenses play a more significant role in limiting bacterial pathogens. The human system is built with many lines of defense against different pathogens, and the loss of one of these arms may increase susceptibility to infection by a specific pathogen. The study of PIDs associated with EBV-driven lymphoproliferative disorders have taught us that the SAP and ITK signaling pathways are crucial for the development of NKT cells and the cytotoxicity of CTLs and NK cells, which are essential for limiting EBV infection and lymphoma development. Studying a family of ICL patients for my thesis, I have discovered a new PID with two key disease manifestations: CAEBV infection and lymphoma development. Not only did this etiology reveal an unexpected new component for regulating ITK activation, it also leads to an interesting connection to the NK cell cytoxicity defects in XLP.

1.6 References

1. Matzinger, P. An innate sense of danger. *Annals of the New York Academy of Sciences* **961**, 341-2 (2002).

2. Aghamohammadi, A. *Primary Immunodeficiency Diseases: Definition, Diagnosis and Management*. (Springer-Verlag: 2008).

3. Notarangelo, L.D. Primary immunodeficiencies. *J Allergy Clin Immunol* **125**, S182-94 (2010).

4. Savides, C. & Shaker, M. More than just infections: an update on primary immune deficiencies. *Current opinion in pediatrics* **22**, 647-54 (2010).

5. Blackburn, M.R. & Thompson, L.F. Adenosine deaminase deficiency: unanticipated benefits from the study of a rare immunodeficiency. *Journal of immunology (Baltimore, Md. : 1950)* **188**, 933-5 (2012).

6. Buckley, R.H. Primary immunodeficiency diseases: dissectors of the immune system. *Immunological reviews* **185**, 206-19 (2002).

7. Al-Herz, W. *et al.* Primary Immunodeficiency Diseases: An Update on the Classification from the International Union of Immunological Societies Expert Committee for Primary Immunodeficiency. *Frontiers in Immunology* **2**, 1-26 (2011).

8. Kumar, A., Teuber, S.S. & Gershwin, M.E. Current perspectives on primary immunodeficiency diseases. *Clinical & developmental immunology* **13**, 223-59 (2006).

9. Puel, A. *et al.* Chronic mucocutaneous candidiasis in humans with inborn errors of interleukin-17 immunity. *Science (New York, N.Y.)* **332**, 65-8 (2011).

10. Chan, a C. *et al.* ZAP-70 deficiency in an autosomal recessive form of severe combined immunodeficiency. *Science (New York, N.Y.)* **264**, 1599-601 (1994).

11. Elder, M.E. *et al.* Human severe combined immunodeficiency due to a defect in ZAP-70, a T cell tyrosine kinase. *Science* **264**, 1596-1599 (1994).

12. Arpaia, E., Shahar, M., Dadi, H., Cohen, A. & Roifman, C.M. Defective T cell receptor signaling and CD8+ thymic selection in humans lacking zap-70 kinase. *Cell* **76**, 947-958 (1994).

13. Negishi, I. *et al.* Essential role for ZAP-70 in both positive and negative selection of thymocytes. *Nature* **376**, 435-8 (1995).

14. Zhan, Y. *et al.* Responses against complex antigens in various models of CD4 T-cell deficiency: surprises from an anti-CD4 antibody transgenic mouse. *Immunol Res* **30**, 1-14 (2004).

15. Gatenby, P.A. Reduced CD4+ T cells and candidiasis in absence of HIV infection. *Lancet* **1**, 1027-1028 (1989).

16. Jowitt, S.N., Love, E.M., Yin, J.A. & Pumphrey, R.S. CD4 lymphocytopenia without HIV in patient with cryptococcal infection. *Lancet* **337**, 500-501 (1991).

17. Cozon, G., Greenland, T. & Revillard, J.P. Profound CD4+ lymphocytopenia in the absence of HIV infection in a patient with visceral leishmaniasis. *N Engl J Med* **322**, 132 (1990).

18. Unexplained CD4+ T-Lymphocyte Depletion in Persons Without Evident HIV Infection -- United States. *MMWR Morb Mortal Wkly Rep* **41**, 541-545 (1992).

19. Update: CD4+ T-Lymphocytopenia in Persons Without Evident HIV Infection -- United States. *MMWR Morb Mortal Wkly Rep* **41**, 578-579 (1992).

20. Smith, D.K., Neal, J.J. & Holmberg, S.D. Unexplained opportunistic infections and CD4+ T-lymphocytopenia without HIV infection. An investigation of cases in the United States. The Centers for Disease Control Idiopathic CD4+ T-lymphocytopenia Task Force. *N Engl J Med* **328**, 373-379 (1993).

21. Kojima, M. *et al.* EBV(+) B-cell lymphoproliferative disorder associated with subsequent development of Burkitt lymphoma in a patient with idiopathic CD4(+) T-lymphocytopenia. *J Clin Exp Hematop* **48**, 55-59 (2008).

22. Kanno, H. *et al.* Epstein - Barr virus-positive malignant lymphoma of salivary gland developing in an infant with selective depletion of CD4-positive lymphocytes. *Leuk Lymphoma* **48**, 183-186 (2007).

23. Lobato, M.N., Spira, T.J. & Rogers, M.F. CD4+ T lymphocytopenia in children: lack of evidence for a new acquired immunodeficiency syndrome agent. *Pediatr Infect Dis J* **14**, 527-535 (1995).

24. Lin, S.J., Chao, H.C., Yan, D.C. & Kuo, M.L. Idiopathic CD4+ T lymphocytopenia in two siblings. *Pediatr Hematol Oncol* **18**, 153-156 (2001).

25. Freier, S. *et al.* Hereditary CD4+ T lymphocytopenia. *Arch Dis Child* **78**, 371-372 (1998).

26. Seligmann, M. *et al.* Profound and possibly primary "idiopathic CD4+ T lymphocytopenia" in a patient with fungal infections. *Clin Immunol Immunopathol* **71**, 203-207 (1994).

27. Reith, W. & Mach, B. The bare lymphocyte syndrome and the regulation of MHC expression. *Annu Rev Immunol* **19**, 331-373 (2001).

28. Poodt, A.E. *et al.* TACI mutations and disease susceptibility in patients with common variable immunodeficiency. *Clin Exp Immunol* **156**, 35-39 (2009).

29. Spickett, G.P. *et al.* Common variable immunodeficiency: how many diseases? *Immunol Today* **18**, 325-328 (1997).

30. Primary immunodeficiency diseases. Report of a WHO Scientific Group. *Clin Exp Immunol* **99 Suppl 1**, 1-24 (1995).

31. Racioppi, L. *et al.* Defective dendritic cell maturation in a child with nucleotide excision repair deficiency and CD4 lymphopenia. *Clin Exp Immunol* **126**, 511-518 (2001).

32. Joachims, M.L., Chain, J.L., Hooker, S.W., Knott-Craig, C.J. & Thompson, L.F. Human alpha beta and gamma delta thymocyte development: TCR gene rearrangements, intracellular TCR beta expression, and gamma delta developmental potential--differences between men and mice. *J Immunol* **176**, 1543-1552 (2006).

33. Collins, A., Littman, D.R. & Taniuchi, I. RUNX proteins in transcription factor networks that regulate T-cell lineage choice. *Nat Rev Immunol* **9**, 106-115 (2009).

34. Singer, A., Adoro, S. & Park, J.H. Lineage fate and intense debate: myths, models and mechanisms of CD4- versus CD8-lineage choice. *Nat Rev Immunol* **8**, 788-801 (2008).

35. Palacios, E.H. & Weiss, A. Function of the Src-family kinases, Lck and Fyn, in T-cell development and activation. *Oncogene* **23**, 7990-8000 (2004).

36. Molina, T.J. *et al.* Profound block in thymocyte development in mice lacking p56lck. *Nature* **357**, 161-164 (1992).

37. Legname, G. *et al.* Inducible expression of a p56Lck transgene reveals a central role for Lck in the differentiation of CD4 SP thymocytes. *Immunity* **12**, 537-546 (2000).

38. Hubert, P. *et al.* Defective p56Lck activity in T cells from an adult patient with idiopathic CD4+ lymphocytopenia. *Int Immunol* **12**, 449-457 (2000).

39. Sawabe, T. *et al.* Defect of lck in a patient with common variable immunodeficiency. *Int J Mol Med* **7**, 609-614 (2001).

40. Goldman, F.D. *et al.* Defective expression of p56lck in an infant with severe combined immunodeficiency. *The Journal of clinical investigation* **102**, 421-9 (1998).

41. Wilkinson, B., Downey, J.S. & Rudd, C.E. T-cell signalling and immune system disorders. *Expert Rev Mol Med* **7**, 1-29 (2005).

42. Laurence, J. *et al.* Apoptotic depletion of CD4+ T cells in idiopathic CD4+ T lymphocytopenia. *J Clin Invest* **97**, 672-680 (1996).

43. Roger, P.M. *et al.* Overexpression of Fas/CD95 and Fas-induced apoptosis in a patient with idiopathic CD4+ T lymphocytopenia. *Clin Infect Dis* **28**, 1012-1016 (1999).

44. *Epstein-Barr virus*. (Caister Academic Press: Norfolk, 2005)

45. Maeda, E. *et al.* Spectrum of Epstein-Barr virus-related diseases: a pictorial review. *Japanese journal of radiology* **27**, 4-19 (2009).

46. Thorley-Lawson, D. a & Gross, A. Persistence of the Epstein-Barr virus and the origins of associated lymphomas. *The New England journal of medicine* **350**, 1328-37 (2004).

47. Michelow, P., Wright, C. & Pantanowitz, L. A review of the cytomorphology of epstein-barr virus-associated malignancies. *Acta cytologica* **56**, 1-14 (2012).

48. Rezaei, N., Mahmoudi, E., Aghamohammadi, A., Das, R. & Nichols, K.E. X-linked lymphoproliferative syndrome: a genetic condition typified by the triad of infection, immunodeficiency and lymphoma. *British journal of haematology* **152**, 13-30 (2011).

49. Nichols, K.E., Ma, C.S., Cannons, J.L., Schwartzberg, P.L. & Tangye, S.G. Molecular and cellular pathogenesis of X-linked lymphoproliferative disease. *Immunological reviews* **203**, 180-99 (2005).

50. Filipovich, A.H., Zhang, K., Snow, A.L. & Marsh, R. a X-linked lymphoproliferative syndromes: brothers or distant cousins? *Blood* **116**, 3398-408 (2010).

51. Marsh, R. a *et al.* XIAP deficiency: a unique primary immunodeficiency best classified as X-linked familial hemophagocytic lymphohistiocytosis and not as X-linked lymphoproliferative disease. *Blood* **116**, 1079-82 (2010).

52. Rumble, J.M. *et al.* Phenotypic differences between mice deficient in XIAP and SAP, two factors targeted in X-linked lymphoproliferative syndrome (XLP). *Cellular immunology* **259**, 82-9 (2009).

53. Rigaud, S. *et al.* XIAP deficiency in humans causes an X-linked lymphoproliferative syndrome. *Nature* **444**, 110-114 (2006).

54. Linka, R.M. *et al.* Germline Mutations within the IL2-Inducible T Cell Kinase Impede T Cell Differentiation or Survival, Cause Protein Destabilisation, Loss of Membrane Recruitment and Lead to Severe EBV Lymphoproliferation. *American Society of Hematology Meeting* (2010) at http://ash.confex.com/ash/2010/webprogram/Paper32792.html

55. Huck, K. *et al.* Girls homozygous for an IL-2 – inducible T cell kinase mutation that leads to protein deficiency develop fatal EBV-associated lymphoproliferation. **119**, (2009).

56. Stepensky, P. *et al.* IL-2-inducible T-cell kinase deficiency: clinical presentation and therapeutic approach. *Haematologica* **96**, 472-6 (2011).

57. Rezaei, N., Hedayat, M., Aghamohammadi, A. & Nichols, K.E. Primary immunodeficiency diseases associated with increased susceptibility to viral infections and malignancies. *The Journal of allergy and clinical immunology* **127**, 1329-41.e2; quiz 1342-3 (2011).

58. Khurana, D., Arneson, L.N., Schoon, R.A., Dick, C.J. & Leibson, P.J. Differential Regulation of Human NK Cell-Mediated Cytotoxicity by the Tyrosine Kinase Itk. *The Journal of Immunology* 3575-3582 (2007).

Chapter 2 : Clinical and genetic characterization of XMEN disease

2.1 Introduction

Historically, genetic etiologies of PIDs were identified by positional cloning and/or candidate gene sequencing, which often depends on identifying many affected families and knowing the functions of candidate genes. Thus, genetic etiologies can take years to identify by this process, and only one-third to one half of ~3000 suspected Mendelian disorders have genes identified by this arduous process. At the dawn of the genomics era in the 21st century, many new technologies have recently been developed to provide an unbiased approach to identify genetic mutations underlying rare genetic diseases. For example, our lab has successfully identified a constitutively active mutation in NRAS in an autoimmune lymphoproliferative syndrome (ALPS) patient through the use of gene expression microarrays to look for signature gene expression patterns[1]. Array comparative genomic hybridization (CGH) has also been utilized to identify a large deletion in the first case of Dock8 immunodeficiency syndrome (DIDS)[2]. As next generation sequencing (NGS) became cheaper, many scientists utilized NGS in conjunction with deoxyribonucleic acid (DNA) target capture technologies to discover gene mutations in rare diseases by exome sequencing. While exome sequencing can greatly accelerate the process to identify coding genetic variants in proband families, it also uncovers many irrelevant variants (>20,000 per exome) due to sequencing errors or common single nucleotide polymorphisms (SNPs). Thus, the challenge of disease gene identification is to sort through these variants properly to find the "needle in the haystack". Once the mutation is pinpointed, the ultimate validation of disease causation by the mutation is to demonstrate its impact on a function related to the

disease and/or to identify mutation(s) in the same gene from unrelated patients with similar disease[3–5].

Current strategies to identify genetic defects by whole exome sequencing (WES) were developed based on the assumption that rare diseases are caused by a highly penetrant coding mutation in a single gene that alters its function[3–5]. While this is probably true in most cases, it is certainly not true in every case. First of all, about 15% of known Mendelian disorders are caused by non-coding mutations, and this could be an underestimate due to ascertainment bias[3]. This is tempered by the fact that the majority of non-coding sequences are not functional so that mutations with a deleterious effect on protein function are more likely to be found in the coding regions of the genome. Secondly, mutations in different proteins involved in the same molecular pathway can often lead to a similar disease that is indistinguishable at the phenotypic level (i.e. genetic heterogeneity). Variation in disease manifestation due to incomplete penetrance (i.e. not every mutant gene carrier has the disease) or variable expressivity (i.e. same mutation showing different disease phenotypes) is observed in a number of PIDs given that the immune system is often affected by host-pathogen or environmental interactions[3–5]. Nonetheless, genetic heterogeneity and phenotypic variations are less probable if the affected subjects are from the same kindred.

Even when these assumptions hold true, there are a still several caveats that limit the success of using exome sequencing to identify genetic defects. First, the targeted exome may not equate to the true human exome as the commercial target capture kits may not include all expressed genes (e.g. microRNAs are not usually

included) and our current knowledge of expressed genes is incomplete. Second, exome capture sequencing will usually yield reliable coverage for ~88% of the exome mostly due to below 100% capture efficiencies and difficulty sequencing GC-rich regions. Third, various filtering strategies to eliminate variants that are unlikely to cause disease, such as synonymous coding variants or SNPs present in the normal population, could eliminate a potentially disease causing variant. For instance, a synonymous variant may actually introduce or ablate a splice site. For recessive diseases, the true mutation may be considered as a normal variant in SNP databases because it is carried by normal females without symptoms. Lastly, exome sequencing does not readily detect all structural variations (large insertions or deletions, inversions, translocations, and duplications) in the genome due to the short sequence reads. In addition to these known pitfalls, there are also potential false-positive hits due to errors in alignments resulting from presence of gene duplications and pseudogenes. Despite all these problems, current strategies to pinpoint the causative mutation (which often involves filtering according to the genetic model and prioritizing according to gene function and/or expression, potential pathogenicity of mutation, and/or conservation of mutated loci), have been estimated to be successful at deciphering genetic etiologies of rare diseases ~60% of the time[3–5].

This thesis began in 2009 with the search of the genetic etiology of two young brothers affected by ICL and a history of chronic viral infections since birth. Although viral infections are common in children, the lack of daycare exposure in the social history of these two boys made their clinical history noteworthy.

Moreover, we were able to strongly suggest that these two boys have an X-linked genetic disease by showing skewed lyonization in the mother's X chromosomes. Since WES technology was still under development at the time, I initially took many different approaches to search for the genetic etiology. But what ultimately led me to find the causative mutation was my novel approach of using NGS read coverage data to search for deletions. This led me to uncover a 10 base-pair (bp) deletion spanning an intron-exon junction in MagT1. Subsequently, I validated this mutation by identifying 5 additional patients from 5 different kindreds with loss-of-function mutations in MagT1. Comparison of the clinical phenotypes between these patients and other known PIDs suggests that this disease is highly similar to XLP and ITK-deficiency in their unique susceptibility to CAEBV infection and lymphoma development. Hence, this disease has been named X-linked immunodeficiency with Mg^{2+} defect, EBV infections, and neoplasia (XMEN) disease.

2.2 Results

A family of two boys with CAEBV and decreased thymic out of $CD4^+$ T cells

We initially characterized two young Caucasian brothers (patient A.1 and A.2) who had a history of recurrent infections with sinusitis, otitis media, chronic non-bloody diarrhea, viral pneumonia, herpes simplex virus infections, and chronically elevated titers of EBV (Figure 2-1). These patients exhibited low $CD4^+$ T cell counts in the absence of HIV infection, but other lymphocyte populations were normal or elevated (Figure 2-2A-B). Although patient A.2 does not strictly fit the definition of ICL, both patients' $CD4^+$ T cells were consistently low relative to $CD8^+$ T cells, leading to a decreased CD4:CD8 ratio (Figure 2-2A-B, Figure 2-3A). Moreover,

compared to normal controls, $CD31^+$ cells were decreased among the patient's $CD4^+CD27^+CD45RO^-$ naïve T cells, indicating diminished thymic output (Figure 2-3C)[6,7]. Nevertheless, expression of T cell surface markers (CD2, CD3, CD4, CD8, CD27) in the peripheral blood were not decreased in the patients, and the peripheral T cells exhibited polyclonally rearranged TCR genes (data not shown). Serum immunoglobulin levels and responses to vaccinations were intermittently defective (Figure 2-2C), perhaps suggesting defective $CD4^+$ T cell helper function. Established causes of low $CD4^+$ T cell counts, including infections with human immunodeficiency virus (HIV) or cytomegalovirus (CMV), Bare-Lymphocyte syndrome, Wiskott- Aldrich syndrome, and DiGeorge syndrome were excluded. XLP and ITK deficiency were also ruled out by Western blotting and sequencing (data not shown). These patients also did not exhibit lack of MHC class II expression (data not shown) as seen in BLS or dermatological abnormalities from sunlight sensitivity as seen in TDD and XP. Thus, they appear to have a novel immunodeficiency characterized by an inability to clear EBV and decreased thymic output of $CD4^+$ T cells.

Figure 2-1: Patients have elevated EBV titers.

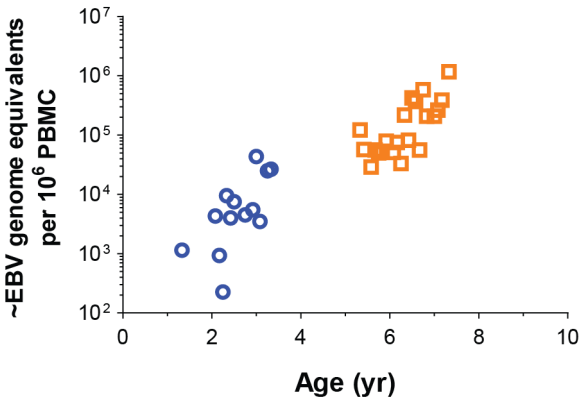

EBV genome copies detected in patient A.1 (orange squares) and A.2 (blue circles) by PCR in the clinical microbiology lab. Estimated conversion of EBV genome equivalents/million PBMC = EBV genome equivalents/mL whole blood/X 10. Performed by the NIH Clinical Core Lab; Data gathered by Helen Su.

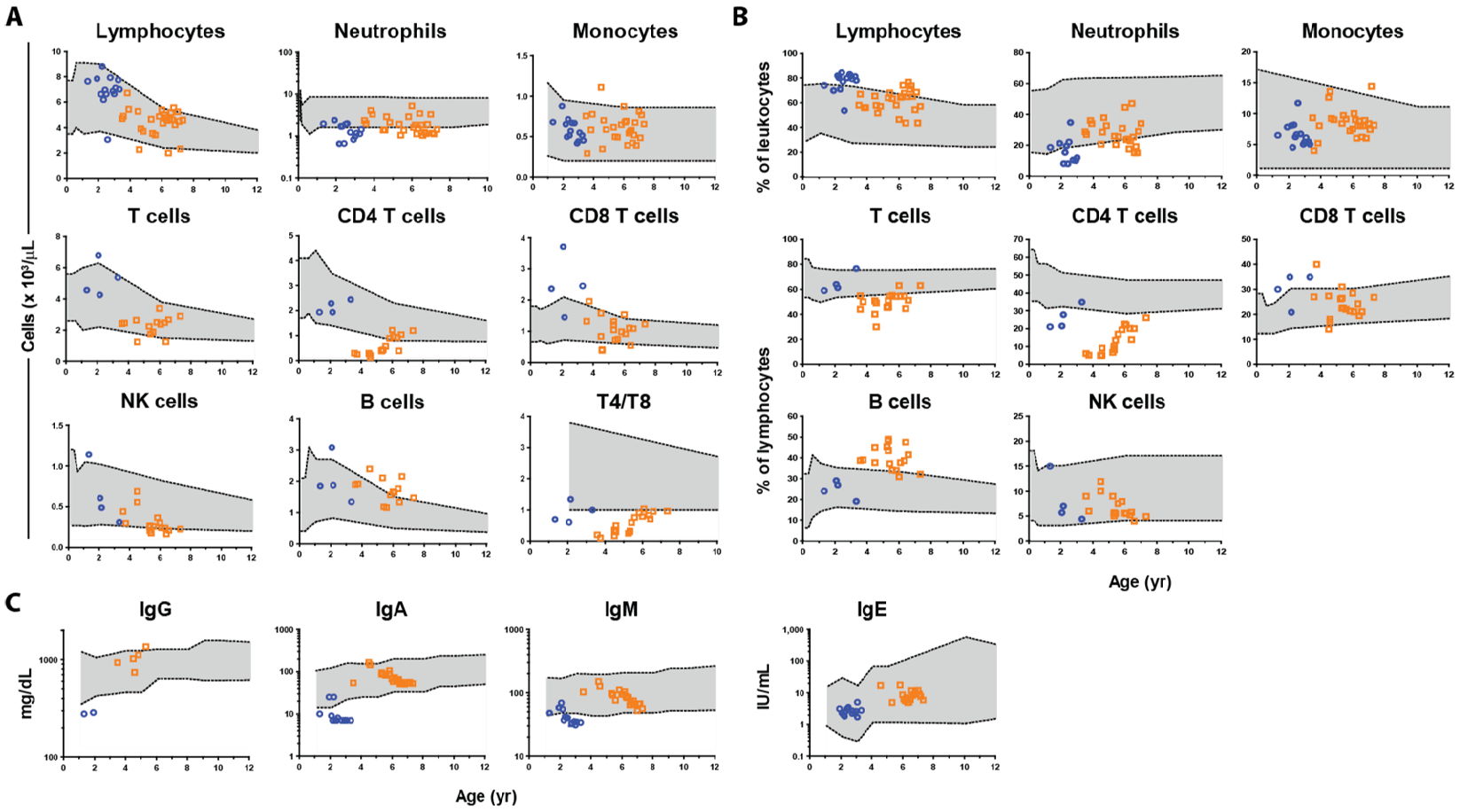
A
Lymphocytes
Neutrophils
Monocytes
T cells
CD4 T cells
CD8 T cells
NK cells
B cells
T4/T8
Cells (x 10³/μL
B
% of leukocytes
% of lymphocytes
Age (yr)
C
IgG
IgA
IgM
IgE
mg/dL
IU/mL
Age (yr)

Figure 2-2: ICL patients have abnormally low CD4:CD8 T cell ratio.

Absolute cell count (**A**) and relative percentage (**B**) of various immune cell populations and immunoglobulin levels (**C**) documented by clinical flow cytometry labs for patient A.1 (orange squares) and patient A.2 (blue circles) during various hospital admissions. T4/T8 = CD4/CD8 T cell ratio. Shaded grey area represents the range of age-matched normal control values (10th to 90th percentiles for lymphocyte subgroups[8] and 95% confidence interval for serum immunoglobulin[9]). Performed by the NIH Clinical Core Lab; Data gathered by Helen Su and Helen Matthews.

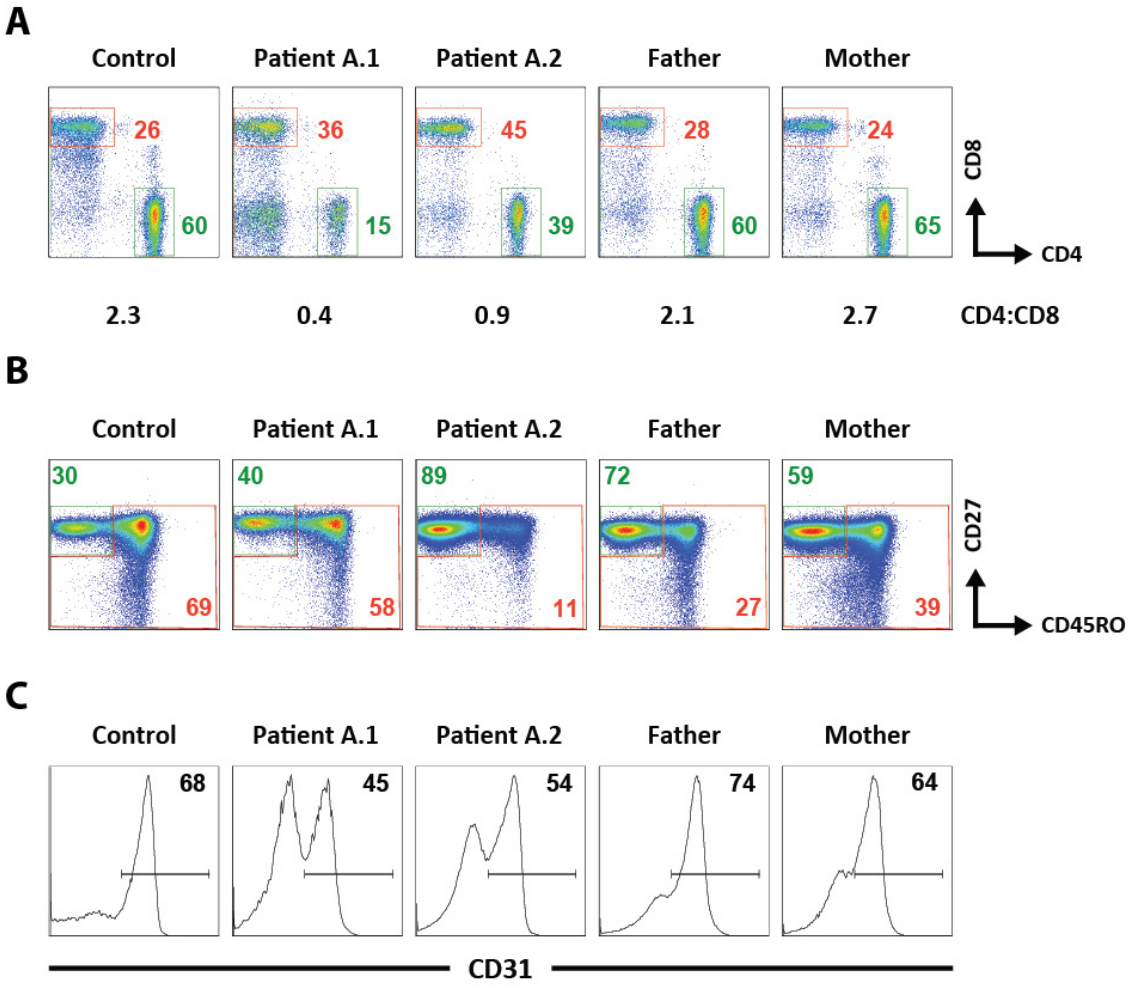

Figure 2-3: Patients have decreased thymic output of CD4⁺ T cells.

(**A**) Flow cytometry staining of CD4 and CD8 on gated CD3⁺ T cells. Percentage of CD4⁺ (green) and CD8⁺ (red) populations as well as the CD4:CD8 ratio (bottom) are displayed. (**B**) Flow cytometry

staining of CD27 and CD45RO on gated $CD4^+$ T cells. Percentages of naïve (green) and memory (red) cells are displayed. Similar percentages were observed in the $CD8^+$ T cells (not shown). (**C**) Histograms of CD31 expression in naive $CD4^+$ T cells with the percentage of $CD31^+$ cells displayed.

X-linked genetic disease model suggested by skewed lyonization

Given that the pedigree of this family revealed only two affected males, which is consistent with an X-linked genetic model, we tested this inheritance pattern by assessing the mother's X chromosome inactivation. Lyonization, the process of random X chromosome inactivation by methylation in females, usually generates mosaicism in inactivation of heterozygous alleles in X-linked genes. When an X chromosome contains a genetic mutation that confers a selective disadvantage (e.g. decreased proliferation or survival of the cells), skewed lyonization typically reflects the reduced fitness of cells inactivating the wild-type X-chromosome due to a deleterious mutation on the active X chromosome[10]. Skewed lyonization in affected cell populations of female carriers has been observed in a number of PIDs including XLA, XSCID, and XLP[11–13]. To assess lyonization, we digested genomic DNA from T cells with the methylation-sensitive restriction endonuclease (*HpaII*) to eliminate all active non-methylated X-chromosome DNA and analyzed the proportion of the remaining undigested (inactive) allele(s) by polymerase chain reaction (PCR) of a locus with variable trinucleotide repeats (Figure 2-4A). In this assay, male X-chromosome DNA is undetectable after *HpaII* digestion given its obligate hemizygous activity, while non-skewed females should display both alleles in roughly equal proportion (B). The mother of the two affected boys exhibited only a

single active allele, revealing completely skewed lyonization in her T cells; both sons inherited their mother's inactivated allele (B). This not only suggests the mother carries an X-linked genetic defect inherited by her two sons, but it also suggests that the defective gene is important to the fitness and survival of T cells or an earlier progenitor cell.

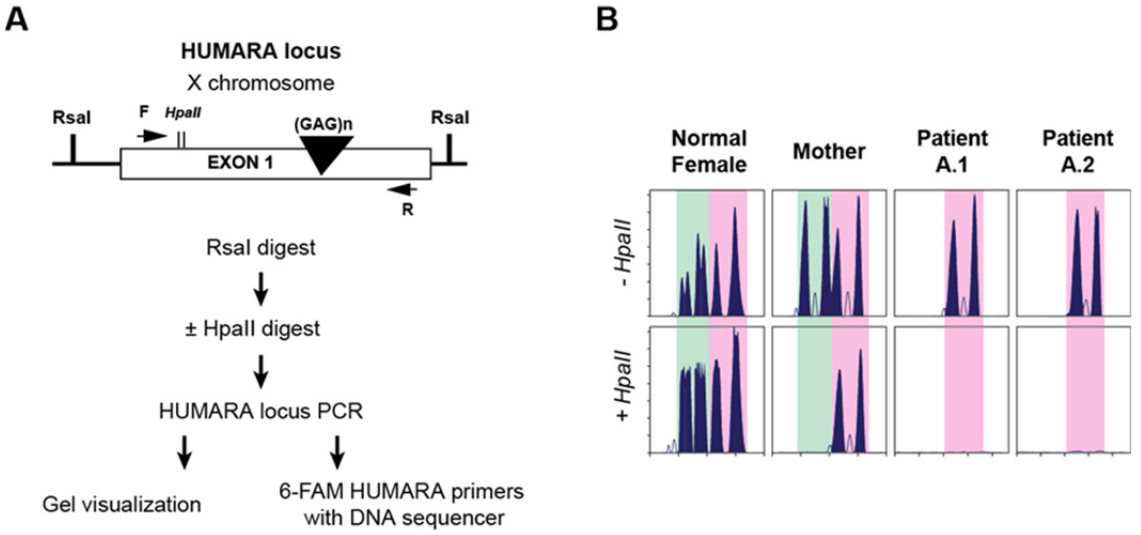

Figure 2-4: Skewed lyonization in patients' mother suggests X-linkage

(**A**) Schematic diagram of lyonization assay on the HUMARA locus. (**B**) Lyonization assay results: each pair of peaks highlighted in green and pink represent different alleles of each X-chromosome. Assay was established and performed by Jeremiah Davis.

MAGT1 mutation uncovered by X-chromosome exome sequencing

Our initial approaches to find the X-linked genetic mutation included both biased and unbiased approaches. I used the functional candidate gene approach by searching for X-chromosome genes whose mouse knockout models exhibit CD4 lymphopenia: *ARHGEF6, CXCR3, IGBP1, IL13RA1, SASH3*. We also performed gene

expression microarrays on sorted naïve ($CD27^{+}CD45RO^{-}$) and memory T cells from patients, parents, and two adult normal controls and identified about 25 X chromosome genes in the patients downregulated relative to normal controls. I carried out DNA sequencing by conventional methods on all these genes using either complementary DNA (cDNA) or genomic DNA (gDNA) and did not find any nonsynonymous coding mutations (data not shown). Large structural mutations were ruled out by performing a CGH array with a resolution of 1 kilobases (data not shown). When we finally gained access to a Solexa NGS machine, we performed X-chromosome exon-capture and single-end Illumina platform next-generation sequencing on the captured genomic DNA from the mother and her two sons. This yielded 18-20 million reads per subject with at least 10x coverage in ~90% of target regions (Figure 2-5A-B). Although some reads were distributed on all chromosomes, there was a 20-fold increase in reads that mapped to the X chromosome indicating that the specific capture of X chromosome exonic sequences was successful (Figure 2-5A). From the coding variants obtained, I excluded all SNPs and 1-2 bp deletion insertion polymorphisms (DIPs) that were not present in both boys, not heterozygous in the mother, or that were found in her cDNA. Using these filters, no nonsense mutations were found, and only two missense mutations were consistent with our search criteria: *MTMR8* (g.63488667A>G; p.Ile622Thr) and *FAM127C* (g.134155953A>G; the variant is now consider non-coding in the 3'UTR). These mutations were found to be common polymorphisms present in about 10% of 100 normal controls that I tested (data not shown).

A

Subject	Patient A.1	Patient A.2	Mother
Sex	Male	Male	Female
Capture	X-exome	X-exome	X-exome
Total Reads	18,521,042	19,149,336	19,708,313

Contig	Average coverage	Average coverage	Average coverage
chr1 contig	0.11	0.12	0.08
chr10 contig	0.11	0.12	0.08
chr11 contig	0.11	0.12	0.08
chr12 contig	0.12	0.13	0.09
chr13 contig	0.08	0.09	0.06
chr14 contig	0.10	0.11	0.07
chr15 contig	0.11	0.12	0.08
chr16 contig	0.12	0.13	0.09
chr17 contig	0.12	0.13	0.09
chr18 contig	0.09	0.10	0.07
chr19 contig	0.15	0.16	0.11
chr2 contig	0.10	0.12	0.08
chr20 contig	0.11	0.13	0.09
chr21 contig	0.07	0.08	0.06
chr22 contig	0.09	0.10	0.07
chr3 contig	0.10	0.11	0.08
chr4 contig	0.09	0.10	0.07
chr5 contig	0.11	0.13	0.09
chr6 contig	0.11	0.12	0.08
chr7 contig	0.09	0.11	0.07
chr8 contig	0.10	0.11	0.08
chr9 contig	0.10	0.12	0.08
chrX contig	2.25	2.17	3.05
chrY contig	0.17	0.17	

B

Patient A.1		Patient A.2		Mother	
coverage		coverage		coverage	
Mean	92.89	Mean	86.17	Mean	121.24
Total bases	1,990,773	Total bases	1,990,773	Total bases	1,990,773
1x	92.50%	1x	92.47%	1x	92.69%
5x	90.96%	5x	90.88%	5x	91.29%
10x	89.35%	10x	89.23%	10x	89.89%
20x	86.38%	20x	85.97%	20x	87.47%
25x	84.89%	25x	84.21%	25x	86.27%
50x	75.80%	50x	73.70%	50x	79.66%
100x	45.87%	100x	39.74%	100x	62.01%

Figure 2-5: X-chromosome exome targeted DNA sequencing leads to enriched and >10X coverage on 90% of X chromosome exons.

(**A**) Total reads detected and average coverage in each chromosome from aligning all reads to the whole human genome. Enrichment of read coverage on X-chromosome indicated by red arrow. (**B**) X-chromosome exon coverage statistics displaying the mean coverage of all bases in exons, total number bases in target, and the percent of bases with minimum coverage displayed.

Given the limitations of targeted exome sequencing (<100% coverage; inability to detect large DIPs (>2bp); lack of coverage for microRNAs, gene regulatory regions, and non-targeted genes) and the CLCbio Genomics Workbench software for NGS analysis (inability to report splicing mutations and target regions missing coverage), I considered the types of mutations that could have been missed in my first analysis: 3-1000 bp DIPs, splicing mutations, coding mutations with insufficient or lack of coverage, microRNA mutations, and non-coding mutations. I tried searching for splicing mutations by filtering for SNPs in non-coding regions with high coverage, which usually correspond to intron regions adjacent to exons due to the exon capture. To complete coverage for genes with missing coverage, I filtered for genes with low coverage SNPs and carried out additional DNA sequencing in the region around those SNPs. To identify genes with potential non-coding mutations leading to loss of expression, I performed real-time gene expression assessments on genes downregulated in the gene expression microarrays. I also started DNA sequencing regions encoding microRNAs on the X-chromosome. Unfortunately, none of these approaches yielded a mutation consistent with the genetic model (data not shown).

In the meantime, CLCbio has been working with me to develop a computational tool to report the coverage of targeted regions. After I validated this tool using the genes that I found to have low and missing coverage earlier, I used it to identify genes with missing coverage in the patients but have sufficient coverage in the mother; I hypothesized that such genes would have deletions in the patients. This analysis revealed two such genes (Figure 2-6). One of them (*MAGEA2*) appears

to be an alignment error due to gene triplication. For the other gene (*MAGT1)*, a 10 bp region with a break of high continuous coverage on both sides was evident in the patients' NGS alignment (Figure 2-7A). The base calls at the end of the aligned reads overlapping this 10bp region were disregarded by the program because mismatched base calls at the ends of short reads are deemed not reliable. However, I observed that the nucleotides were the *same* mismatched calls on every read, and they match the reference after the 10bp interval. I found this to be the case when examining the sequencing coming in from either the 5' or 3' end, suggesting the presence of a possible 10bp deletion. The mother's alignment also has these consistent mismatched base calls in some of the aligned reads, suggesting she could be heterozygous for this deletion. To confirm my hypothesis, I created a new reference sequence with this 10bp deletion and aligned it against the reads that did not assemble with the initial reference. Supporting my conclusion, a large number of reads aligned perfectly with the new reference sequence harboring a deletion of this 10 bp region from both patients (Figure 2-7B) and mother (data not shown).

	Patients	Mother
Gene	**Min coverage**	**Min coverage**
AFF2	0	2
AVPR2	0	2
CT47A6	0	1
CTAG2	0	4
CTAG2	0	4
FAM120C	0	1
GAB3	0	1
GAB3	0	1
GYG2	0	1
LOC100288052	0	1
LOC100289651	0	1
LOC644717	0	1
MAGEA2	0	131
MAGEA2	0	131
MAGEA2	0	131
MAGEC1	0	2
MAGED2	0	1
MAGED2	0	1
MAGED2	0	1
MAGT1	0	92
MXRA5	0	2
PRAF2	0	1
SMC1A	0	1
VCX2	0	1
WDR42C	0	1

Figure 2-6: Genes with missing coverage in the patients but not in the mother

From the set of genes reported as having minimum (min) coverage of 0 in target regions from the patients on the CLCbio targeted resequencing plug-in tool, those genes that did not have a minimum coverage of 0 in the mother were filtered in Microsoft EXCEL and reported on this table. Only two genes show sufficient coverage throughout the whole gene in the mother but have missing coverage in the coding region in the patients, suggesting a potentially deleted region.

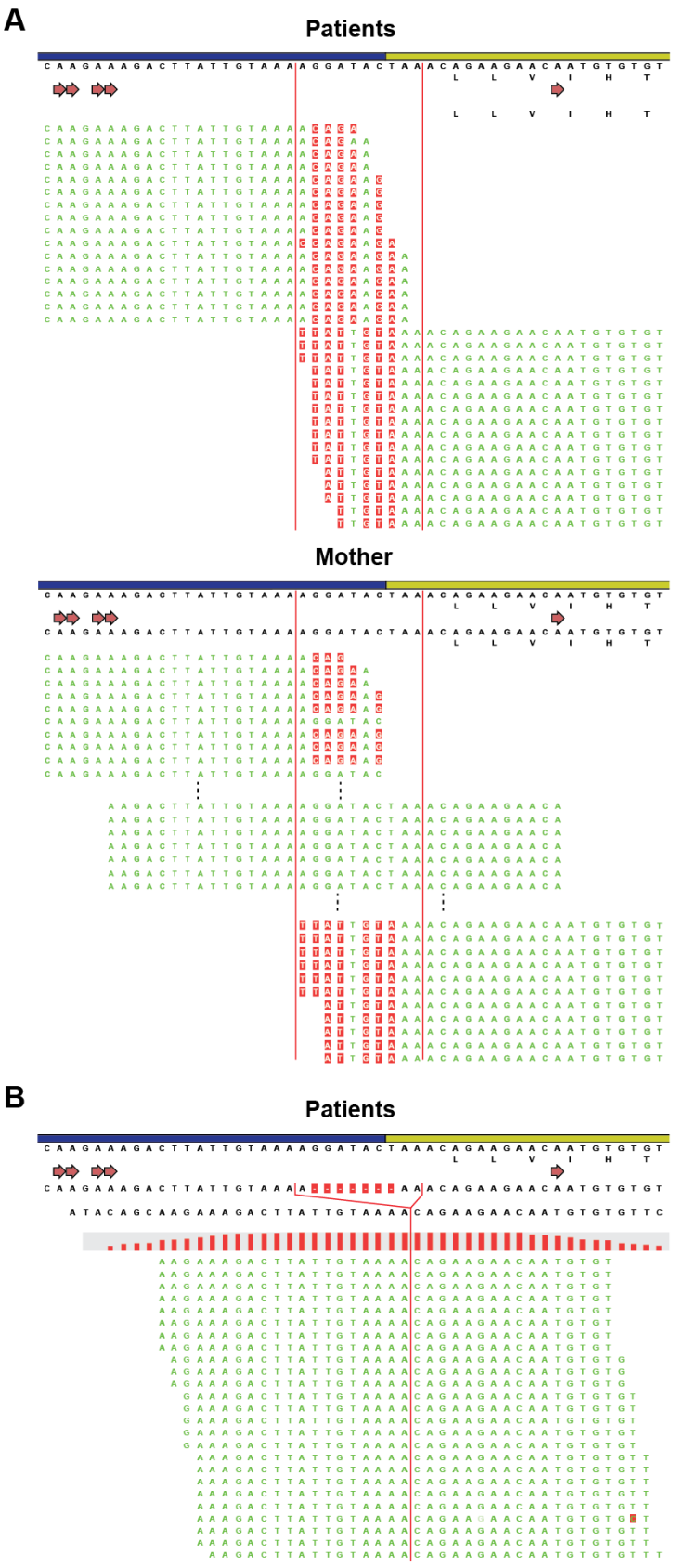
A
Patients
Mother
B
Patients

Figure 2-7: Patients' X-exome sequencing alignment suggests a 10bp deletion at an intron-exon junction of *MAGT1.*

(**A**) Region in the *MAGT1* gene with missing coverage (highlighted in pink) in the patients but not in the mother. Yellow bar indicates a coding exon, and aligned reads are shown in green with disregarded reads shaded. (**B**) Alignment of unaligned reads from the patients using a new reference (purple) with the potential 10 bp deletion removed.

MAGT1 mutation leads to loss of expression

The 10 bp deletion removes a splice donor site located in the 3' exon-intron junction of exon 7 in *MAGT1*, a gene coding for a magnesium transporter[14–16]. Direct conventional DNA sequencing of gDNA confirmed the deletion in the two brothers and heterozygosity of the deletion in the mother (Figure 2-8A). This mutation was also carried by the maternal grandmother and maternal great-grandmother of the patients (data not shown). cDNA amplification from both brothers, showed their predominant *MAGT1* splice variant was ~150 bp smaller than the normal splice variant of approximately 1100 bases and the loss of both exon 7 and 8 was confirmed by cDNA sequencing (Figure 2-8B-C).

Consistent with the mother's skewed lyonization, we only found the normal *MAGT1* splice variant expressed in her T cells (Figure 2-8B-C). This deletion was not detected in a number of other immunodeficient patients and 100 normal individuals (data not shown). Since exon 9 is not in frame with exon 6 in *MAGT1*, an premature stop codon was introduced; and nonsense-mediated decay likely caused a decrease of the mRNA expression by ~80% (Figure 2-9A). Neither truncated nor normal

MagT1 protein were detectable in the patient cells by Western blot or immunofluorescence staining (Figure 2-9B-C).

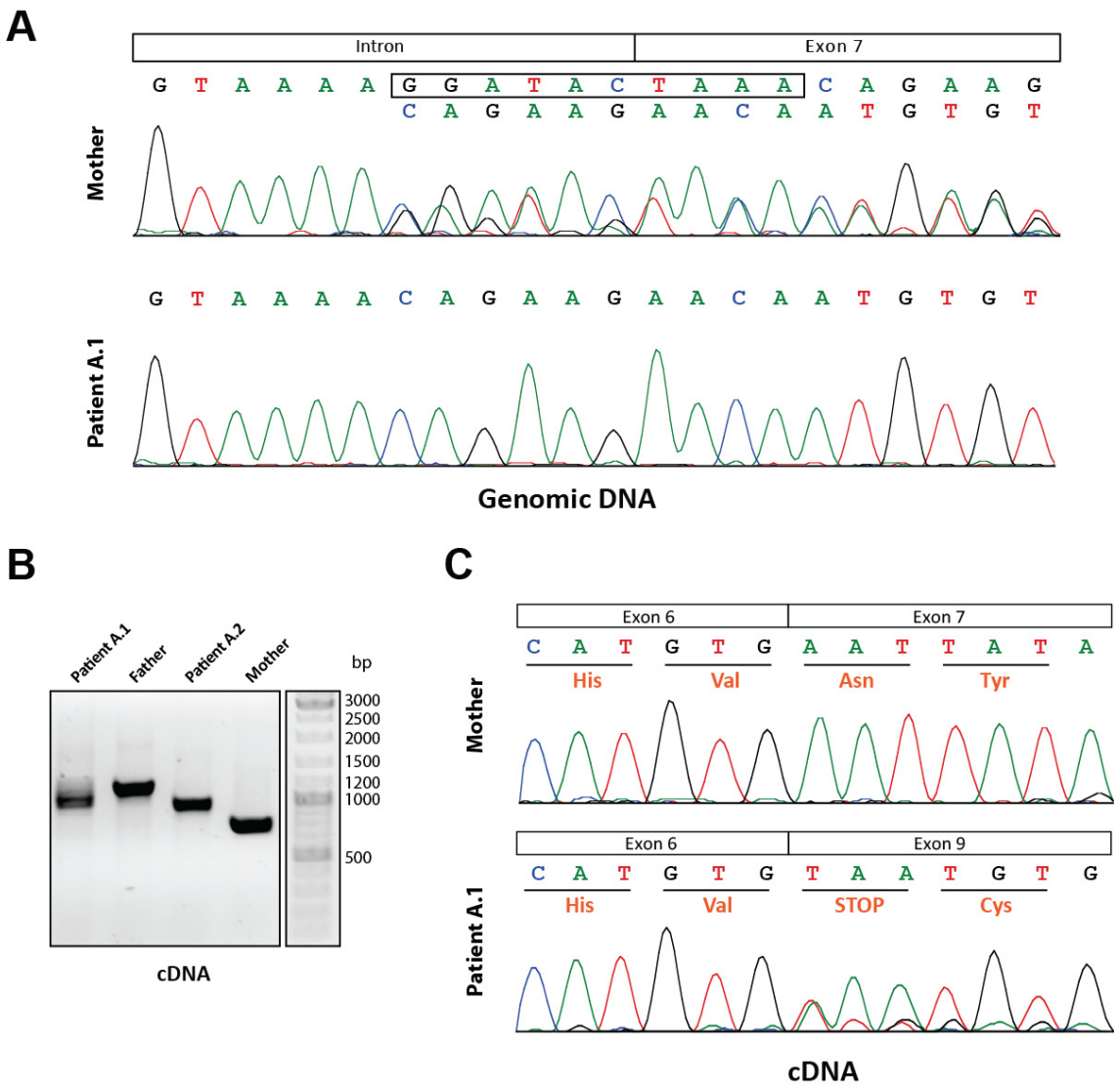

Figure 2-8: Patients A.1 and A.2 have 10 bp deletion in *MAGT1* leading to altered splicing and early termination.

(**A**) Sanger sequencing of *MAGT1* gDNA sequence from patients A.1 and mother. The normal allele from mother is shown on top, and boxed reads represent deleted regions in the mutant allele. (**B**) PCR amplification of *MAGT1* cDNA from patients A.1 and A.2 and their parents. (**C**) Sanger DNA

sequencing of *MAGT1* cDNA from patient A.1 and the mother. Expected translation from open reading frame is shown.

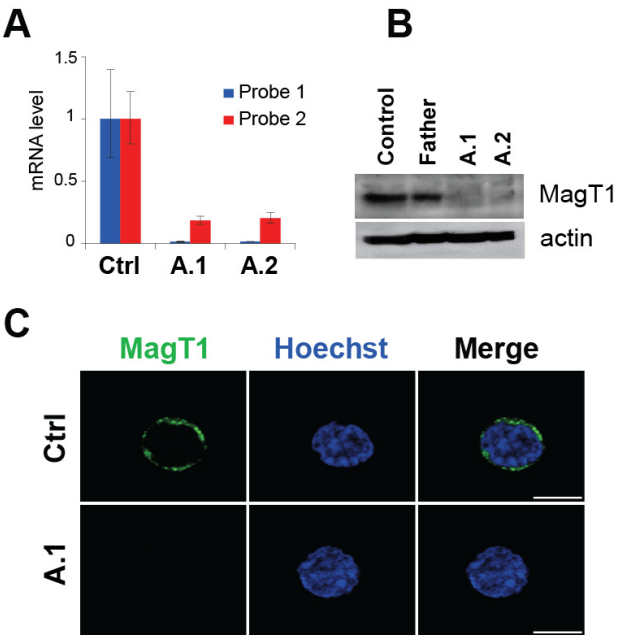

Figure 2-9: *MAGT1* mutation leads to loss of protein expression

(**A**) RT-PCR showing decreased expression of *MAGT1* mRNA in T cells from patients (A.1, A.2) and normal control (Ctrl). Probe 1 detects region overlapping exon 7 and 8 that contains the deletion; probe 2 detects region overlapping exon 1 and 2. (**B**) Expression of MagT1 and actin control in T cells by immunoblot. (**C**) Confocal images of T cells stained with anti-MagT1 antibody (scale bar: 5 μm). Real –time assay in (**A**) was performed by Chryssa Kanellopoulou.

By screening more than 60 additional male patients with ICL and/or CAEBV infections, I have uncovered 5 additional patients from 5 different kindreds harboring mutations in *MAGT1* (Figure 2-10). The *MAGT1* mutations were spread throughout the gene with one mutation (g.29684C>T) being shared by two kindreds. All were loss of function mutations leading to an early stop codon and decreased MagT1 mRNA probably due to nonsense-mediated decay of the transcripts (Figure 2-9A). Thus, MagT1 deficiency constitutes a novel human PID.

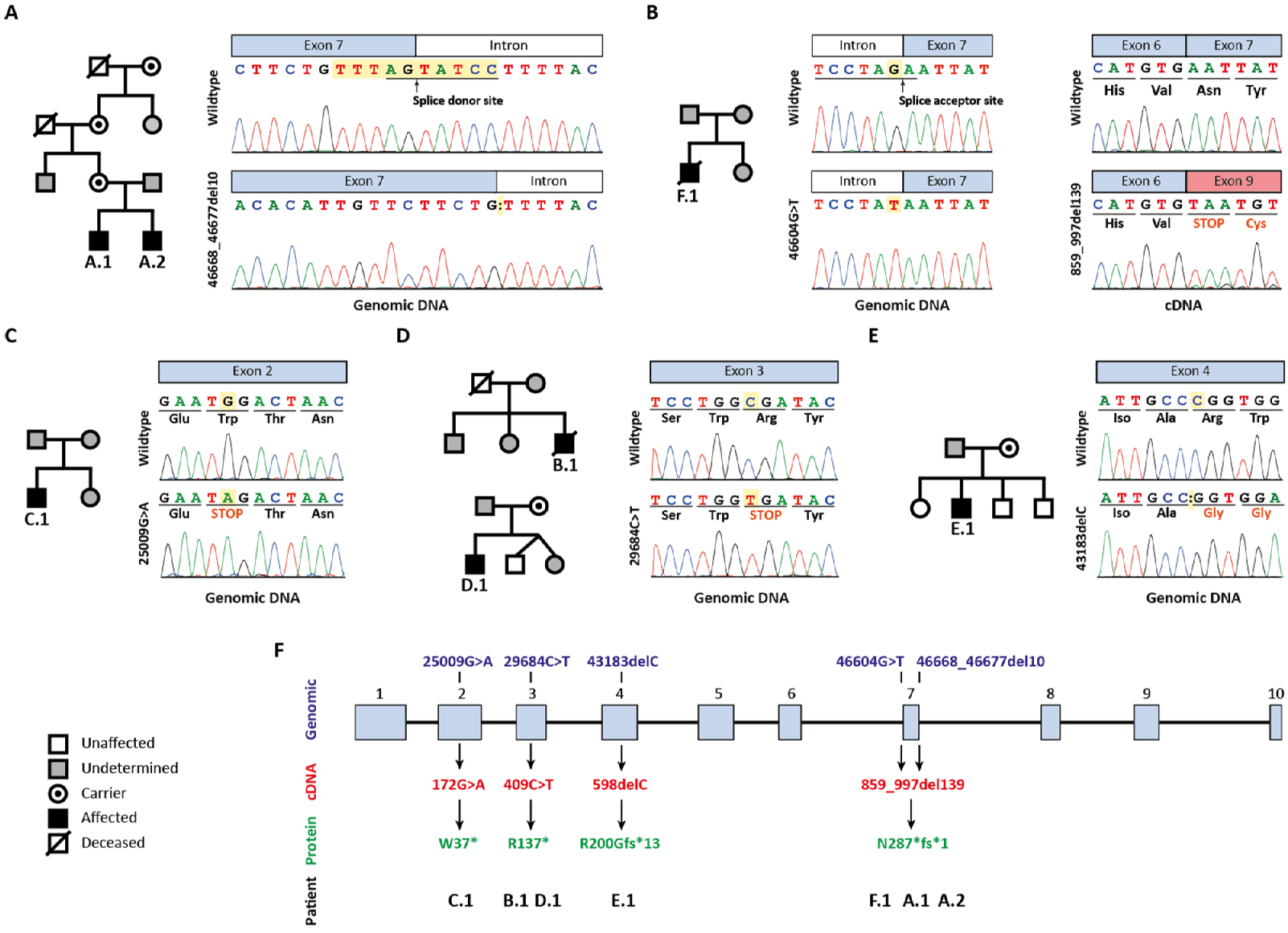
A
Exon 7
Intron
Wildtype
Splice donor site
46668_46677del10
Genomic DNA
A.1
A.2
B
F.1
Splice acceptor site
46604G>T
Exon 6
Exon 9
859_997del139
cDNA
C
Exon 2
25009G>A
C.1
D
B.1
D.1
Exon 3
29684C>T
E
E.1
Exon 4
43183delC
F
25009G>A
29684C>T
43183delC
46604G>T
46668_46677del10
Genomic
cDNA
Protein
172G>A
409C>T
598delC
859_997del139
W37*
R137*
R200Gfs*13
N287*fs*1
Patient
C.1
B.1 D.1
E.1
F.1
A.1
A.2
Unaffected
Undetermined
Carrier
Affected
Deceased

Figure 2-10: XMEN patients with loss of function mutations in *MAGT1.*

(**A**-**E**) Pedigree of each family (left), and DNA sequencing of gDNA representative of a normal control (top) or a patient (bottom) illustrating the mutation. In (**B**), DNA sequencing of cDNA confirming altered splicing is shown next to the gDNA sequencing. (**F**) Schematic representation of *MAGT1* exons (boxes) and introns (lines) showing the location and annotation of each mutation found in the affect individuals according to Human Genome Variation Society recommendations (http://www.hgvs.org/mutnomen/) using GenBank Reference Sequences NC_000023.10 (DNA), NM_032121.5 (mRNA), and NP_115497.4 (protein) based on NCBI Build 37.3. Coding DNA variations are described with the A of the ATG translation initiation codon designated as nucleotide +1. Marshall Lukacs performed sequencing for (**C**) and relatives of patient D.1 and E.1.

MAGT1 deficient patients have increased susceptibility to EBV-associated lymphomas

With the exception of one patient (B.1), all patients have a decreased CD4:CD8 T cell ratio and borderline low neutrophils (Table 2-1, Figure 2-12). All patients exhibit borderline high level of B cells, which could be a consequence of EBV infection. However, some of the patients (C.1 and D.1) currently have non-detectable levels of EBV (Gulbu Uzel and Taco Kuijpers, personal communication). Variable deficiencies in immunoglobulin levels (IgG, IgA, and IgM) and vaccination responses were found in some of the patients (Table 2-1, Figure 2-12). Except for the younger patients, all 4 of the older patients have developed lymphomas as early as 7 years of age (Table 2-1). Patient E.1 and F.1 had both two independent episodes of lymphomas. Patient B.1 suffered from CAEBV infection involving lung and liver and died subsequent to lymphoma development and transplant complications at age

45, while patient F.1 died at the age of 22 also from bone marrow transplant complications after he developed recurrent Hodgkin's lymphoma. These data indicate that the most serious sequellae of this otherwise mild PID condition is EBV-associated lymphomas.

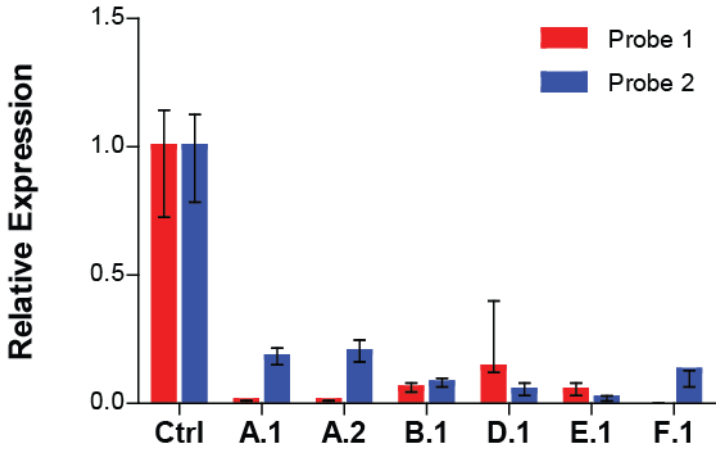

Figure 2-11: XMEN patients have decreased transcript levels

RT-PCR showing decreased expression of *MAGT1* mRNA in T cells from XMEN patients (A.1, A.2, B.1, D.1, E.1, and F.1) and normal control (Ctrl). Probe 1 detects region overlapping exon 7 and 8 that contains the deletion; probe 2 detects region overlapping exon 1 and 2. Cells from patient C.1 were not available for evaluation. Real-time for patients A.1, A.2, and B.1 was performed by Chryssa Kanellopoulou. Real-time for patients D.1 and E.1 was performed by Marshall Lukacs.

Table 2.1: Clinical phenotypes of XMEN patients							
Subject	**A.2**	**C.1**	**A.1**	**D.1**	**E.1**	**F.1**	**B.1**
Age (yo)	3	4	7	14	14	20	45
Age of death (yo)						21	45
Infection phenoypes							
Epstein-Barr Virus	+	+	+	+	+	+	+
Herpes simplex virus	+	-	+	-	-	-	-
Viral pneumonia	+	-	+	-	-	-	-
Otitis Media	+	-	+	-	-	-	-
Sinusitis	+	+	+	-	-	+	-
Other immune disorders							
Auto-immunity	-	-	**+ (ITP)**	**+ (ITP)**	-	-	-
Cancers (age onset)							
Lymphoma	None	None	None	**Non-Hodgkin (12 yo)**	**Burkitt's (7, 14 yo)♮**	**Hodgkin (17, 22 yo) ♭**	**Lymphoma (45 yo)**
Vaccinations Titers							
Tetanus Toxoid	+	+	-	ND	+	+/-	ND
Haemophilus influenzae type B	+	ND	+	ND	ND	ND	ND
Diphtheria	ND	ND	+	ND	+	+	ND
Pneumococcal	+/-	+	+	ND	-	-	ND
Peripheral blood cell numbers (normal range)							
Total T cells (cells/μL)	**4562** (1900-5900)	**3470** (700-4500)	**1738** (1400-3700)	**798** (1200-2600)	**1028** (980-5700)	**1289** (1400-3300)	**239** (650-2108)§
% T cells	**61.2** (53-75)	ND	**54.3** (53-75)	**48.6** (53-75)	**53.6** (53-75)	**69** (55-83)	**83.9** (57.3-86.4)§
CD4+ T cells (cells/μL)	**1935** (1400-4300)	**1170** (300-2400)	**432** (700-2200)	**149** (650-1500)	**291** (400-2100)	**100** (300-1400)	**212** (358-1259)§
% CD4 T cells	**27.8** (32-51)	ND	**13.5** (28-47)	**19.1** (31-47)	**17** (31-47)	**40** (28-57)	**74.4** (28.6-57.2)§
CD8+ T cells (cells/μL)	**2364** (500-1700)	**1990** (300-1800)	**717** (490-1300)	**501** (370-1100)	**582** (370-1100)	**76** (20-90)	**25** (194-836)§
% CD8 T cells	**20.8** (14-30)	ND	**22.4** (16-30)	**43** (18-35)	**34** (18-35)	**34** (10-39)	**8.6** (12.9-46.9)§
CD4/CD8 Ratio	**0.7** (0.9-3.7)	**0.6** (0.9-3.4)	**0.6** (1.4-1.7)	**0.55** (0.9-3.4)	**0.5** (0.9-3.4)	**1.1** (1.0-3.6)	**8.5** (1.0-3.6)§
B cells (cells/μL)	**1849** (610-2600)	**1984** (200-2100)	**1185** (390-1400)	**2891** (270-860)	**0** (RITX)	**1200** (110-570)	**40** (49-424)§
% B cells	**26.9** (16-35)	ND	**37.1** (14-33)	**46** (13-27)	**0** (RITX)	**44** (6-23)	**14.1** (6-23)§
NK cells (cells/μL)	**487** (160-950)	**600** (100-1000)	**175** (130-720)	**170** (100-480)	**120** (100-480)	**300** (70-480)	**5** (87-505)§
% NK cells	**15** (3-15)	ND	**5.4** (4-17)	**5** (3-22)	**7** (3-22)	**11** (3-22)	**1.7** (4.6-29.8)§
Eosinophils (cells/μL)	**150** (30-530)	**180-160** (30-530)	**61** (30-520)	**34** (30-520)	**44** (30-520)	**40** (40-540)	**8** (40-540)§
% Eosinophils	**1.85** (0-4.1)	ND	**1.2** (0-4.7)	**1.5** (0.8-7)	**1.2** (0.8-7)	**1** (0.8-7)	**0.2** (0.8-7)§
Neutrophils (cells/μL)	**651** (1500-8500)	**5720** (1500-8500)	**1045** (1500-8500)	**3057** (1800-7700)	**2155** (1800-7700)	**1360** (1800-7700)	**3352** (1800-7700)§
% Neutrophils	**8** (22.4-69)	ND	**20.4** (28.6-74.5)	**37.9** (28.6-74.5)	**55** (28.6-74.5)	**34** (34-67.9)	**88.2** (34-67.9)§
Monocytes (cells/μL)	**651** (190-940)	**800** (190-940)	**497** (190-850)	**706** (190-850)	**482** (190-850)	**280** (300-820)	**129** (300-820)§
% Monocytes	**8.1** (4.2-12.2)	ND	**9.7** (4.2-12.3)	**13** (4.2-12.3)	**9.9** (4.2-12.3)	**7** (4.2-12.3)	**3.4** (4.2-12.3)§
Immunoglobulin's levels							
IgG (mg/dL)	**286** (424-1051)	**1030** (620-1300)	**1160** (633-1280)	**1690** (639-1349)	**611** (639-1349)	**619** (639-1349)	**734** (642-1730)§
IgA (mg/dL)	**7** (14-23)	**56** (50-200)	**87** (25-154)	**14.8** (45-236)	**35.6** (45-236)	**29.9** (70-312)	**128** (91-499)§
IgM (mg/dL)	**55** (48-1680)	**115** (60-200)	**92** (43-1960)	**29** (56-352)	**87** (56-352)	**38** (56-352)	**14** (34-342)§
IgE (IU/mL)	**2000** (310-2950)	ND	**1750** (1070-6890)	**2100** (206-1952)	**1500** (206-1952)	**5** (1.53-114)	**5** (0-90)§

ITP, idiopathic thrombocytopenia

ND, not determined (blood could not be obtained from deceased patient)

+/-, positive for some serotypes, negative for others

♮ B cell lymphomas of two different restrictions: first lambda light chain and then kappa light chain; no MYC/IGH gene rearrangements were found.

♭ Presumably two independent lymphomas based on the timing of onset

RITX, on Rituximab treatment

§ Lymphocyte numbers in peripheral blood were measured a few months prior to death but before chemotherapy and transplant

Data assembled with assistance from Helen Su, Helen Matthews, and Benjamin Chaigne-Delalande

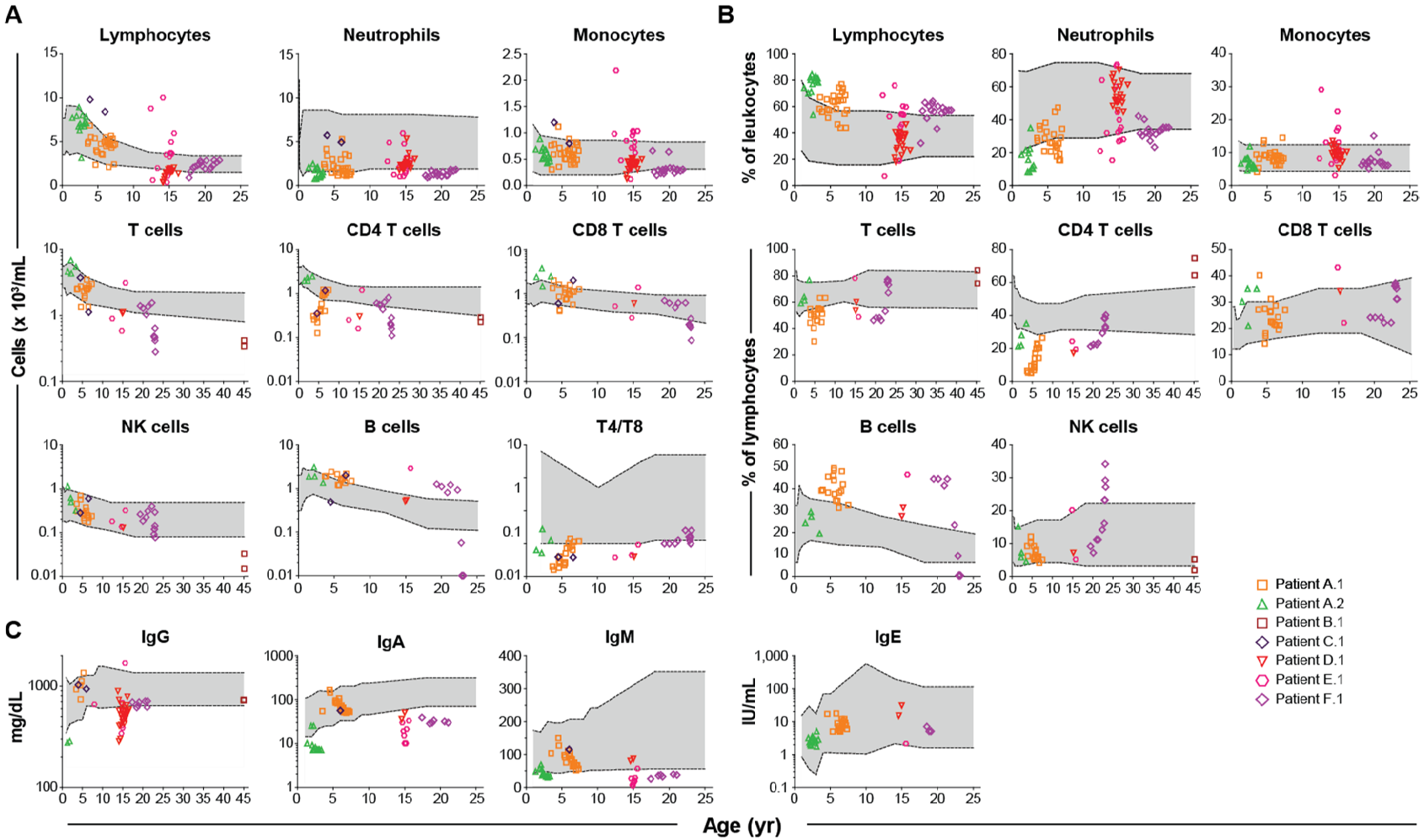
A
Lymphocytes
Neutrophils
Monocytes
T cells
CD4 T cells
CD8 T cells
NK cells
B cells
T4/T8
Cells (x 10³/mL
B
% of leukocytes
% of lymphocytes
C
IgG
IgA
IgM
IgE
mg/dL
IU/mL
Age (yr)
Patient A.1
Patient A.2
Patient B.1
Patient C.1
Patient D.1
Patient E.1
Patient F.1

Figure 2-12: Cellular and humoral abnormalities in XMEN patients

Absolute cell count (**A**) and relative percentage (**B**) of various immune cell populations and immunoglobulin levels (**C**) documented by clinical flow cytometry labs for XMEN patients during various hospital admissions. T4/T8 = CD4/CD8 T cell ratio. Shaded grey area represents the range of age-matched normal control values (10th to 90th percentiles for lymphocyte subgroups[8] and 95% confidence interval for serum immunoglobulin[9]). Data assembled with assistance from Helen Su, Helen Matthews, and Benjamin Chaigne-Delalande

2.3 Discussion

By using exome capture NGS, we have successfully identified a novel human primary immunodeficiency characterized by loss of MagT1 gene function and an increased susceptibility of developing EBV-associated lymphomas. While our initial patients were children when they came into medical attention with ICL, many of our older patients had no significant medical history prior to developing lymphoma. Very high EBV titers are detectable in some of these patients (A.1 and A.2), while others do not currently have detectable levels (C.1 and D.1). Unlike XLP and ITK deficiency, these XMEN patients do not exhibit symptoms of FIM or HLH, and their first signs of disease may be fatal systemic EBV infiltration and lymphoma. Even though deficient NKT cells or iNKT cells have been implicated in the disease pathogenesis of XLP and ITK deficiency[17,18], these cells are not deficient in XMEN patients (Gulbu Uzel, personal communication). Although none of our patients are EBV free, further screening would be necessary to determine if there are XMEN patients who develop lymphoma without EBV, as in some cases of XLP. Given that female carriers express no symptoms and affected males can survive to adulthood,

there could be a fairly substantial number of carriers in the normal population, as supported by the two unrelated females who carried the same mutation in *MAGT1* in our cohort.

Our initial XMEN patients (A.1 and A.2) have decreased staining for CD31 in the naïve $CD4^+$ T cell population, which is indicative of lower thymic output of $CD4^+$ T cells unless the $CD31^+$ population is preferentially dying faster[6,7]. Because the CD31 expression is assessed in the gated naïve $CD4^+$ T cell pool, it is not affected by expansion of the effector T cell population. Moreover, the decrease in thymic output of $CD4^+$ T cells in the two boys is probably underestimated when compared against adult normal controls since thymic output decreases with age. Given that the absolute number $CD4^+$ T cell counts is decreased in these patients, their absolute number of early thymic emigrant $CD4^+$ T cells should be diminished given their lower percentage of $CD31^+$ naïve CD4 cells. Consistent with that, all of our living XMEN patients have a low CD4:CD8 T cell ratio, and a few ICL cases suffering from EBV-associated lymphoma have been reported previously[19,20]. Interestingly, in a recent mouse model of EBV-driven lymphoma, $CD4^+$ T cells were shown to be superior to $CD8^+$ T cells and NKT cells in restricting tumor outgrowth[21]. Thus, all male patients with a decreased CD4:CD8 T cell ratio and/or persistently high EBV titers should be screened for XMEN disease.

The role of MagT1 in the immune system was never characterized prior to this study, and our initial mutation search by the traditional candidate gene approach was consequently unfruitful. Nonetheless, our unbiased searches were not straightforward either given the many limitations of each technique. In the end, the

gene was successfully found because of two key guiding principles: (1) follow the X-linked genetic model derived from the skewed lyonization data and (2) remember types of mutations that are not readily detected, especially the more deleterious ones such as deletions and splicing mutations. While exome sequencing can readily detect nonsense mutations, large DIPs and many splicing variants are not reported. Recently, it has been suggested up to 39% of loss of function variants in human genomes are frameshifting DIPs not readily detected by NGS[22]. I used a novel approach to search for large DIPs by comparing the patients' read coverage to that of the mother. This led me to identify a region with read coverage features indicative of a 10 bp deletion. Thus, developing NGS analysis tools to report such variants based on these features will help advance gene identification of rare diseases by exome sequencing. Oddly, even though we detected downregulation of *MAGT1* transcript by real-time PCR, it was not in the list of downregulated genes from the gene expression microarray. This may be due to the fact that microarray quality control analyses consider genes below detection level as not reliable for statistical analyses and do not report them. Thus, improving the analysis algorithms or the sensitivity of microarrays may advance detection of loss of expression genes in rare diseases. On the other hand, it would interesting to see if whole transcriptome sequencing would be a better alternative for this purpose as it could detect splicing and coding changes simultaneously.

MagT1 is a transmembrane protein identified in 2005 as one of two mammalian channels highly specific for Mg^{2+} transport[14,16]. It consists of 367 amino acids encoding for a signal peptide, a large N-terminal segment, four or five

transmembrane domains, and a small C-terminal tail. It shares no homology to any other known transporter except for TUSC3, a nonselective transporter for Mg^{2+} and several other divalent cations[15]. Its expression has been suggested to be ubiquitous[14,15], but the gene expression microarray in the UCSC Genome Browser database indicates elevated expressions in certain tissues, particularly in all hematopoietic cells. The skewed lyonization in the mother's T cells suggests that it may play a role in the fitness or survival of T cells during development. MagT1 has been shown to be vital to zebrafish development[15], but its physiologic function in mammals has not been investigated prior to this study. We now turn to dissecting its function in the immune system specifically in T cells and NK cells given the significant role of these cells in controlling EBV disease.

2.4 Materials and Methods

Human subject samples

All human subjects in this study provided informed consent in accordance with Helsinki principles to be enrolled in research protocols approved by the institutional review board of the National Institute of Allergy and Infectious Diseases, NIH. Normal control and patient PBMCs were isolated from whole blood by Ficoll-Paque PLUS (GE Healthcare) density gradient centrifugation, washed twice in phosphate buffered saline (PBS) and resuspended at 10^6 cells/ml in complete RPMI 1640 medium (Lonza) containing 10% fetal bovine serum (FBS), 2 mM glutamine, and penicillin and streptomycin (100 U/ml each, Invitrogen). To expand T cells for gDNA purification, PBMCs were stimulated 1 μg/ml each of anti-CD3ε and anti-CD28 monoclonal antibodies (BD Biosciences) and transferred to complete

RPMI-1640 media supplemented with 100 U/ml recombinant human interleukin 2 (rhIL-2) (R&D) after 3 days. gDNA were isolated from expanded T cells using DNeasy Blood and Tissue kit (Qiagen). Buccal swabs were processed for gDNA using the QIAamp DNA Mini kit (Qiagen).

Flow cytometry

PBMCs from patients and normal controls were stained with CD3 or CD2, CD4, CD8, CD27, CD45RO, and CD31 (BD biosciences or courtesy of D. Douek's lab) at recommended concentration for 30min. in the dark. Stained cells were washed 1-2 times and acquired on BD LSRII flow cytometer. Data analyses were performed with Flowjo software (Treestar).

Lyonization assay

Lyonization assay was adapted from a previous study[23]. Briefly, gDNA (1 μg) samples were first digested with *RsaI* (NEB) and then split into two for treatment with or without *HpaII* (NEB). Each digestion was carried out for at least 2h and heat inactivated at 65 ^{o}C for 20 min. Digested DNA was purified by QIAquick PCR purification kit (Qiagen) and PCR amplified using 6-FAM-conjugated primers for the HUMARA locus: 5'-TGCGCGAAGTGATCCAGAACC-3', 5'-TGGGCTTGGGGAGAACCATCC-3' (Fig. 2.4a). The amplified products were analyzed on a 310 Gene Analyzer (ABI) as recommended using ROX500 (ABI) as size standard.

Exome sequencing and analysis

3 ug gDNA from T cells was processed using Genomic DNA Sample Prep Kit (Illumina) for SureSelect Human X Chromosome (Agilent) target enrichment

according to manufacturer instructions. Captured DNA was subject to cluster generation using Single-Read Cluster Generation Kit v2 (Illumina) and NGS using SBS Sequencing Kit v3 (Illumina) on the Illumina Genome Analyser IIx. The data were imported into CLCbio Genomics Workbench software and aligned to the human genome reference (hg19) annotated with SNPs (130) downloaded from UCSC Genomics browser. Detection of SNPs and DIPs was performed on alignments in the software, and genes with missing coverage were identified using the targeted resequencing plug-in tool (CLCbio). Candidate genes were filtered using available filters on the software and in Excel spreadsheets. From the Illumina sequencing data, all SNPs and 1–2 bp DIPs that were not present in both brothers, not heterozygous in the mother, or that were found in her cDNA were excluded. Large DIPs (.1 kb) were screened by using comparative genomic hybridization 244K arrays (Agilent) as described previously[2]. To detect 3–1,000 bp DIPs, the targeted resequencing plug-in tool (CLCbio) was used to identify genes with missing coverage in the patients but not in the mother. SNPs and DIPs consistent with these search criteria were ruled out as common polymorphisms in the normal population by DNA sequencing in 100 normal controls.

Sanger DNA sequencing

DNA sequencing was performed as described previously[2]. *MAGT1* exons were amplified from gDNA using intronic primers flanking exons listed below (Table 2-2). All sequencing was performed using gDNA isolated from activated T cells except for the sequencing of the grandmother and great-grandmother of patient A.1 and A.2 where gDNA isolated from buccal cells was used. To make cDNA, RNA was isolated

from T cells by Trizol (Invitrogen) and RNeasy mini columns (Qiagen) and digested with amplification grade DNase I (Invitrogen) before reverse transcription with SuperScript Vilo (Invitrogen). *MAGT1* sequence including exons 6-10 was amplified from cDNA using these primers: 5'-TTCCTGCAAAAGGGAAACC-3' and 5'-GTCTTGCTGAGGGCTAGACG-3'.

Table 2-2: Primers for amplifying *MAGT1* exons

Exon	5' primer	3' primer
1	TTAGCGGACCAATGAAAACG	TCTCACGAATTCCACAACTCC
2	AATTATCATCCAGCCCAACTACC	CCTTCTGGGATTGAGAAATGG
3	CCTGCTATTGCTTGCTTGG	GCAATCCCATTTAATGTCTTATAGC
4	CACTTTCCTTGGGCAAACC	GCCTCCCAGTAAGATTCAAAGG
5	GGATCATTTTTCCGAAAGTAACC	TTTCCTCAGGTAAGAAATAAAATGC
6	TTATCGAATTGTGATCCTTGG	CTGGCACTGTTCTCACAGG
7	ACCCGGAGTATGTCACATGG	AACTCCACTATTCTCCCAAATCC
8	CAATAACTGAATGTCCAGACAGG	AGTGGTGGAATGTTTCATGC
9	AAGGGGAAGGCAGATTCC	AAAGCAATATCAACTCTAATCATTCC
10	TGATACCCAAAGATTATCATGTACG	TTTCCCCATCTTTGGATAAGG

Real-time PCR

MAGT1 mRNA levels were assessed using cDNA from T cells and Taqman Gene Expression Assays (ABI): Hs00259564 (probe 1) and Hs00794271 (probe 2). Expression levels were normalized to simultaneous duplicate assessments of hypoxanthine-guanine phosphoribosyltransferase (*HPRT*) mRNA using Taqman Gene Expression Assay (ABI): Hs1003267. Reaction mixes were amplified for 40 cycles (95 ^{o}C for 15 s, 60 ^{o}C for 1 min) using PRISM 7900HT Sequence Detection System (Applied Biosystems).

Immunoblotting

10^7 expanded T cells were pelleted and immediately lysed in 1% Triton X-100, 1% NP40, 50 mM Tris pH 8, 150 mM NaCl, 20 mM EDTA, 1 mM Na_3VO_4, 1 mM NaF, phosphatase inhibitor cocktail (Sigma) and complete protease inhibitor cocktail (Roche). Protein concentration was quantitated by BCA assay (Pierce). 30μg of cell lysates were separated on 4-20% gradient Tris-Glycine SDS–PAGE gel (Invitrogen) and transferred onto a nitrocellulose membrane (Biorad). Membrane was blocked with 5% non- fat dry milk for 15 min. before incubating with 1:1000 anti-MAGT1 polyclonal antibody (Proteintech) overnight, all in PBS containing 0.1% Tween-20 (wash buffer). Membranes were washed at least 3x before incubation with 1:10000 horseradish peroxidase (HRP)-conjugated anti-rabbit Ig antibody (Southern Biotechnology) for 1 hour, washed 3x, and detected with Supersignal West enhanced chemiluminescence (ECL) substrates (Pierce). For loading control, membranes were subsequently blotted with 1:30,000 monoclonal anti-β-

Actin−Peroxidase Conjugate antibody (Sigma-Aldrich) for 15 min. before exposure with ECL.

Immunofluorescence

Expanded T cells were dropped on poly-L-lysine coated slides and fixed with 3% paraformaldehyde in PBS, permeabilized with 0.05% Triton X-100 for 3 min at room temperature, and blocked with PBS containing 10% FBS. All slides were stained with anti-MAGT1 polyclonal antibody in 0.5% BSA-PBS for 45 min at room temperature. Slides were washed and incubated with an Alexa 488-conjugated donkey anti-rabbit antibodies (Invitrogen) for 45 min. Nuclei were stained with Hoechst 33342 (50 ng/ml, Invitrogen). Slides were washed in PBS, rinsed, and mounted with a coverslip using Fluoromount-G (Southern Biotechnology). All images were collected on a Leica TCS-NT/SP5 con- focal microscope (Leica Microsystems) using a 633 oil immersion objective NA 1.32, 'zoom X'.

2.5 References

1. Oliveira, J.B. *et al.* NRAS mutation causes a human autoimmune lymphoproliferative syndrome. *Proc Natl Acad Sci U S A* **104**, 8953-8958 (2007).

2. Zhang, Q. *et al.* Combined immunodeficiency associated with DOCK8 mutations. *N Engl J Med* **361**, 2046-2055 (2009).

3. Gilissen, C., Hoischen, A., Brunner, H.G. & Veltman, J. a Disease gene identification strategies for exome sequencing. *European journal of human genetics : EJHG* 1-8 (2012).doi:10.1038/ejhg.2011.258

4. Bamshad, M.J. *et al.* Exome sequencing as a tool for Mendelian disease gene discovery. *Nature Reviews Genetics* **12**, 745-755 (2011).

5. Ng, S.B., Nickerson, D. a, Bamshad, M.J. & Shendure, J. Massively parallel sequencing and rare disease. *Human molecular genetics* **19**, R119-24 (2010).

6. Junge, S. *et al.* Correlation between recent thymic emigrants and CD31+ (PECAM-1) CD4+ T cells in normal individuals during aging and in lymphopenic children. *Eur J Immunol* **37**, 3270-3280 (2007).

7. Kohler, S. & Thiel, A. Life after the thymus: CD31+ and CD31- human naive CD4+ T-cell subsets. *Blood* **113**, 769-774 (2009).

8. Shearer, W.T. *et al.* Lymphocyte subsets in healthy children from birth through 18 years of age: the Pediatric AIDS Clinical Trials Group P1009 study. *J Allergy Clin Immunol* **112**, 973-980 (2003).

9. Jason W Custer, R.E.R. *The Harriet Lane handbook: a manual for pediatric house officers.* (Elsevier Mosby: Philadelphia, 2009).

10. Wengler, G.S. *et al.* A PCR-based non-radioactive X-chromosome inactivation assay for genetic counseling in X-linked primary immunodeficiencies. *Life Sci* **61**, 1405-1411 (1997).

11. Fearon, E.R., Winkelstein, J.A., Civin, C.I., Pardoll, D.M. & Vogelstein, B. Carrier detection in X-linked agammaglobulinemia by analysis of X-chromosome inactivation. *N Engl J Med* 427-31 (1987).

12. Puck, J.M., Nussbaum, R.L. & Conley, M.E. Carrier detection in X-linked severe combined immunodeficiency based on patterns of X chromosome inactivation. *The Journal of clinical investigation* **79**, 1395-400 (1987).

13. Filipovich, A.H., Zhang, K., Snow, A.L. & Marsh, R. a X-linked lymphoproliferative syndromes: brothers or distant cousins? *Blood* **116**, 3398-408 (2010).

14. Goytain, A. & Quamme, G.A. Identification and characterization of a novel mammalian Mg2+ transporter with channel-like properties. *BMC Genomics* **6**, 48 (2005).

15. Zhou, H. & Clapham, D.E. Mammalian MagT1 and TUSC3 are required for cellular magnesium uptake and vertebrate embryonic development. *Proc Natl Acad Sci U S A* **106**, 15750-15755 (2009).

16. Quamme, G.A. Molecular identification of ancient and modern mammalian magnesium transporters. *Am J Physiol Cell Physiol* **298**, C407-29 (2010).

17. Latour, S. Natural killer T cells and X-linked lymphoproliferative syndrome. *Current opinion in allergy and clinical immunology* **7**, 510-4 (2007).

18. Linka, R.M. *et al.* Germline Mutations within the IL2-Inducible T Cell Kinase Impede T Cell Differentiation or Survival, Cause Protein Destabilisation, Loss of Membrane Recruitment and Lead to Severe EBV Lymphoproliferation. *American Society of Hematology Meeting* (2010).at http://ash.confex.com/ash/2010/webprogram/Paper32792.html

19. Kojima, M. *et al.* EBV(+) B-cell lymphoproliferative disorder associated with subsequent development of Burkitt lymphoma in a patient with idiopathic CD4(+) T-lymphocytopenia. *J Clin Exp Hematop* **48**, 55-59 (2008).

20. Kanno, H. *et al.* Epstein - Barr virus-positive malignant lymphoma of salivary gland developing in an infant with selective depletion of CD4-positive lymphocytes. *Leuk Lymphoma* **48**, 183-186 (2007).

21. Zhang, B. *et al.* Immune Surveillance and Therapy of Lymphomas Driven by Epstein-Barr Virus Protein LMP1 in a Mouse Model. *Cell* **148**, 739-751 (2012).

22. MacArthur, D.G. *et al.* A Systematic Survey of Loss-of-Function Variants in Human Protein-Coding Genes. *Science* **335**, 823-828 (2012).

23. Allen, R.C., Zoghbi, H.Y., Moseley, a B., Rosenblatt, H.M. & Belmont, J.W. Methylation of HpaII and HhaI sites near the polymorphic CAG repeat in the human androgen-receptor gene correlates with X chromosome inactivation. *American journal of human genetics* **51**, 1229-39 (1992).

Chapter 3 : Role of MagT1 in T cell activation

3.1 Introduction

Mg^{2+} is the most abundant divalent cation in mammalian cells and is an essential cofactor for ATP, nucleic acids, membranes and numerous enzymes in animals and plants[1–3]. It has long been considered to be a passive cofactor or a slow chronic regulator due to its high abundance and the low chemical concentration difference across the plasma membrane compared to Ca^{2+} [4]. Ca^{2+} is a well-established second messenger with transient influxes promoted by the 10, 000 fold difference between free intracellular $[Ca^{2+}]_i$ (0.1 μM) and extracellular $[Ca^{2+}]_e$ (1 mM)[5]. Whether Mg^{2+} can serve as a second messenger in intracellular signaling as well is controversial[6–10]. The gradient between $[Mg^{2+}]_i$ (0.2-1 mM) and $[Mg^{2+}]_e$ (1-2 mM) less than 10. Hence, detecting small Mg^{2+} flutuations over the high bound intracellular magnesium background (10-30 mM) has been difficult, especially given the limited sensitivity and specificity of Mg^{2+} detection probes. Nevertheless, the intracellular magnesium concentration is strictly maintained ~100-fold lower than its electrochemical equilibrium potential, which theoretically allows for regulated Mg^{2+} influxes[8,11]. Mg^{2+} has been found to enhance lymphocyte activation in suboptimal Ca^{2+} concentrations by phytohemagglutinin (PHA) but not ionomycin[12–14]. Since ionomycin bypasses proximal TCR signals, optimal T cell activation could require a magnesium-generated process upstream of Ca^{2+} signaling. Mg^{2+} sensitive probes have revealed changes in $[Mg^{2+}]_i$ in lymphocytes following lectin stimulation[15,16]. Nevertheless, whether extracellular Mg^{2+} promotes cellular activation signals is unknown.

The selective persistence of viral rather than bacterial infection history in the XMEN patients suggested a potential deficiency in the T cell rather than B cell or

myeloid compartment[17]. PIDs with mutations in TCR signaling molecules illustrate the importance of this pathway to T lymphocyte selection during ontogeny and for peripheral responses against foreign pathogens[18]. Mutations in ZAP-70 tyrosine kinase in SCID patients illustrated its role in thymic development of $CD8^+$ T cells and peripheral T cell activation[19,20]. Likewise, genetic defects in SCID patients in ORAI1 revealed that it was a critical store-operated Ca^{2+} channel[21]. Thus, I hypothesized that MagT1 could play role in the TCR signaling pathway and provide an explanation for the synergistic effect between Ca^{2+} and Mg^{2+} observed more than 30 years ago. Indeed, this hypothesis led us to uncover a second messenger role for Mg^{2+} required for temporal orchestration of PLCγ1 activation by ITK.

3.2 Results

XMEN patients exhibit a proximal T cell activation defect

Assessment of primary T cell activation in total PBMCs through the TCR revealed a T cell activation defect in XMEN patients exhibited by decreased upregulation of activation markers (CD69, CD25, CD95, and CTLA-4) on both $CD4^+$ and $CD8^+$ T cells upon soluble OKT3 (agonistic αCD3) stimulation (Figure 3-1A, Table 3.1). Nevertheless, the patient T cells were capable of expanding in long-term culture like the normal cells (data not shown). However, restimulation of these expanded patient T cells with OKT3 to assess early TCR signaling events also revealed a profound defect in the induction of NF-κB and NFAT nuclear translocation (Figure 3-1B-C). By contrast, the patients' T cells were fully activated by the second messenger inducers phorbol 12-myristate 13-acetate and ionomycin (PMA/Iono), implying a proximal TCR activation defect (Figure 3-1A-C). Consistent

with the lack of bacterial infections in XMEN disease, these patients showed no defect in B cell receptor (BCR) or Toll-like receptor (TLR) stimulation of B cells (Figure 3-2-B).

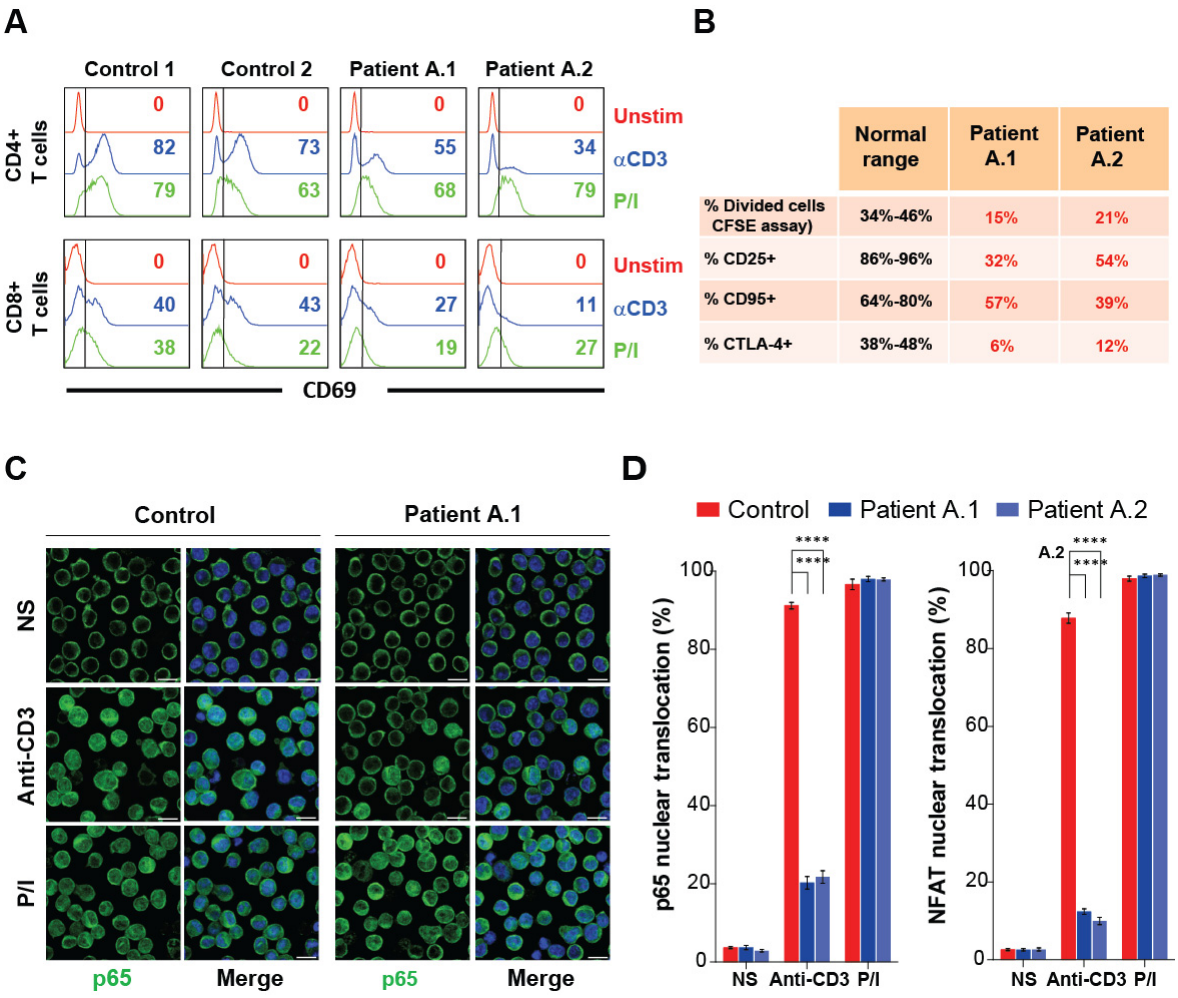

Figure 3-1: Patients have a proximal TCR activation defect

(**A**) Flow cytometry histograms of CD69 expression in CD4+ (top) and CD8+ (bottom) T cells after 12 h stimulation with anti-CD3 (blue), PMA/ Ionomycin (P/I, green) or unstimulated (Unstim, red). Numbers represent percent cells in indicated gates. (**B**) Percent cells positive for the listed activation markers in the CD4+ T cell gate after 72h stimulation with anti-CD3 as assessed by flow cytometry as in (**A**). Carboxyfluorescein succinimidyl ester (CFSE) proliferation assay was analyzed by the Proliferation function on FlowJo. (**C**) Confocal imaging of p65 nuclear translocation after anti-CD3 or

P/I stimulation (scale bar: 10 μm). (D) Percent cells with p65 (left) and NFAT (right) nuclear translocation. Error bars represent s.e.m. (n=3), **** (P<0.0001). Benjamin Chaigne-Delalande performed stimulations, staining and imaging for (**C**) and (**D**).

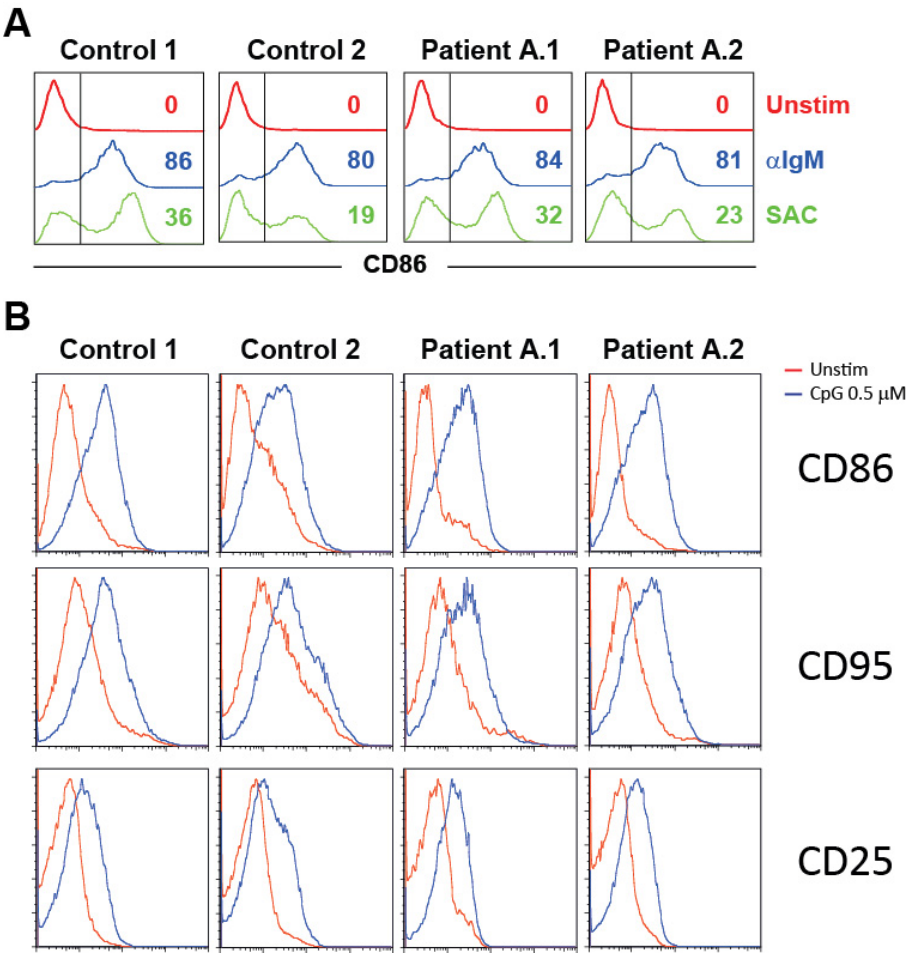

Figure 3-2: Patient B cells do not have an activation defect.

(**A**) Flow cytometry histograms of CD86 surface expression in purified B cells after 72 hours of stimulation with anti-IgM, staphylococcus aureus cowan (SAC) or unstimulated (Unstim). (**B**) flow cytometry histograms of CD86, CD95, and CD25 expression in purified B cells with (CpG 0.5 μM) or without (Unstim) CpG oligodeoxynucleotide (ODN 2395) stimulation for 72h.

TCR-induced Mg^{2+} and Ca^{2+} influx defects in patients

Given that the role of MagT1 in mammals is not well understood except for its function as a Mg^{2+}-selective transporter[22,23], we hypothesize MagT1 may regulate total intracellular magnesium and/or a transient Mg^{2+} flux to affect T cell activation. We first measured ion uptake by sequential addition of Ca^{2+} and Mg^{2+} in normal and patients' lymphocytes using fluorescent probes sensitive for Ca^{2+} (fluo3-AM and Fura Red-AM) or Mg^{2+} (MagFluo4-AM), which exhibited no detectable cross-reactivity (Figure 3-3A). Equal probe loading of the cells was demonstrated by the maximal flux induction with the ionophore calcimycin, and specificity of the flux signals for divalent cation binding was shown by quenching the signals with the chelator ethylenediaminetetraacetic acid (EDTA). Initial experiments showed a lower basal level of free Mg^{2+} and defective passive Mg^{2+} influx in patients, whereas there were no defects for Ca^{2+} (Figure 3-3A). By contrast, the total Ca^{2+} and Mg^{2+} in the patients' $CD4^+$ and $CD8^+$ T cells determined by inductively coupled plasma mass spectrometry were normal, indicating that MagT1 deficiency chiefly affects free Mg^{2+} and that bound Mg^{2+} and the general metabolic processes requiring it should be unaffected (Figure 3-3B). The reliability of these measurements is also indicated by the lack of a difference in the sulfur content of these cells, which is known to be highly stable.

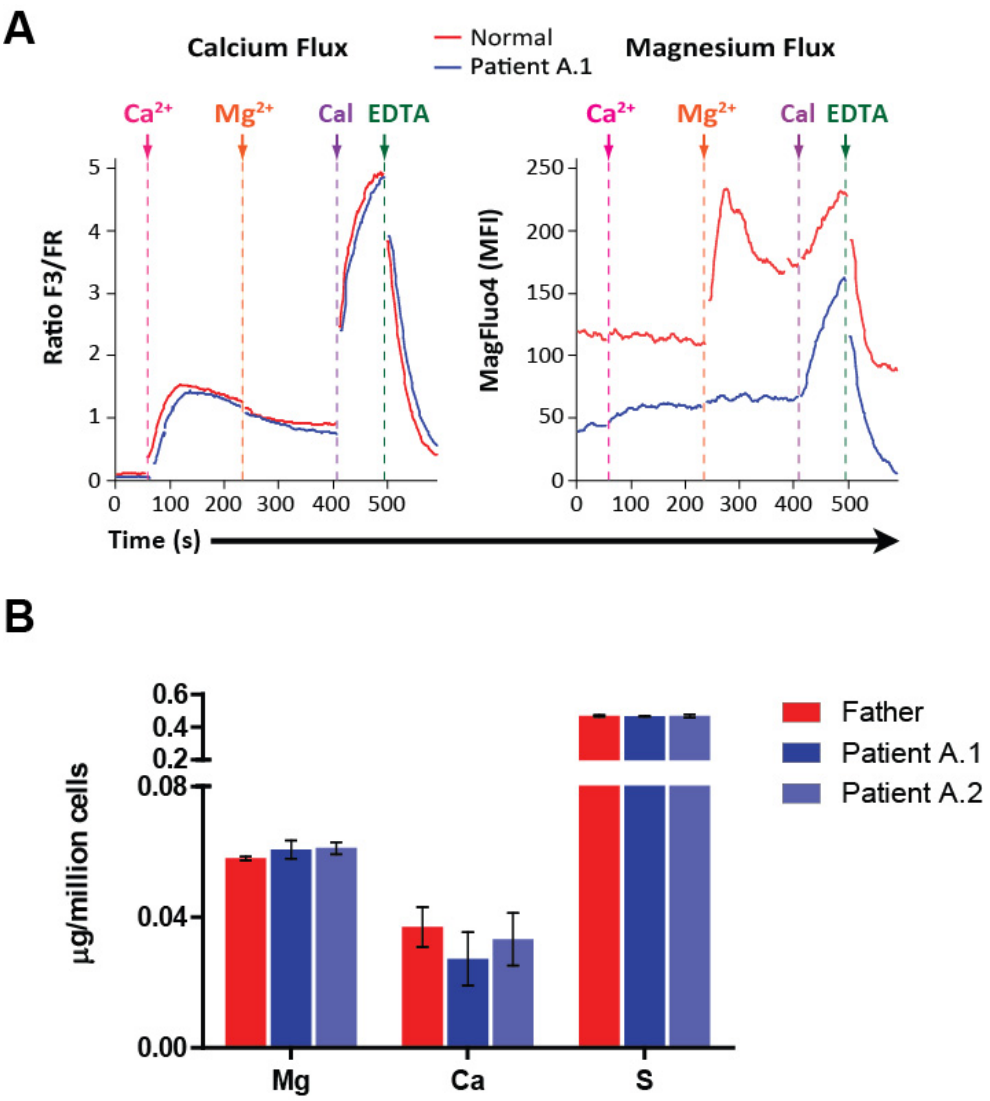

Figure 3-3: Patient cells have defective Mg^{2+} uptake but normal total magnesium level

(**A**) Flow cytometry kinetic profiles of Ca^{2+} (left panel) and Mg^{2+} (right panel) uptake in T cells from normal donor and patient T cells loaded with either Fluo3-AM/Fura Red-AM or Magfluo4-AM upon sequential addition of 1 mM Ca^{2+}, 2 mM Mg^{2+}, 5mM calcimycin (Cal), and 2 mM EDTA. (**B**) Total magnesium (Mg), calcium (Ca), and sulfur (S) levels measured in activated $CD8^+$ T cells by inductively coupled plasma mass spectroscopy[24]. Error bars represent s.e.m. (n=3). Similar results were obtained for $CD4^+$ T cells. Benjamin Chaigne-Delalande performed flux assays for (**A**) and David Killilea performed mass spectrometry for (**B**)

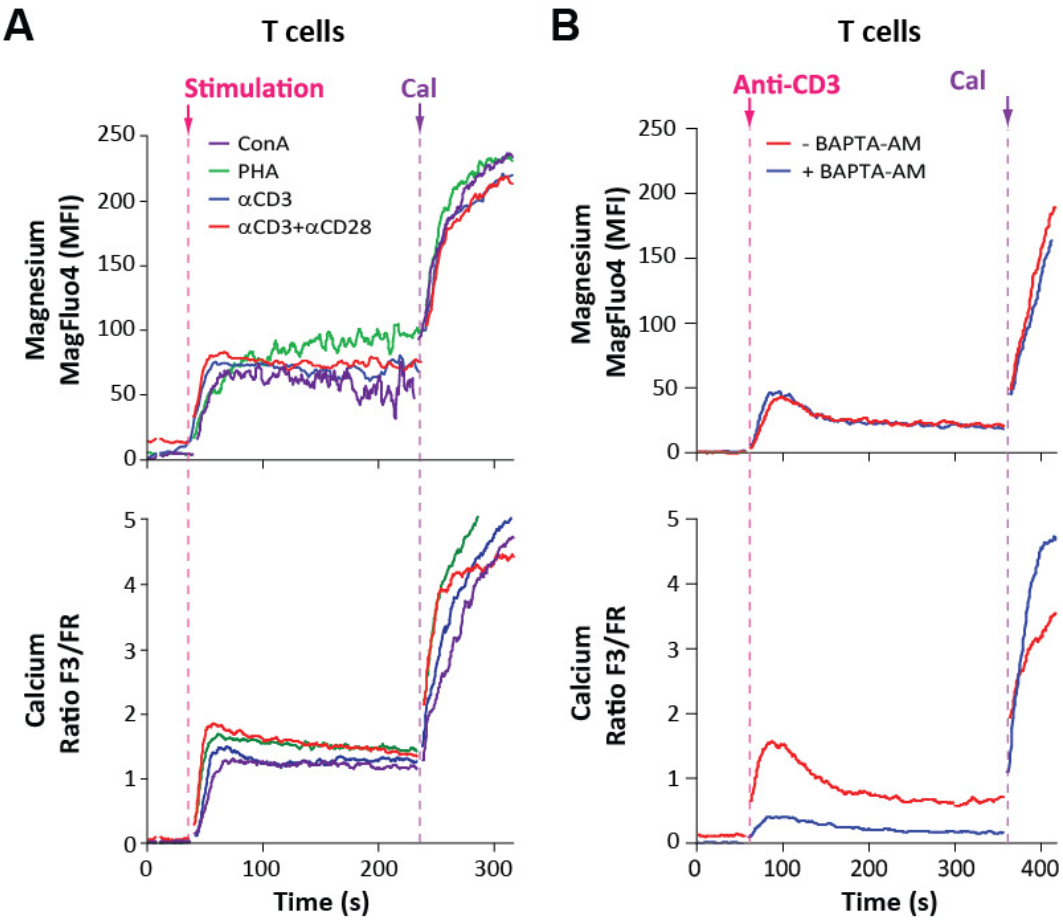

Figure 3-4: TCR stimulation induces Mg^{2+} flux coincident with Ca^{2+} flux.

Flow cytometry kinetic profiles of Mg^{2+} (upper panels) and Ca^{2+} (lower panels) flux in: (**A**) normal PBMCs stimulated with 10μg/mL concanavalin A (ConA), 10μg/mL phytohemagglutinin (PHA), 1μg/mL αCD3, or 1μg/mL αCD3 and 1μg/mL αCD28 or (**B**) normal T cells pre-incubated with or without 5μM BAPTA-AM before stimulation with 1μg/mL anti-CD3. Benjamin Chaigne-Delalande performed flux assays in (**A**) and (**B**).

We next examined whether various TCR stimuli would affect free Mg^{2+} transport. We observed a robust transient Mg^{2+} influx together with the well-documented Ca^{2+} influx in normal T cells stimulated with various TCR agonists (Figure 3-4A). The apparent Mg^{2+} influx was not due to cross-detection of the Ca^{2+} influx because the specific Ca^{2+} chelator 1,2- bis(o-aminophenoxy)ethane-N,N,N',N'-tetraacetic acid acetoxymethyl ester (BAPTA-AM) abolished the Ca^{2+} fluorescence but not the Mg^{2+} fluorescence (Figure 3-4B). The Mg^{2+} influx was not detectable in the patients' T cells even with as much as 5 μg/ml αCD3 stimulation. (Figure 3-5A-B). Surprisingly, we also found that the Ca^{2+} influx was severely compromised in the patient T cells across a broad dose range of αCD3 (Figure 3-5A-B). The TCR-induced Mg^{2+} influx was selective since stimulation of T cells with secondary lymphoid tissue chemokine (SLC/CXCL21), Fas-ligand (FasL), and tumor necrosis factor-α (TNFα) caused no Mg^{2+} influx and the Ca^{2+} influxes induced by SLC and FasL were normal in the patient cells (Figure 3-6A). Also, no Mg^{2+} influx was discernible in B lymphocytes following anti-IgM and anti-CD40 stimulation, and the ensuing Ca^{2+} influx was not diminished in patient B cells (Figure 3-6B). Although the patient B cells exhibited reduced basal free Mg^{2+}, their B cell activation was normal (Figure 3-2A-B). This provided a strong argument that the impairment of function in T cells was not due to an impairment of the co-factor function mediated by bound Mg^{2+}.

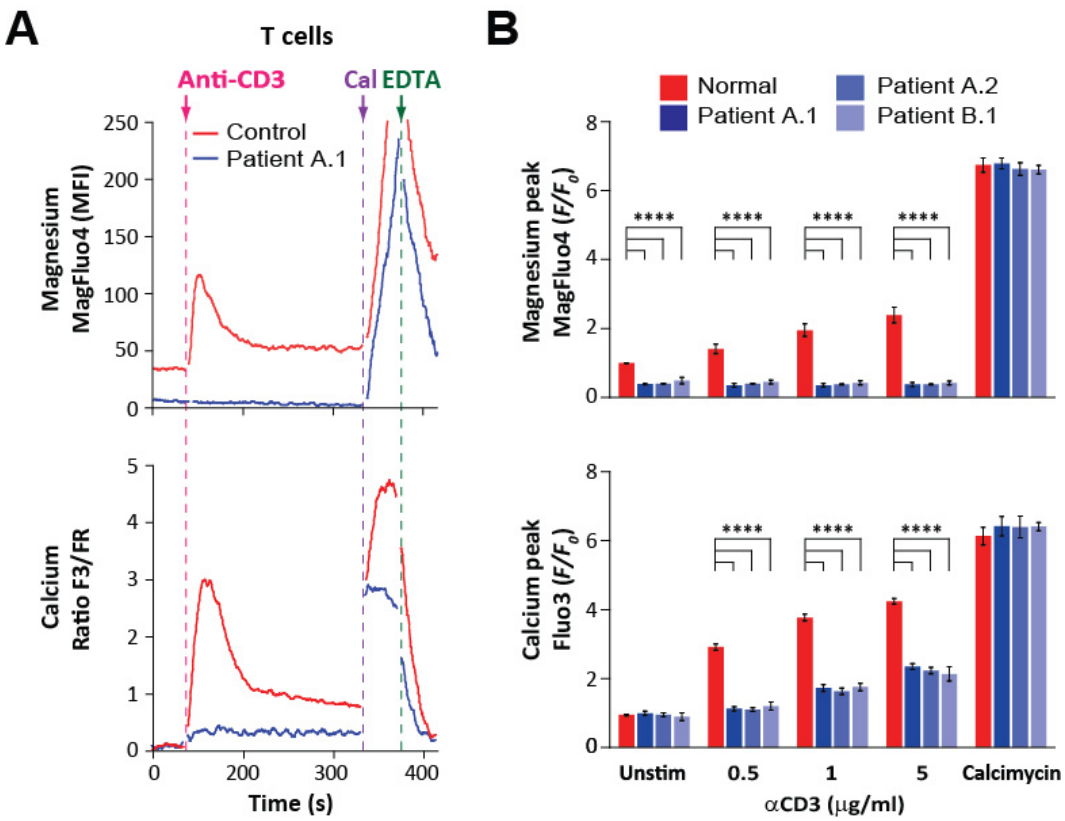

Figure 3-5: Patients have defective Mg^{2+} and Ca^{2+} fluxes upon TCR stimulation.

(**A**) Flow cytometry kinetic profiles of Mg^{2+} (upper panels) and Ca^{2+} (lower panels) fluxes in T cells sequentially stimulated with 1μg/mL αCD3, 10μM Cal, and 2mM EDTA. (**B**) Peak value of fluxes in T cells upon stimulation with indicated αCD3 concentrations. Error bars represent s.e.m. (n=3), **** (P<0.0001). Benjamin Chaigne-Delalande performed flux assays in (**A**) and (**B**).

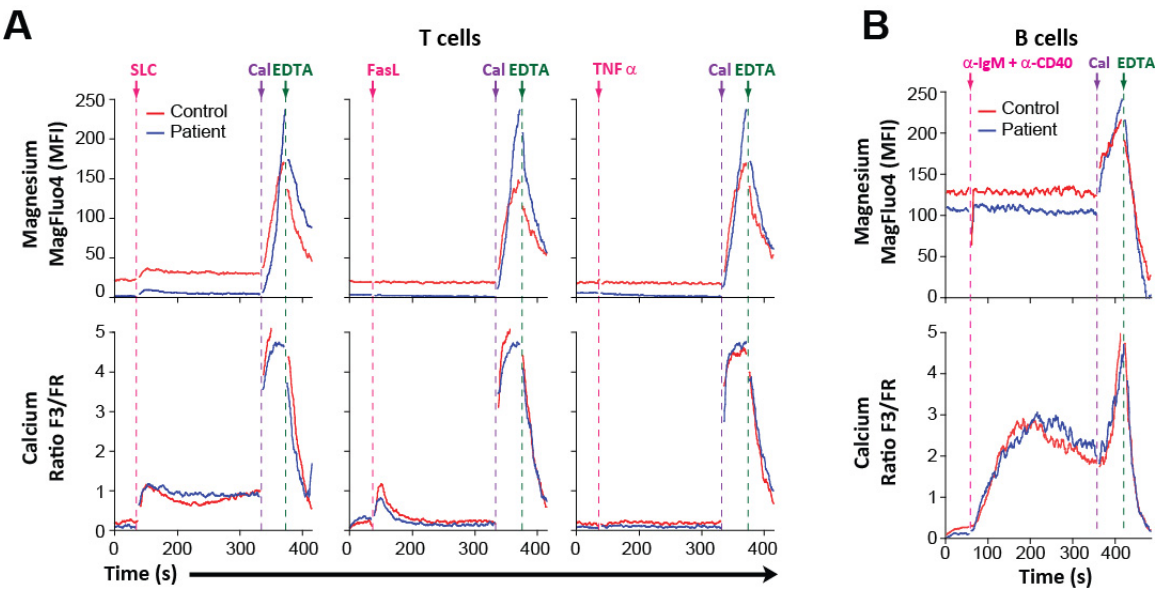

Figure 3-6: MagT1-mediated Mg^{2+} flux is specific to TCR stimulation.

Flow cytometry kinetic profiles of Mg^{2+} (upper panels) and Ca^{2+} (lower panels) fluxes in: (A) activated T cells from normal control (red) or patient A.1 (blue) stimulated with SLC/CCL21 (100 ng/ml), FasL (1 μg/ml) or TNFα (50 ng/ml) (B) B cells from normal control or patient A.1 stimulated with anti-IgM (30 μg/ml) and anti-CD40 (1 μg/ml). Benjamin Chaigne-Delalande performed flux assays in (A) and (B)

We then tested the hypothesis that the defective Ca^{2+} influx in the patients was secondary to the loss of the Mg^{2+} influx. We first explored the relationship between the TCR stimulated influxes in normal T cells by modulating $[Mg^{2+}]_e$ and $[Ca^{2+}]_e$. Both Mg^{2+} and Ca^{2+} influxes were optimal when $[Mg^{2+}]_e$ and $[Ca^{2+}]_e$ = 1 mM, respectively, but abolished when $[Mg^{2+}]_e$ and $[Ca^{2+}]_e$ = 0, respectively (Figure 3-7A). Moreover, when $[Mg^{2+}]_e$ = 0, the Ca^{2+} influx was decreased, but when $[Ca^{2+}]_e$ = 0, the Mg^{2+} influx was minimally affected (Figure 3-7A). These results show that the TCR-induced Ca^{2+} influx is partially dependent on $[Mg^{2+}]_e$. Thus, we infer that the Ca^{2+}

influx defect in T cells associated with MagT1 deficiency is secondary to the loss of the TCR-stimulated Mg^{2+} influx. Conversely, when $[Mg^{2+}]_e = 0$, the Ca^{2+} influx in B cells after the BCR stimulation is normal, which is consistent with the absence of BCR-induced Mg^{2+} influxes (Figure 3-7B). Moreover, the loss of the TCR-induced Ca^{2+} influx in the absence of extracellular Mg^{2+} is not likely to be due to a deficiency in Mg^{2+} as a cofactor required for ATP-dependent processes since B cells had no comparable defect. This is underscored by the fact that both B and T cells from the MagT1 deficient patients had the same partial reduction in the free $[Mg^{2+}]_i$, but only the latter exhibited functional defects in antigen receptor signaling.

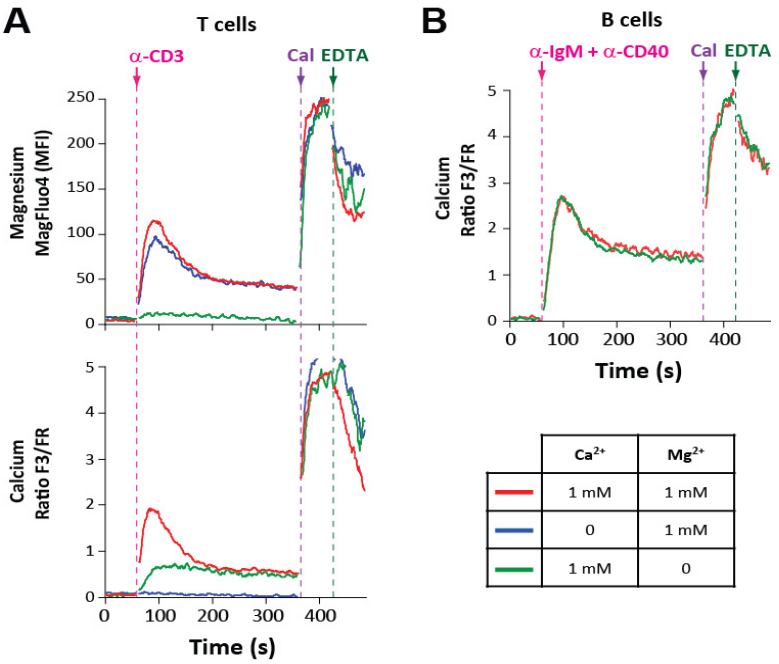

Figure 3-7: TCR-induced Ca^{2+} flux depends on the Mg^{2+} flux but not vice versa.

Flow cytometry kinetic profiles of Mg^{2+} (upper panel) and Ca^{2+} (lower panel) fluxes in: (**A**) normal T cells or (**B**) normal B cells stimulated as in figure 3.5a in the presence of extracellular Mg^{2+} and/or Ca^{2+}. Benjamin Chaigne-Delalande performed all flux assays in (**A**) and (**B**)

Knockdown and reconstitution of MagT1

To demonstrate that decreased MagT1 expression can account for the immunological and signaling defects observed in the patients, we knocked down MagT1 in normal human T cells by transient small interfering RNA (siRNA) transfections. We found that the TCR-stimulated Mg^{2+} and Ca^{2+} influxes were decreased in proportion with the degree of MagT1 mRNA knockdown (Figure 3-8A-B). Similar to the patients' T cell phenotype, MagT1 knockdown impeded TCR-induced p65 nuclear translocation (Figure 3-8C-D). These results verify that MagT1 is necessary for normal T cell activation.

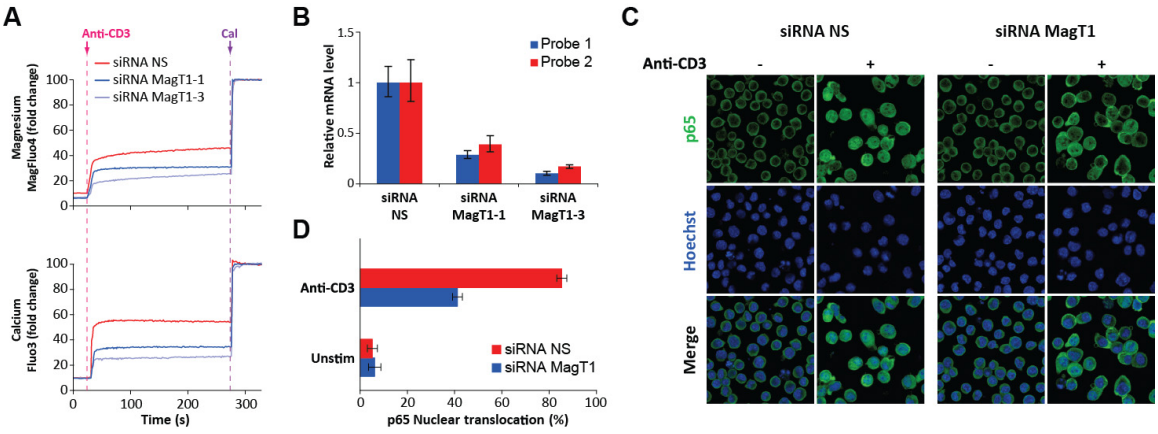

Figure 3-8: MagT1 knockdown recapitulates TCR signaling defects.

(**A**) Fluorimetric kinetic profiles of Mg^{2+} (upper panel) and Ca^{2+} (lower panel) fluxes in normal T cells transfected with non-specific (NS) or MagT1-specific siRNAs. (**B**) RT-PCR assessing the efficiency of *MAGT1* mRNA knockdown in transfected T cells used in (**A**). (**C**) Confocal imaging of p65 nuclear translocation in transfected cells after anti-CD3 (1 μg/ml) stimulation. Nuclei are counterstained with Hoechst 33342. (Scale bar: 10 μm). (**D**) Percent of cells with nuclear p65 after anti-CD3 stimulation in transfected cells. Error bars represent s.e.m. (n=3). Benjamin Chaigne-Delalande

performed flux assays in (**A**) as well as stimulations, staining, and imaging for (C) and (D). Chryssa Kanellopoulou performed real-time assays for (**B**).

To determine whether MagT1 deficiency is sufficient to explain the patients' functional defects, we reconstituted MagT1 expression by lentiviral transduction of patient T cells. Positively transduced cells marked by a coexpressed fluorescent marker (mCherry) were examined by live cell confocal imaging of the influxes. We found that expressing wild type MagT1 in the patients' T cells restored a TCR-stimulated Mg^{2+} influx (Figure 3-9A). MagT1 restoration also improved the TCR-stimulated Ca^{2+} influx, thereby validating our conjecture that it is contingent upon the Mg^{2+} influx (Figure 3-9A). The expression of MagT1 also augmented other activation events of the patients' T cells, such as TCR-induced CD69 upregulation (Figure 3-9B). Thus, MagT1 is necessary and sufficient for the Mg^{2+} influx required for optimal T cell activation, and MagT1 deficiency is the proximate cause of the T cell activation defect in this PID.

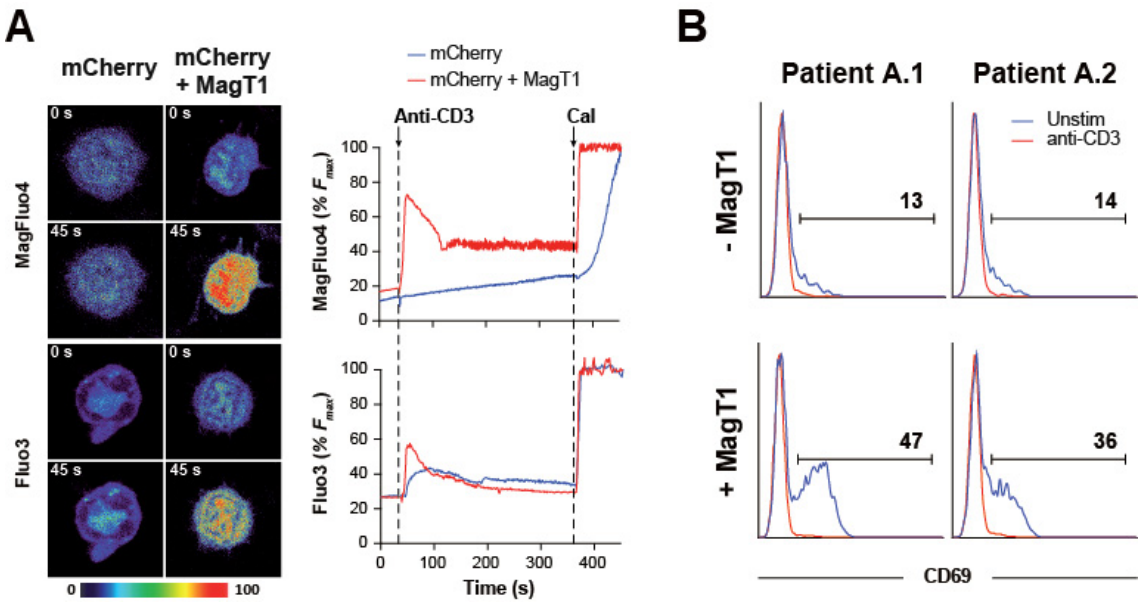

Figure 3-9: MagT1 reconstitution in patient cells rescues TCR activation.

(**A**) Time-lapse imaging (left, s = sec) and cytometric graph (right) of Mg^{2+} (upper) and Ca^{2+} (lower) flux in T cells transduced with lentiviruses expressing mCherry or mCherry + MagT1. (**B**) Flow cytometry histograms of CD69 expression on gated $CD4^+$ T cells from anti-CD3 (1 μg/ml) stimulated or unstimulated (Unstim) PBMCs transduced with lentiviruses expressing MagT1 or not. Percent cells $CD69^+$ are shown for the indicated gates. Benjamin Chaigne-Delalande performed flux assays in (**A**).

Loss of MagT1 impairs PLCγ1 activation and ITK function

To understand the molecular mechanism of the Ca^{2+} influx defect observed in MagT1- deficient patients, we examined proximal TCR signaling components (Figure 2-10D). TCR engagement causes clustering and Lck-mediated tyrosine phosphorylation of the CD3ζ chain and the subsequent recruitment of ZAP-70, which phosphorylates the scaffold proteins Linker of Activated T cells (LAT) and Src homology 2 (SH2) domain-containing leukocyte protein of 76 kDa (SLP76)[25,26].

These phosphorylated scaffolds then bind ITK, which activates PLCγ1 and thereby generates inositol triphosphate (IP_3) and diacylglycerol (DAG) as second messengers to trigger Ca^{2+} mobilization and protein kinase C-θ (PKC-θ) activation, respectively. The Ca^{2+} influx modulates the protein phosphatase calcineurin, which together with PKC θ, activates downstream transcription factors such as NF-κB and NFAT[27]. We found that TCR cluster formation and LAT and PLCγ1 recruitment to these clusters were intact in patient T cells after αCD3 stimulation (Figure 2-10A). Moreover, early TCR activation events including the activation of Lck, CD3ζ, ZAP-70, and LAT induced by TCR ligation were normal in the patient T cells (Figure 2-10B). Again, this normal series of early activation events excludes a general defect in Mg^{2+} as a co-factor for ATP-requiring processes accounting for the TCR signaling defects in MagT1 deficient T cells. By contrast, PLCγ1 phosphorylation was markedly delayed by almost one hour in the patient T cells compared to healthy control T cells (Figure 2-10B). Consistent with the delayed activation of PLCγ1, the activating phosphorylation of PKC θ and IP_3 generation downstream of PLCγ1 were comparably and significantly delayed (Figure 2-10B-C). On the other hand, we found that TCR signaling events that do not require PLCγ1 such as the phosphorylation of the mitogen activated protein kinases (MAPKs) p38 and extracellular signal regulated kinase 1/2 (Erk1/2) were intact in the patient T cells (Figure 2-10B).

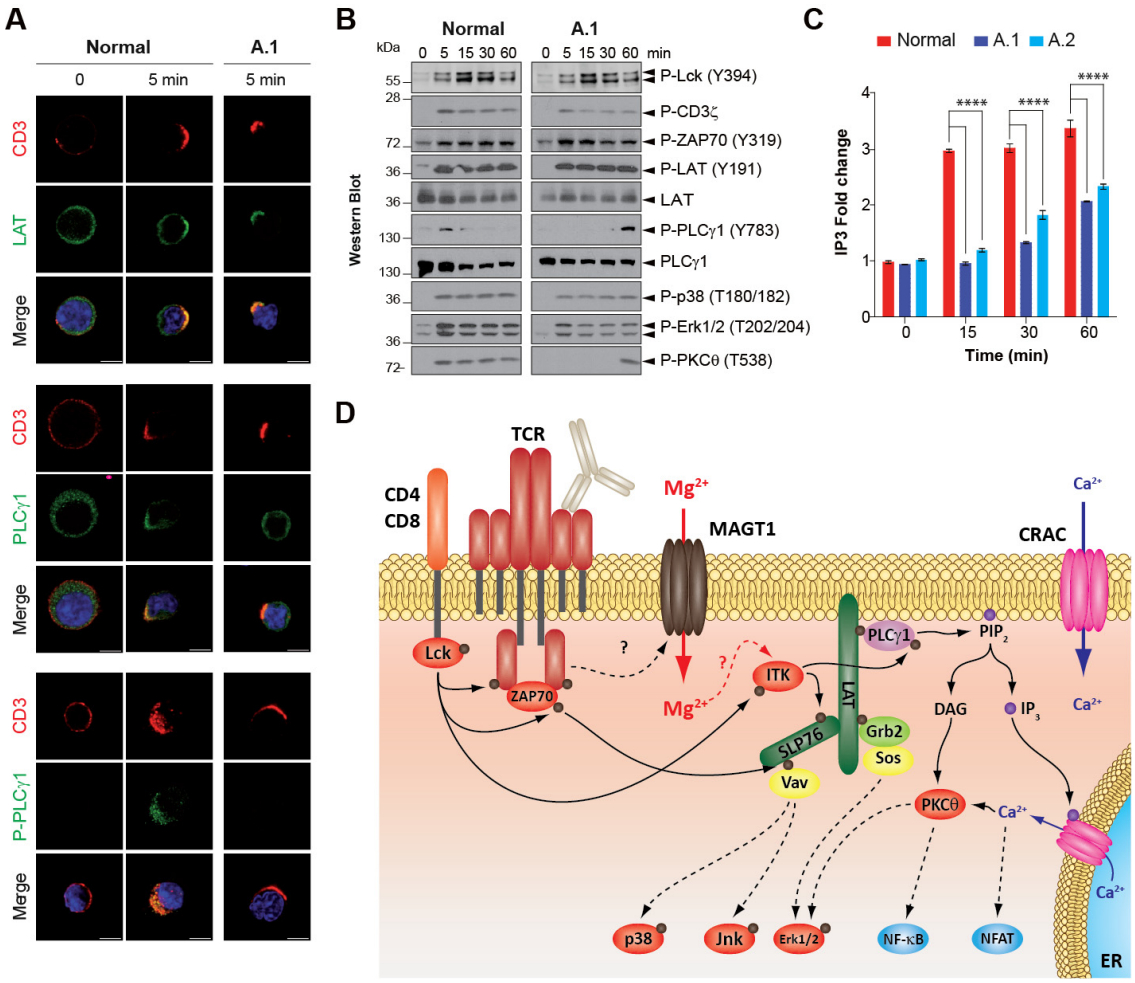

Figure 2-10: MagT1 deficiency impairs PLCγ1 activation upon TCR stimulation.

(**A**) Confocal images of TCR clustering induced by αCD3 stimulation on T cells. (Scale bar: 5 μm). (**B**) Immunoblot of phosphoproteins and (**C**) quantification of cellular IP_3 level in T cells stimulated with αCD3 for indicated times by enzyme-linked immunosorbent assays (ELISAs). Error bars represent s.e.m. (n=3). ****(P<0.0001). (**D**) Hypothetical schematic depicting how the MagT1 mediated Mg^{2+} influx participates in TCR signaling. Solid arrows indicate direct effects; dotted arrows indicate indirect effects. Benjamin Chaigne-Delalande performed all stimulations, stainings, imaging, immunoblotting, and ELISAs for (**A**)-(**C**) and created figure (**D**).

This deficiency in PLCγ1 and PKC θ activation following TCR stimulation was recapitulated by RNAi silencing of *MAGT1* and Mg^{2+} depletion in normal T lymphocytes (Figure 3-11A-B). Consistent with this defect being a kinetic block, upregulation of CD69 and CD25 upon OKT3 stimulation of primary T cell activation in long-term PBMC cultures is only temporally inhibited in the patients. However, this temporal defect in TCR induced gene upregulation does not appear to be completely rescued by PMA/IONO stimulation (Figure 3-13), suggesting that signaling events downstream of second messenger induction may require MagT1 function as well. Thus, Mg^{2+} can temporally regulate signal transduction pathways involving PLCγ1, and MagT1-deficiency profoundly delays the activation of the PLCγ1 branch of TCR signaling. Also the defects in late but not early TCR events is consistent with the concept that early events trigger MagT1 to induce a Mg^{2+} influx, which is required for certain downstream signaling events in the T cell activation program.

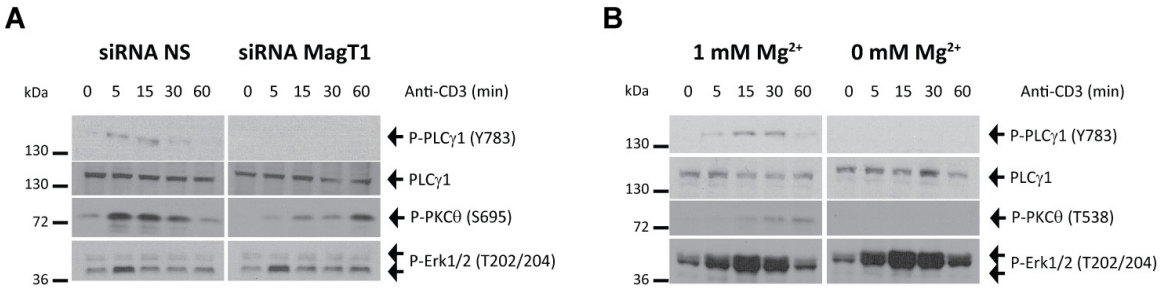

Figure 3-11: Recapitulates P-PLCγ1 and PKCθ defects in normal T cells.

Immunoblot of phosphoproteins in normal T cells stimulated with 1 μg/ml αCD3 for indicated times (**A**) after transfection with non-specific (NS) or MagT1-specific siRNA or (**B**) in 0% FCS RPMI media with or without Mg^{2+} after 4h starvation in the same media. Benjamin Chaigne-Delalande performed knockdown, stimulations, and immunoblots in (**A**) and (**B**).

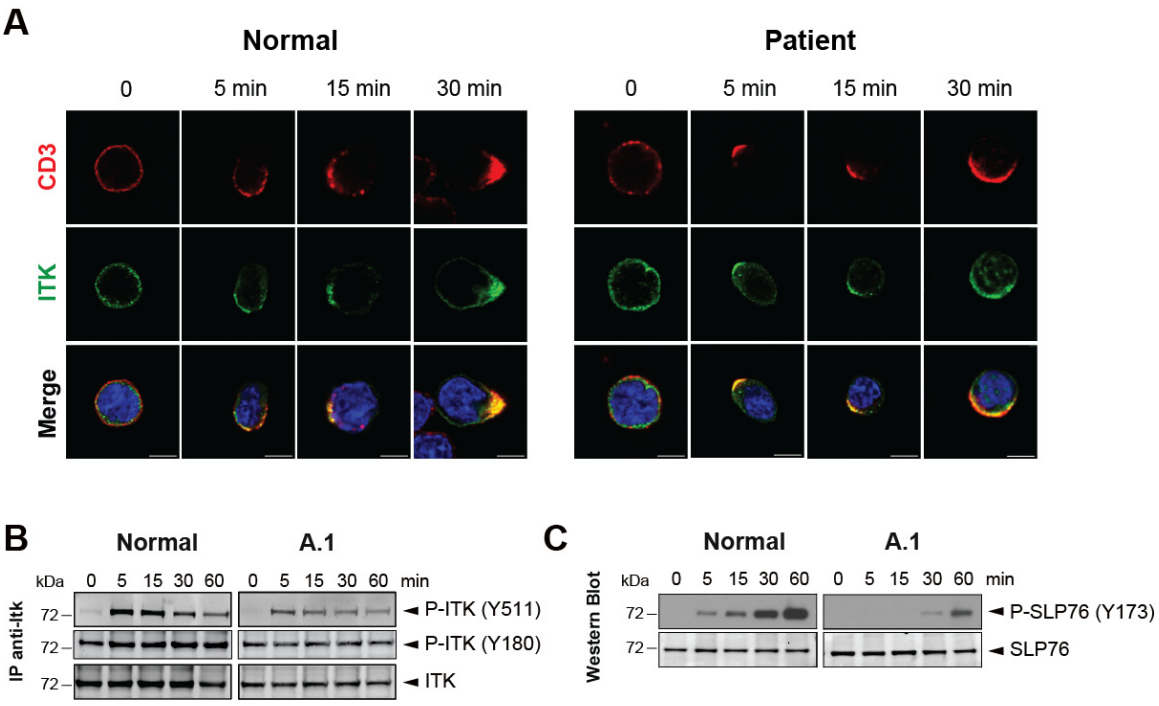

Figure 3-12: MagT1 deficiency impairs ITK-mediated phosphorylations.

(**A**) Confocal images of TCR clustering induced by αCD3 stimulation for various times on T cells. (Scale bar: 5 µm). Immunoblot of (**B**) ITK after immunoprecipitation and (**C**) SLP76 in T cells stimulated with αCD3 for indicated times. Benjamin Chaigne-Delalande performed stimulations, stainings, imaging, and immunoblots in (**A**)-(**C**).

PLCγ1 is activated by members of the tyrosine kinase expressed in hepatocellular carcinoma (Tec) family of nonreceptor tyrosine kinases, of which ITK is most highly expressed and functionally important in T cells[28,29]. Activation of ITK is regulated at many levels, including its recruitment to the plasma membrane by phosphatidylinositol (3,4,5) trisphosphate (PIP_3), association with the phosphorylated SLP76/LAT complex, phosphorylation of its activation loop by Lck, and disruption of its inhibitory self-association. Upon activation, ITK will phosphorylate a number of targets in the TCR signaling complex besides PLCγ1,

including itself and SLP76 at Y173[29,30]. While ITK Y511 phosphoryation by Lck and its recruitment to the TCR signaling complex as assessed by confocal imaging appears intact, the autophosphorylation at residue Y180 and also on Y173 of SLP76 is delayed in the patients (Figure 3-12A-C). Thus, the ability of ITK to phosphorylate its various substrates seems specifically impaired in the absence of MagT1.

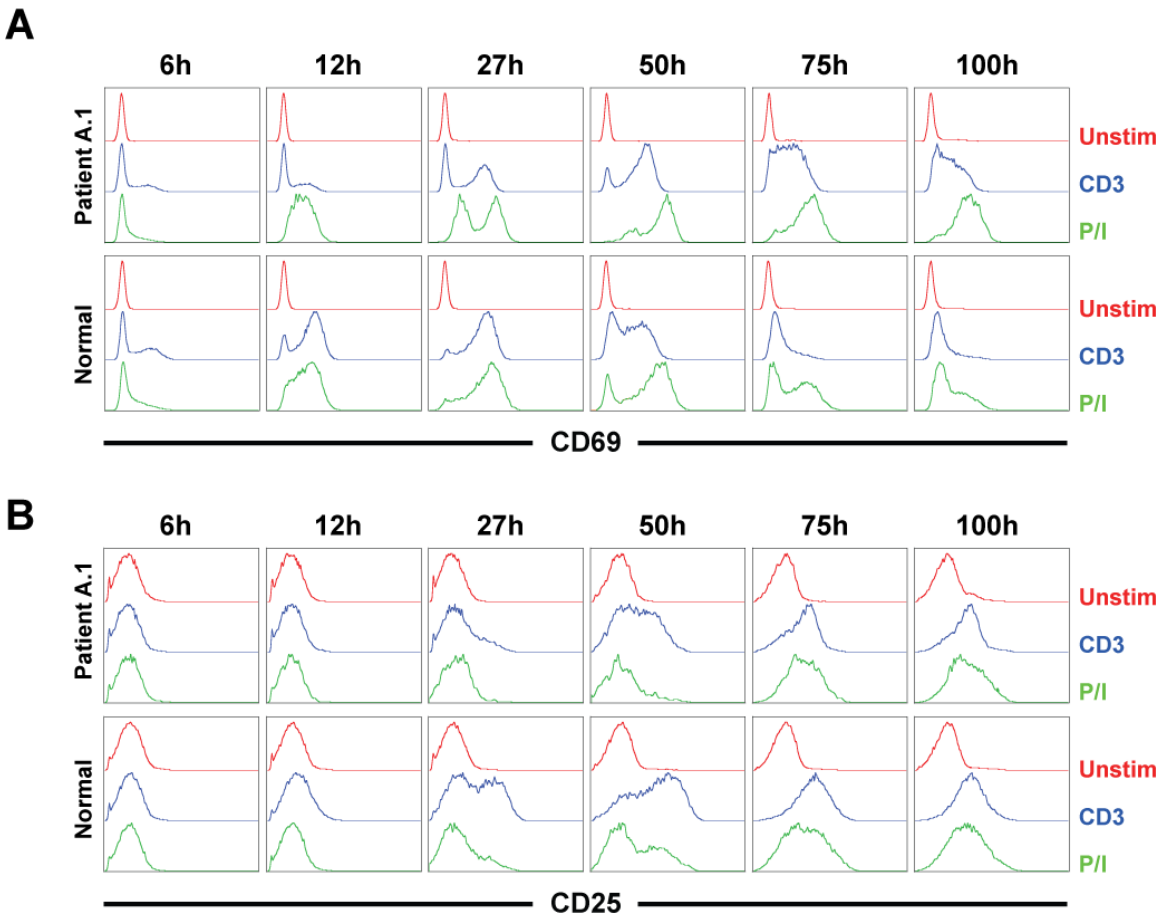

Figure 3-13: Delayed upregulation of CD69 and CD25 in patients.

Flow cytometry histograms of (**A**) CD69 and (**B**) CD25 expression over time in $CD4^+$ T cells after stimulation with anti-CD3 (blue), PMA/ Ionomycin (P/I, green) or unstimulated (Unstim, red).

3.3 Discussion

Mg^{2+} has been well recognized as an essential cofactor for many biological processes, but its role as a second messenger in rapid intracellular signaling has been debated[6–10]. We have found a physiologically relevant transient Mg^{2+} influx mediated by MagT1 during T cell activation that is required for ITK-mediated phosphorylations. Sutherland articulated three fundamental features of a second messenger: 1) its levels must increase rapidly in response to a stimulus which is typically the engagement of a cell surface receptor (first messenger), 2) it needs to alter the rate of one or more cellular processes, and 3) it exerts cell-type specific activity because different cells harbor different complements of enzymes[31]. Here, we find that Mg^{2+} fulfills these requirements and is a kinetic regulator of signaling in T cells. We found no difference in total Mg^{2+} content between our patients and healthy controls, indicating that MagT1 does not influence general Mg^{2+} homeostasis, total cellular Mg^{2+}, or its cofactor function. Unlike prior studies that detected non-instantaneous Mg^{2+} fluxes after several minutes or hours of stimulation[11,15,16], we measured rapid and transient free Mg^{2+} influxes after TCR engagement that is gated by a Mg^{2+} specific transporter. How TCR engagement leads to the induction of MagT1 remains to be determined. It does not appear to be dependent on Lck or ZAP-70 activity as the Mg^{2+} flux is not defective in wildtype or analogue sensitive ZAP-70 expressing Jurkat cells[32] inhibited by PP2 (4-amino-5-(4-chlorophenyl)-7-(dimethylethyl)pyrazolo[3,4-*d*]pyrimidine) or 3-MB-PP1 (4-amino-1-*tert*-butyl-3-(*p*-methylphenyl) pyrazolo [3,4-D] pyrimidine), respectively (data not shown; Jurkat cells and 3-MB-PP1 were gifts from Art Weiss). The transient Mg^{2+} influxes serve to

promote the function of ITK by an unknown mechanism thereby enhancing the corresponding Ca^{2+} influx in T cells. The incomplete rescue of the delay in T cell activation in long-term cultures by PMA/IONO suggests that MagT1 may have roles in downstream T cell signaling. B cells, which depend on Btk for the BCR-induced Ca^{2+} influx, have no requirement for MagT1-mediated Mg^{2+} influxes despite their expression of MagT1. However, our data do not preclude the possibility that MagT1 may have a function in immature B cells during development since XMEN patients do have elevated B cells that exhibit a decreased memory phenotype (data not shown). Overall, our findings shed new light on older observations that extracellular magnesium promotes lymphocyte activation synergistically with calcium by T cell but not B cell mitogens and that mice fed Mg^{2+} deficient diets have lower calcineurin activity in their splenocytes[12–14,33,34].

We have pinpointed a proximal step in the TCR signaling pathway requiring MagT1 function by its effect on the phosphorylation ITK substrates, but we have yet to determine what is the molecular event(s) that is directly sensitive to the Mg^{2+} flux. The Mg^{2+} responsive protein could be ITK itself or an unknown Mg^{2+} binding protein that regulates the activity, conformation, or localization of ITK. Self-oligomerization of ITK at TCR clusters is thought to inhibit its activity[29], but we have not been able to assess this in cells from our patients yet. ITK autophosphorylation appears defective in XMEN patients, which is consistent with the decreased phosphorylation of its other substrates. However, this is not required for its catalytic activity and is thought to primarily enhance its self-oligomerization as part of a negative feedback loop[29]. *In vitro* biochemical assays with purified recombinant

protein may reveal whether the catalytic activity and self-oligomerization of ITK are directly sensitive to Mg^{2+}. An experimental search for a novel Mg^{2+} sensitive ITK regulator may be accomplished by an RNAi screen for novel proteins that affect ITK-mediated phosphorylations or by immunoprecipitation of ITK to identify novel binding partners by mass spectrometry, both in the presence and absence of Mg^{2+}. One potential candidate is the Ca^{2+}/calmodulin-activated Ser-Thr kinase (CASK), a constitutive active kinase sensitive to Mg^{2+} inhibition with a prominent role in the brain[35]. Although CASK has no known functions in the immune system, it is highly expressed in T lymphocytes compared to other immune cells according to the UCSC genome browser database. Thus, CASK or a similar regulator could serve as a negative regulator of ITK, and the MagT1-mediated Mg^{2+} flux may relieve this inhibition. Examining the Ca^{2+} flux in CASK knockdown or knockout T cells in the absence of extracellular Mg^{2+} could be used to test this hypothesis.

The apparent role of the MagT1-mediated Mg^{2+} flux on ITK's function is consistent with the phenotypes observed in the ITK knockout mice. Like XMEN patients, ITK-/- mice have decreased CD4:CD8 ratio in T cells and elevated B cells in the periphery. Consistent with a defect in thymic output of $CD4^+$ T cells in XMEN patients, positive selection of $CD4^+$ T cells is specifically impaired in ITK-/- mice. Lymphocytes from ITK-/- mice exhibit a partial proliferation defect upon anti-TCR stimulation that can be bypassed by PMA/IONO stimulation or interleukin-2 (IL-2) supplementation, which was also found in XMEN patients (data not shown)[36]. Similar phenotypes were also observed in the double knockout mice of ITK and resting lymphocyte kinase (Rlk), the other Tec kinase member expressed in T cells.

Like the XMEN patients, PLCγ1 activation appears delayed and Ca^{2+} flux is partially impaired in the $ITK^{-/-}Rlk^{-/-}$ mice, consistent with the notion of Tec kinases being amplifiers of TCR signaling[28,37].

The integrity of early TCR activation events in the XMEN patient T cells explains how MagT1 acts as a TCR-gated transporter that controls a new step (Mg^{2+} flux) in the later contingent series of TCR signaling events[38]. The selective requirement of this Mg^{2+} influx for the activation of T cells but not B cells suggests that MagT1 may be a potentially useful therapeutic target for diseases requiring T cell specific immunomodulation.

3.4 Materials and Methods

Flow cytometry

For primary T cell activation assessments, PBMCs purified from whole blood were stimulated at 10^6 cells/mL with 1 μg/ml αCD3 or with 0.8 ng/ml PMA (Sigma) and 0.4 μM ionomycin (Sigma). Cells were harvested at various time points (12-72h) for flow cytometry staining with anti-CD2, anti-CD4, anti-CD8 and various activation markers antibodies (CD69, CD25, CD95, CTLA-4) as described in Chapter 2. All agonistic and flow staining antibodies were from BD biosciences. For CFSE dilution assays, cells resuspended at 10^7 cells/mL in PBS were labeled with 2.5 μM CFSE (Invitrogen) for 5 min at 37 ^oC in the dark and washed 3X with RPMI + 10% FBS before stimulation as described above. For B cell activation assessments, B cells enriched by negative selection using the B cell isolation kit II (Miltenyi) were stimulated with 10 μg/ml αIgM (BD biosciences), SAC (Sigma), or 0.5 μM CpG

(Invivogen) for 72 h and stained for CD69, CD25, CD86, and CD95 (BD biosciences) upregulation in flow cytometry.

Lentiviral transduction

Full-length MAGT1 was amplified by PCR from normal control T-cell cDNA and subcloned into the *BamI* and *NotI* restriction sites of LeGO-iG50 plasmid and into *XhoI* and *BamHI* restriction sites of the pLenti-bicistronic (Applied Biological Materials, ABM) plasmid. mCherry was also subcloned into the *SnaBI* and *NotI* restriction sites of pLenti-bicistronic plasmid. These constructs were each cotransfected with lentiviral second-generation packaging mix (ABM) in 1:1 mix into HEK293T (70% confluent) using Turbofect transfection reagent (Fermentas). After 2 days, virus supernatants were harvested and concentrated by overnight ultracentrifugation at 20,000g at 4 ^{o}C. Virus pellets were resuspended in 10% RPMI and stored at 280 ^{o}C. Unstimulated PBMCs purified from whole blood by Ficoll were transduced using virus made from LeGO-iG as described[39]. Three days after transduction, half of the transduced PBMCs were activated with 1 mg/mL OKT3 and analyzed for activation by flow cytometry. Day 4 stimulated T cells were transduced similarly using virus made from pLenti-bicistronic vector. Two days after transduction, cells were harvested for influx measurements by confocal imaging.

RNAi

For RNAi gene silencing of MAGT1, total T cells purified by Pan T cell isolation kit (Miltenyi Biotech) were transfected using P3 Primary Cell 4D-Nucleofector X kit (Lonza) with either Stealth RNAi Negative Control Duplexes or Stealth siRNA targeting MAGT1 (Invitrogen): siMAGT1-1 (59-

GCCCAAAGAAAGAAGGAGAUGGUGU-39), siMAGT1-3 (59-UCAUGUUCACUGCUCUCCAACUGCA-39). Transfected cells were cultured in 10% RPMI media for at least 4 h before stimulation with 1 mg/ml each of anti-CD3 and anti-CD28 for 48 h. Transfection was repeated again with the same siRNA, and transfected cells were cultured in 10%FBS RPMI media supplemented with 100 U/ml rhIL-2 for 48–72 h. Subsequently, cells were harvested for fluorimetric influx measurements and microscopic assessment of p65 translocation following stimulation with OKT3 or PMA/ionomycin. At the same time, cells were processed for real-time assessment of MAGT1 mRNA expression as described in Chapter 2.

Confocal imaging

For nuclear translocation of p65 and NFAT, cells were stimulated with either OKT3 or PMA/IONO for 30 min. Then cells were dropped onto poly-L-lysine coated slides and fixed with 3% paraformaldehyde in PBS, permeabilized with 0.05% Triton X-100 for 3 min at room temperature, and blocked with PBS containing 10% FBS. For TCR clustering, activated PBL from normal control and patient were incubated on ice with anti-CD3 antibody (1 μg/ml) for 30 min, washed and stained with Alexa-568 goat anti-mouse antibody for 30 min. Cell were then incubated at 37^{o}C for indicated times on poly-L-lysine coated slides and then fixed and permeabilized. All slides were stained with p65/RelA (Santa Cruz) or NFAT (BD biosciences) in 0.5% BSA-PBS for 45 min at room temperature. Slides were washed and incubated with an Alexa 488-conjugated donkey anti-rabbit antibodies (Invitrogen) for 45 min. Nuclei were stained with Hoechst 33342 (50 ng/ml, Invitrogen). Slides were washed in PBS, rinsed, and mounted with a coverslip using

Fluoromount-G (Southern Biotechnology). All images were collected on a Leica TCS-NT/SP5 confocal microscope (Leica Microsystems) using a 63X oil immersion objective NA 1.32, 'zoom X'. For enumeration of percentage of cells with nuclear NF-kB, NFAT or CD3 clustering, 450–700 cells were scored visually by a single observer.

Calcium and magnesium flux measurements

Cells were loaded with 1 mM MagFluo4-AM (Invitrogen) or 1 mM Fluo3-AM (Invitrogen) and 1 mM Fura Red-AM (Invitrogen) for 20 min at 37 ^{o}C. Then cells were washed in incubation buffer (IB: 120 mM N-methyl-D-glutamine, 20 mM HEPES, 4.7 mM KCl, 1.2 mM KH_2PO_4, 10 mM glucose, pH 7.4) with or without 1.2 mM $CaCl_2$ and/or 1.2 mM $MgSO_4$. The loading efficiency was assessed by adding 1 mM calcimycin, a Ca^{2+}/Mg^{2+} ionophore that induces maximal influxes of both ions. For flow cytometry experiments, intracellular calcium and magnesium were measured using a BD LSRII flow cytometer. Kinetic analyses were done with the FlowJo (TreeStar), with percentage of responding cells defined as .95th percentile of unstimulated baseline. For fluorimeter experiments, cells were seeded in opaque 96-well clear flat bottom plates and assessed with a POLARstar OPTIMA plate reader (BMG LabTech). For confocal microscopy, cells were plated on LabTek II Chamber Slide (Nunc) coated with 0.01% poly-L-lysine, and analyzed with a Leica TCS-NT/SP5 confocal microscope (Leica Microsystems) using a 63X oil immersion objective NA 1.32, 'zoom X'. ConA and PHA were from Sigma. Recombinant FasL and TNFα were from Alexis and recombinant SLC was from PeproTech.

Immunoblotting

Activated T cells were starved for 4 h in RPMI medium without FBS. Then cells were stimulated with OKT3 (1 μg/ml) for indicated times. Stimuli were terminated by addition of ice-cold PBS, and pelleted cells were immediately lysed in 1% Triton X-100, 1% NP40, 50 mM Tris-Cl pH 8, 150 mM NaCl, 20 mM EDTA, 1 mM Na_3VO_4, 1 mM NaF, phosphatase inhibitor cocktail (Sigma) and complete protease inhibitor cocktail (Roche). For Itk immunoprecipitation, 10^7 lysed cells were incubated with 5 μg of anti-Itk antibody (Cell Signaling Technologies) overnight at 4°C with rotation. Protein concentration was quantitated by BCA assay (Pierce). 30 mg of cell lysates were separated on 4-20% gradient Tris-Glycine SDS–PAGE gel (Biorad) and transferred on PVDF membrane (Millipore). Membrane was blocked with BSA for 1 h before incubating with primary antibodies overnight, all in PBS containing 0.1% Tween-20 (wash buffer). Phospho-ZAP-70/SYK(Y319), ITK, SLP76, phospho-LAT (Y191), LAT, phospho-PLCγ1 (Y783), PLCγ1, phospho-p38 (T180/182) and phospho-Erk1/2 (T202/204) antibodies were from Cell Signaling Technology. Lck, phospho-PKC-θ (T538), phospho-CD3ζ (C415.9A), and phospho-LAT (Y131) antibodies were from Santa Cruz. Phospho-Lck (Y394) and phosphor-ITK/Btk (Y511) antibodies were from BD biosciences. Phospho-SLP76 (Y173) and phospho-ITK (Y180) antibodies were obtained from D. Yablonski and O. Witte, respectively. Membranes were washed at least 3x before incubation with 1:10000 horseradish peroxidase (HRP)-conjugated anti-rabbit Ig antibody (Southern Biotechnology) for 1 hour, washed 3x, and detected with Supersignal West enhanced chemiluminescence (ECL) substrates (Pierce). For loading control, membranes were

subsequently blotted with 1:30,000 monoclonal anti-β-Actin−Peroxidase Conjugate antibody (Sigma-Aldrich) for 15 min. before exposure with ECL.

Quantitative total elemental content measurement

10^7 $CD4^+$ and $CD8^+$ T cells separately purified from PBMCs using human CD4 or CD8 Microbeads (Miltenyi Biotech), respectively, were stimulated with anti-CD3 and anti-CD28 for 3 days and subsequently cultured continuously in 10% RPMI media with 100 U/ml IL-2 at ~1–2 million cells per ml. When sufficient cells accumulated, duplicate aliquots of 5, 10, and 15 million cells were pelleted and dried overnight at 32 ^oC. Total magnesium, calcium and sulphur content was measured for each cell pellet by inductively coupled plasma mass spectrometry as described[24].

IP3 measurement

IP_3 levels from stimulated T cells were assessed using an IP_3 ELISA kit (Cusabio) according manufacturer's instructions. Statistical analysis. P values were calculated with the Students t-test using PRISM software (GraphPad Software), with a two-tailed distribution.

Statistical analysis

P values were calculated with the Students t-test using PRISM software (GraphPad Software), with a two-tailed distribution.

3.5 References

1. Yang, W., Lee, J.Y. & Nowotny, M. Making and breaking nucleic acids: two-Mg2+-ion catalysis and substrate specificity. *Molecular cell* **22**, 5-13 (2006).

2. Cowan, J. a Structural and catalytic chemistry of magnesium-dependent enzymes. *Biometals : an international journal on the role of metal ions in biology, biochemistry, and medicine* **15**, 225-35 (2002).

3. Cakmak, I. & Kirkby, E. a. Role of magnesium in carbon partitioning and alleviating photooxidative damage. *Physiologia Plantarum* **133**, 692-704 (2008).

4. Trapani, V. *et al.* Intracellular magnesium detection: imaging a brighter future. *Analyst* **135**, 1855-1866

5. Hogan, P.G., Lewis, R.S. & Rao, A. Molecular basis of calcium signaling in lymphocytes: STIM and ORAI. *Annual review of immunology* **28**, 491-533 (2010).

6. Gasser, A., Bruhn, S. & Guse, A.H. Second messenger function of nicotinic acid adenine dinucleotide phosphate revealed by an improved enzymatic cycling assay. *J Biol Chem* **281**, 16906-16913 (2006).

7. Grubbs, R.D. & Maguire, M.E. Magnesium as a regulatory cation: criteria and evaluation. *Magnesium* **6**, 113-127 (1987).

8. Murphy, E. Mysteries of magnesium homeostasis. *Circ Res* **86**, 245-248 (2000).

9. Permyakov, E.A. & Kretsinger, R.H. Cell signaling, beyond cytosolic calcium in eukaryotes. *J Inorg Biochem* **103**, 77-86 (2009).

10. Takaya, J., Higashino, H. & Kobayashi, Y. Can magnesium act as a second messenger? Current data on translocation induced by various biologically active substances. *Magnes Res* **13**, 139-146 (2000).

11. Romani, A.M. Magnesium homeostasis in mammalian cells. *Front Biosci* **12**, 308-331 (2007).

12. Abboud, C.N., Scully, S.P., Lichtman, A.H., Brennan, J.K. & Segel, G.B. The requirements for ionized calcium and magnesium in lymphocyte proliferation. *J Cell Physiol* **122**, 64-72 (1985).

13. Modiano, J.F., Kelepouris, E., Kern, J.A. & Nowell, P.C. Requirement for extracellular calcium or magnesium in mitogen-induced activation of human peripheral blood lymphocytes. *J Cell Physiol* **135**, 451-458 (1988).

14. Whitney, R.B. & Sutherland, R.M. The influence of calcium, magnesium and cyclic adenosine 3',5'-monophosphate on the mixed lymphocyte reaction. *J Immunol* **108**, 1179-1183 (1972).

15. Ng, L.L., Davies, J.E. & Garrido, M.C. Intracellular free magnesium in human lymphocytes and the response to lectins. *Clin Sci (Lond)* **80**, 539-547 (1991).

16. Rijkers, G.T. & Griffioen, A.W. Changes in free cytoplasmic magnesium following activation of human lymphocytes. *Biochem J* **289 (Pt 2**, 373-377 (1993).

17. Kumar, A., Teuber, S.S. & Gershwin, M.E. Current perspectives on primary immunodeficiency diseases. *Clinical & developmental immunology* **13**, 223-59 (2006).

18. Wilkinson, B., Downey, J.S. & Rudd, C.E. T-cell signalling and immune system disorders. *Expert Rev Mol Med* **7**, 1-29 (2005).

19. Chan, a C. *et al.* ZAP-70 deficiency in an autosomal recessive form of severe combined immunodeficiency. *Science (New York, N.Y.)* **264**, 1599-601 (1994).

20. Arpaia, E., Shahar, M., Dadi, H., Cohen, A. & Roifman, C.M. Defective T cell receptor signaling and CD8+ thymic selection in humans lacking zap-70 kinase. *Cell* **76**, 947-958 (1994).

21. Feske, S. *et al.* A mutation in Orai1 causes immune deficiency by abrogating CRAC channel function. *Nature* **441**, 179-185 (2006).

22. Goytain, A. & Quamme, G.A. Identification and characterization of a novel mammalian Mg2+ transporter with channel-like properties. *BMC Genomics* **6**, 48 (2005).

23. Quamme, G.A. Molecular identification of ancient and modern mammalian magnesium transporters. *Am J Physiol Cell Physiol* **298**, C407-29 (2010).

24. Killilea, D.W. & Ames, B.N. Magnesium deficiency accelerates cellular senescence in cultured human fibroblasts. *Proc Natl Acad Sci U S A* **105**, 5768-5773 (2008).

25. Peterson, E.J. & Koretzky, G.A. Signal transduction in T lymphocytes. *Clin Exp Rheumatol* **17**, 107-114 (1999).

26. Weiss, A. & Littman, D.R. Signal transduction by lymphocyte antigen receptors. *Cell* **76**, 263-274 (1994).

27. Nel, A.E. T-cell activation through the antigen receptor. Part 1: signaling components, signaling pathways, and signal integration at the T-cell antigen receptor synapse. *J Allergy Clin Immunol* **109**, 758-770 (2002).

28. Readinger, J. a, Mueller, K.L., Venegas, A.M., Horai, R. & Schwartzberg, P.L. Tec kinases regulate T-lymphocyte development and function: new insights into the roles of Itk and Rlk/Txk. *Immunological reviews* **228**, 93-114 (2009).

29. Andreotti, A.H., Schwartzberg, P.L., Joseph, R.E. & Berg, L.J. T-cell signaling regulated by the Tec family kinase, Itk. *Cold Spring Harbor perspectives in biology* **2**, a002287 (2010).

30. Sela, M. *et al.* Sequential phosphorylation of SLP-76 at tyrosine 173 is required for activation of T and mast cells. *The EMBO journal* **30**, 3160-72 (2011).

31. Sutherland, E.W. Studies on the mechanism of hormone action. *Science (New York, N.Y.)* **177**, 401-8 (1972).

32. Levin, S.E., Zhang, C., Kadlecek, T. a, Shokat, K.M. & Weiss, A. Inhibition of ZAP-70 kinase activity via an analog-sensitive allele blocks T cell receptor and CD28 superagonist signaling. *The Journal of biological chemistry* **283**, 15419-30 (2008).

33. Flynn, A. Control of in vitro lymphocyte proliferation by copper, magnesium and zinc deficiency. *J Nutr* **114**, 2034-2042 (1984).

34. Sabbagh, F., Lecerf, F., Hulin, A., Bac, P. & German-Fattal, M. Effect of hypomagnesemia on allogeneic activation in mice. *Transpl Immunol* **20**, 83-87 (2008).

35. Mukherjee, K. *et al.* CASK Functions as a Mg2+-independent neurexin kinase. *Cell* **133**, 328-39 (2008).

36. Liao, X.C. & Littman, D.R. Altered T cell receptor signaling and disrupted T cell development in mice lacking Itk. *Immunity* **3**, 757-69 (1995).

37. Schaeffer, E.M. Requirement for Tec Kinases Rlk and Itk in T Cell Receptor Signaling and Immunity. *Science* **284**, 638-641 (1999).

38. Crabtree, G.R. Contingent genetic regulatory events in T lymphocyte activation. *Science* **243**, 355-361 (1989).

39. Cho, N.H. *et al.* Inhibition of T cell receptor signal transduction by tyrosine kinase-interacting protein of Herpesvirus saimiri. *J Exp Med* **200**, 681-687 (2004).

Chapter 4 : Cytotoxicity defects in XMEN patients

4.1 Introduction

NK cells and CTLs are two arms of the immune system highly specialized to kill virally infected and tumor cells. Unlike CTLs, which require antigen-specific TCR stimulation and long-term clonal expansion, NK cells do not have clonal antigen-specific receptors and are triggered to kill innately by the balance of inhibitory and activating receptor engagement. Human inhibitory receptors, which include killer cell inhibitory receptors (KIRs) and the heterodimeric C-type lectin receptor CD94-NKG2A, recognize MHC-class I molecules to prevent killing of cells of self-origin and allow for the recognition of the "missing-self" state[1]. Activating receptors, which detect the "altered-self" state, include the NK-restricted natural cytotoxicity receptors NKp30, NKp44 and NKp46, which may recognize heparin sulfate on tumor cells or hemagglutinin on virally infected cells, and non-NK-restricted receptors (NKG2D, 2B4, DNAM-1, and CD2) that recognize ligands upregulated by stress, transformation, or viral infection[2,3]. Many of these activating receptors are also expressed on CTLs and serve as costimulatory signals with TCR engagement to enhance activation and cytolytic function[4–6]. In addition to these receptors, NK cell activation is also augmented by cytokines released during the early stages of viral infection. IFN-α/β can enhance NK cytotoxicity, and IL-15 serves to induce NK proliferation. IL-12 and IL-18 act synergistically on NK cells to induce the production IFN-γ, which activates T cells and macrophages to limit the infection[1]. Upon engagement with target cells, NK cells or CTLs release cytotoxic granules containing membrane pore-forming molecules called perforin and granzymes, which are proteases that carry out activating cleavage of specific zymogens of

caspases that cleave other proteins to generate the apoptotic phenotype and cell death. In addition, cytolytic lymphocytes can also upregulate the expression of Fas-ligand, a member of the tumor necrosis family, and induce the killing of Fas-expressing targets by apoptosis, which is more significant to immature NK cells that cannot use perforin-dependent killing. Lastly, NK cells can lyse antibody bound cells by antibody dependent cellular cytotoxicity (ADCC) mediated through engagement of its CD16 (FcγRIII) receptor by the Fc portion of the bound IgG[1–3].

The importance of CTL and NK cytotoxicity for the control of herpes virus infections has been underscored by a number of PIDs with impairments in NK cell and/or CTL cytotoxicity function[7]. Susceptibility to uncontrolled infections with herpes simplex virus (HSV), varicella zoster virus (VZV), CMV, and/or EBV has been found in PIDs with CD16 impairment, deficiencies in the perforin degranulation pathway, IFN-γ receptor deficiency, and functional or absolute NK cell deficiencies[7,8]. The specific susceptibility to EBV in XLP could be explained by SAP deficiency impairing cytotoxicity mediated by 2B4, leading to defective killing of EBV-infected cells that highly express its ligand (CD48)[9–11]. The significance of NK and CTL cytotoxicity for herpes virus infections is also suggested by the evolution in herpes viruses of many immune-evasion strategies against this pathway to persist in the host. For instance, human CMV expresses proteins to block the expression of ligands for CD2 and NKG2D. Many herpes viruses, including CMV, HSV, and Kaposi's sarcoma-associated herpesvirus (KSHV), express proteins to downmodulate MHC class I molecules or prevent their peptide loading to evade recognition by CTLs. To

elude NK cells, human CMV also expresses decoy molecules to mimic MHC class I molecules that bind to NK inhibitory receptors[2,3].

To avoid antitumor immunity, many tumor cells also acquire mutations to escape from NK cell and CTL mediated cytotoxicity. Many cases of diffuse large B cell lymphomas have mutations that downmodulate the expression of HLA class I to prevent recognition by CTLs[12]. Similarly, several human cancers and cancer cell lines have been found to downregulate NKG2D expression on effector cells through various mechanisms, including persistent overexpression of its ligands on tumor cells and/or secretion of soluble forms of its ligands. Alternatively, they can also prevent the recognition by NKG2D by downregulating the expression of its ligands[3]. The importance of NKG2D-dependent killing to early tumor immunosurveillance is also demonstrated by NKG2D-deficient mice that show accelerated disease in spontaneous models of prostate adenocarcinoma and B cell lymphoma[13]. Mice treated with NKG2D neutralizing antibody are also more susceptible to carcinogen-induced carcinomas[14]. Thus, in addition to recognition of tumor specific antigens by MHC class I and II on CTLs, recognition of NKG2D ligands expressed on tumor cells (but not normal cells) also serves as an essential mechanism of restricting tumor outgrowth[15].

Unlike many herpes viruses and cancer cells, EBV's main mechanism of immune evasion is latency, a state in which it downmodulates the expression of most of its gene expression program. However, lytic induction is also accompanied by expression of several EBV proteins that interfere with HLA class I and II expression or recognition and IFNγ expression to avoid CTL recognition. In addition,

lytic induction also upregulates ligands for DNAM-1 and NKG2D on infected cells, allowing for NK cell mediated cytolysis[16]. Moreover, NKG2D ligands have recently been shown to be highly expressed on tumors from a mouse model of EBV-driven tumorigenesis as well as from patients with EBV^+ post-transplant lymphoproliferative disorder[17]. Induction of complement- or cell-mediated cytotoxicity of these cells by the injection of NKG2D-fc fusion protein reduced tumor growth and increased the survival of these mice. Although depletion of NKG2D, IFNγ, or TNFα alone was not sufficient to promote the emergence of tumors in this model, depletion of TCRαβ and TCRγδ T cells, NK cells, and NKT cells was necessary and sufficient to drive the outgrowth of B cell lymphomas[17]. Thus, the total function of these cells may be crucial for restricting tumor emergence, while their specific effector functions such as NKG2D-mediated killing help limit the expansion of tumors and virus control.

Given the unusual susceptibility of XMEN patients to EBV-driven tumorigenesis, I hypothesized that their NK cells and CTLs would have cytotoxicity defects. Not only did they exhibit profound defects in cytotoxicity function against the leukemia cell line K562 and autologous EBV-transformed lymphoblastoid cell lines (LCLs), they also exhibited a nearly complete loss of NKG2D expression and NKG2D-mediated killing. Moreover, we found that Mg^{2+} depletion and supplementation in the media can decrease and rescue NKG2D expression, respectively. This indicates that MagT1 may regulate the surface expression of NKG2D via a Mg^{2+} dependent mechanism. The unusual loss of NKG2D expression in this disease can also serve as a pre-diagnostic screen for XMEN disease.

4.2 Results

XMEN patient NK cells lack NKG2D synergism for Ca^{2+} flux induction

Like T cells, NK cells also have receptors (CD16, NKp46, and NKp30) that associate with the CD3 ζ-chain and signal through ITAM motifs to induce a Ca^{2+} flux. In contrast, other cytotoxicity receptors such as NKG2D, 2B4, DNAM-1, and CD2 do not signal through ITAMs and but are still capable of inducing a Ca^{2+} flux synergistically through coengagement of some of these receptors[18]. To determine whether these Ca^{2+} fluxes are regulated by a MagT1-dependent Mg^{2+} flux, we assessed these fluxes in IL-2-activated NK cells from patients and normal controls. We detected a Mg^{2+} flux and a Ca^{2+} flux upon anti-CD16 stimulation in normal cells, whereas the patient cells have no detectable Mg^{2+} flux and a slightly diminished Ca^{2+} flux (Figure 4-1A). We also observed that the CD16 induced Ca^{2+} flux in normal NK cells is decreased in the absence of extracellular Mg^{2+}(data not shown), suggesting it may be partially dependent on the Mg^{2+} flux. NKp46 stimulation exhibits a very weak Ca^{2+} flux but no visible Mg^{2+} flux, and this Ca^{2+} flux is comparable between normal and patient cells (Figure 4-1A). Consistent with previous reported findings, we did not detect a Ca^{2+} flux by stimulating NKG2D, 2B4, DNAM-1, and CD2 alone in normal cells (Figure 4-1A). However, costimulating 2B4 or DNAM-1 with CD16 enhances the Ca^{2+} flux but not the Mg^{2+} flux (Figure 4-1B). Strikingly, this enhancement is not present in the patient cells with NKG2D stimulation (Figure 4-1B). In addition, while costimulating 2B4 with DNAM-1 yielded a comparable Ca^{2+} flux in normal and patient cells, NKG2D lacks this synergism with 2B4 for the Ca^{2+} flux in patient cells compared to in normal cells (Figure 4-1C). Thus, the NKG2D-

induced synergistic Ca^{2+} flux is also dependent on MagT1 even though NKG2D does not induce a detectable Mg^{2+} flux.

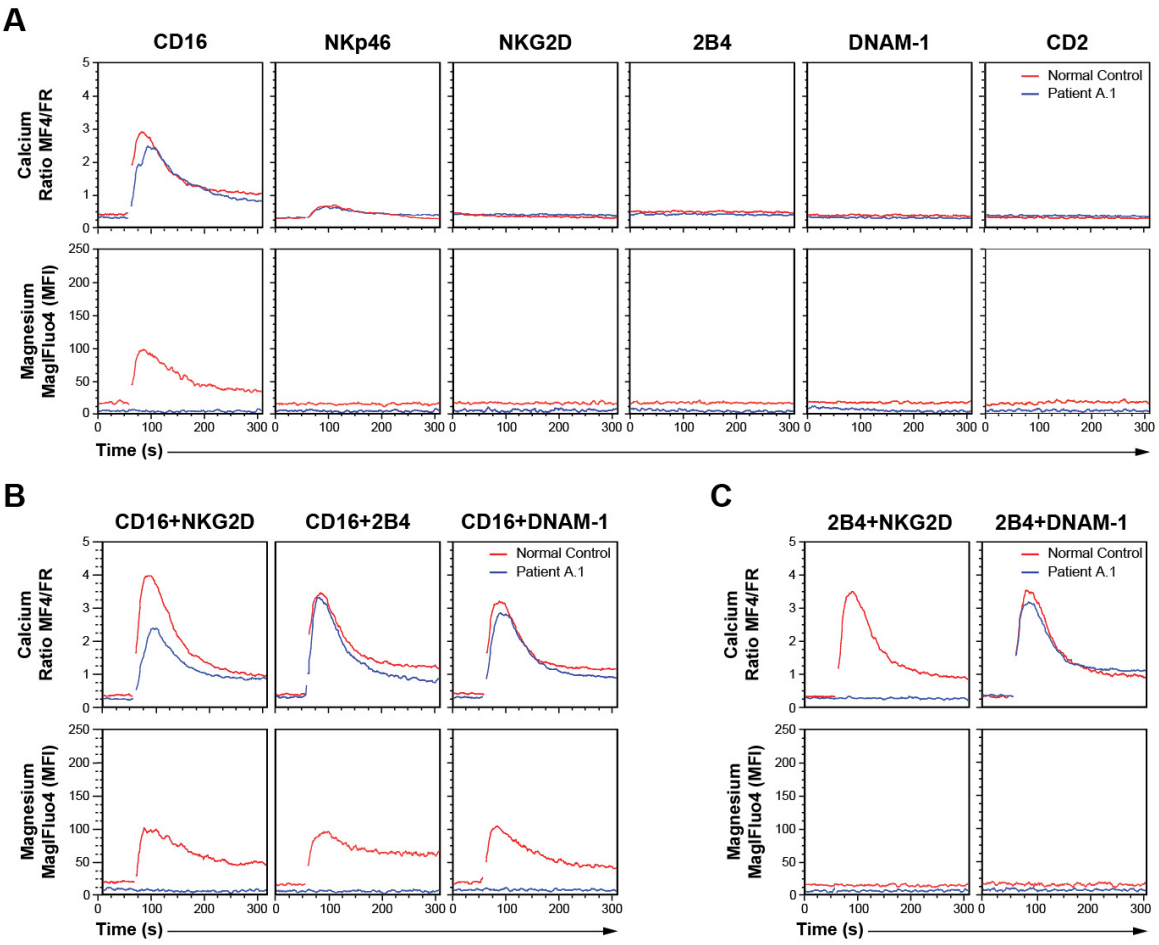

Figure 4-1: XMEN patients lack NKG2D-induced synergistic Ca^{2+} flux

Flow cytometry kinetic profiles of Ca^{2+} (upper panel) and Mg^{2+} (lower panel) flux in IL-2 activated NK cells from normal control (red curve) and patient A.1 (blue curve). Cells were incubated on ice with 10 μg/ml of mouse antibodies to NK cell receptors alone (**A**) or in combination (**B**, **C**) for at least 30 minutes before acquisition. Fluxes were induced by addition of 10 μg/ml goat-anti-mouse F(ab)2 antibody. Flux assays were performed by Benjamin Chaigne-Delalande

XMEN patients lack NKG2D expression

To determine if the loss of NKG2D synergism in Ca^{2+} flux induction was due to loss of expression, we assessed NKG2D surface expression by flow cytometry. To our surprise, the level of NKG2D expression was almost completely lost in patient NK cells examined immediately *ex vivo*. On the other hand, expression of other NK receptors including 2B4, CD16, CD122, CD161, NKp30, NKp46, DNAM-1, and NKp44 were not significantly different from normal NK cells (Figure 4-2A). Moreover, the expression of inhibitory KIR receptors (data not shown) and cytotoxic mediators such as perforin and granzyme B was not significantly compromised either (Figure 4-2B), suggesting these patient cells were truly NK cells. NKG2D is upregulated in patients NK cells with IL-2 or IL-15 and IL-18 stimulation although not to the same extent as normal NK cells (Figure 4-2C). However, NK cell activation as assessed by CD25 upregulation appears normal in patient cells (Figure 4-2D). The loss of NKG2D expression was not only at the surface but also intracellularly in NK cells and CD8+ T cells from all assessed XMEN patients (Figure 4-3A,C). This defect appears to be post-transcriptional as its mRNA expression level is not compromised in the patient cells (Figure 4-3D). The loss of NKG2D expression is not secondary to EBV infection in XMEN patients as another chronic EBV patient without any MagT1 mutations expresses normal surface levels of NKG2D (Figure 4-3B-C). Moreover, two of the XMEN patients did not have detectable levels of EBV at the time of assessment (Gulbu Uzel and Taco Kuijpers, personal communications).

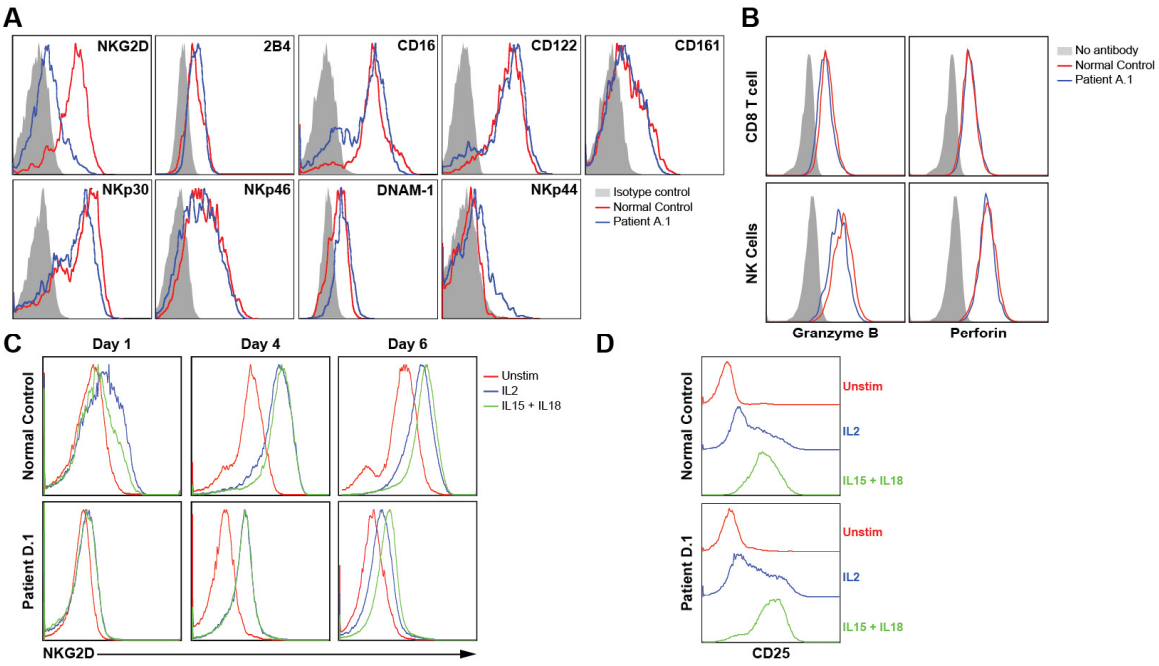

Figure 4-2: Loss of NKG2D expression in patient NK cells.

(**A**) Flow cytometry profile of NK cell receptors on gated NK cells from whole blood of normal control and patient A.1. (**B**) Flow cytometry profile of granzyme B and perforin in NK and CD8+ T cells from normal control donor and patient A.1. (**C**) Flow cytometry profiles of NKG2D expression in NK cells after stimulation with or without IL-2 or IL-15 and IL-18. (**D**) Flow cytometry profiles of CD25 expression in NK cells after 4 days of stimulation with or without IL-2 or IL15 and IL18. Geraldine O'Connor performed (**A**) and Benjamin Chaigne-Delalande performed (**B**).

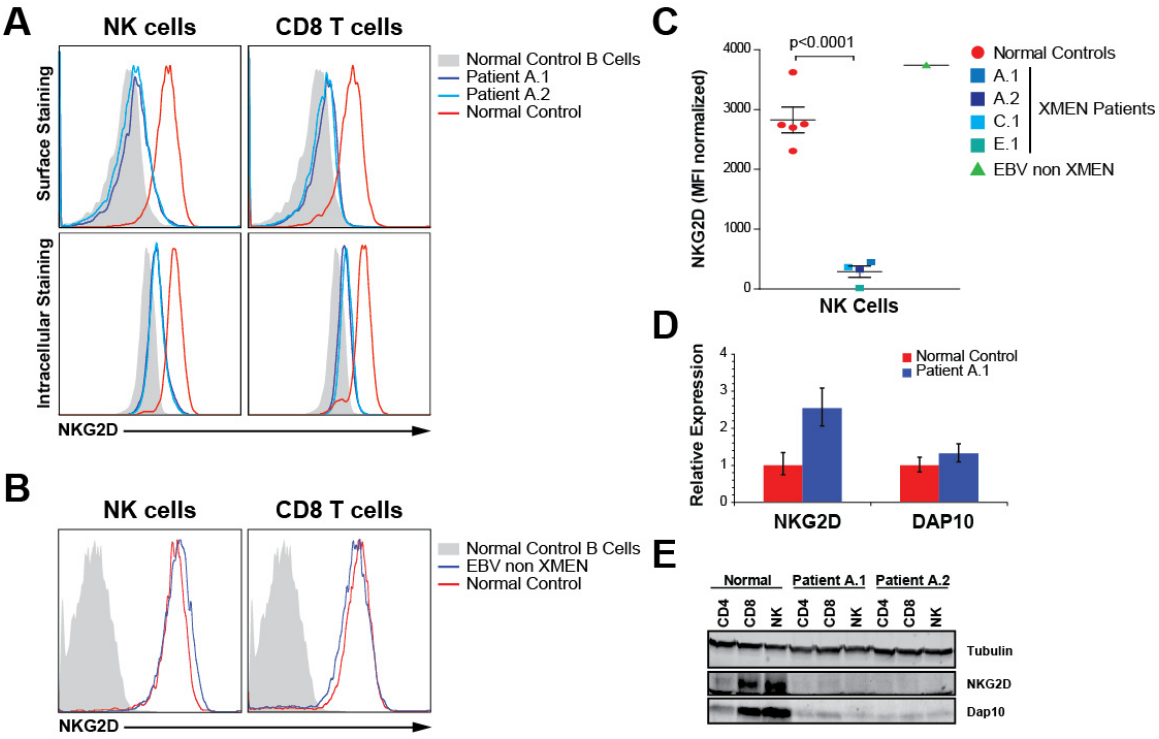

Figure 4-3: Post-transcriptional loss of NGK2D and Dap10 in XMEN patients

(**A**) Flow cytometry profile of NKG2D surface staining (upper panel) and intracellular staining (lower panel) in freshly isolated PBMCs from normal control, patient A.1, and patient A.2. (**B**) Flow cytometry profile of NKG2D surface staining in freshly isolated PBMCs from normal control and a non-XMEN chronic EBV patient. (**C**) The mean fluorescence intensity of NKG2D surface staining on gated NK cells subtracting the background staining of gated $CD4^+$ T cells from freshly isolated PBMCs of normal controls (red) and patients (green or blue). (**D**) RT-PCR showing mRNA expression of *NKG2D* and *DAP10* in patient CD8+ T cells. Values are normalized to HPRT mRNA expression. (**E**) Immunoblotting of NKG2D, DAP10, and Tubulin in $CD4^+$ and $CD8^+$ T cells and NK cells from normal control, patient A.1, and patient A.2. NKG2D expression data for patient C.1 was contributed by Taco Kuijpers and colleagues. Marshall Lukacs performed (**D**) and Benjamin Chaigne-Delalande performed (**E**).

NKG2D is a C-type lectin-like receptor expressed mainly on NK cells, CD8+ T cells, and γδ-T cells. It is associates with the adaptor protein DAP10 in humans to signal for the activation of PLCγ through the phosphatidylinositol-3 kinase (PI3K) pathway. In humans, NKG2D recognizes MHC class I chain-like molecules (MICA and MICB) and the UL16 binding protein (ULBP) family of glycoproteins induced by infection, cellular transformation, or stress like heat shock or DNA damage[19]. Persistent expression of NKG2D ligands in transgenic mouse models has been shown to downmodulate NKG2D. In addition, some human cancers have been found to shed MICA, which can induce the endocytosis and degradation of NKG2D. Lastly, human cancer cells can repress the expression of both NKG2D and its ligands by secreting TGF-β[3], which directly interfere with the transcription of DAP10[20]. We assessed whether any of these mechanisms play a role in the downmodulation of NKG2D in our patients. Although DAP10 protein expression is decreased in our patients (Figure 4-3E), DAP10 mRNA levels are not diminished (Figure 4-3D), which disfavors the TGF–β mediated mechanism. Persistent expression of ligands is also not likely the case as NKG2D ligand expression as detected by NKG2D-Fc or anti-MICA antibody was not found to be elevated in LCLs, *ex vivo* lymphocytes, or *in vitro* cultured CTLs from the patients (Figure 4-4A-B). We did not detect soluble MICA in long-term cultures of CTLs even though the NKG2D level remains suppressed in these cells (Figure 4-4E). The decreased protein expression of DAP10 could be a cause or effect of NKG2D downregulation.

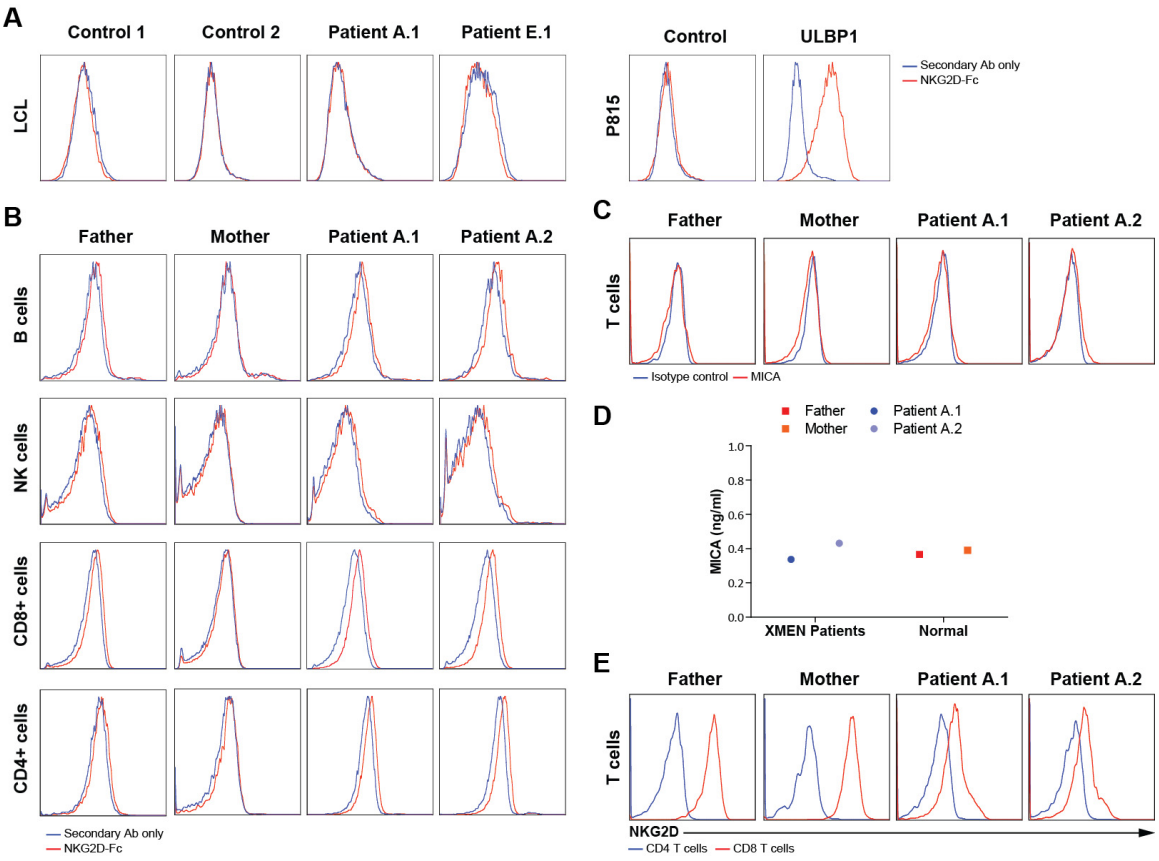

Figure 4-4: NKG2D is repressed in culture without elevation of ligand expression or shedding

Flow cytometry profiles of NKG2D ligand expression detected by NKG2Dfc recombinant protein on (**A**) LCLs and P815 cell lines with or without ULBP1 expression and (**B**) ex vivo lymphocyte subsets of PBMCs. (**C**) Flow cytometry profiles of MICA expression by anti-MICA antibody on activated T cells in culture. (**D**) Quantitation of soluble MICA and (**E**) NKG2D expression on activated T cells from the same cultures as in (**C**). Benjamin Chaigne-Delalande performed (**C**)-(**E**).

XMEN patients exhibit cytotoxicity defects in NK cells and CTLs

Consistent with the loss of NKG2D expression in the patients, the patient NK cells also exhibit profoundly defective killing of K562 cells (Figure 4-5A), a cancer target cell line that can be killed via NKG2D ligation. Moreover, NKG2D-mediated cytotoxicity against an ULBP1-overexpressing P815 cell line is abrogated using the

patient NK cells (Figure 4-5B), supporting the conclusion that the patient NK cells have specific NKG2D-mediated cytotoxicity defects. The patient NK cells also exhibit defective killing of 721.221, an EBV transformed cell line with loss of HLA class I expression (Figure 4-5C). In addition to defective killing as assessed by positive granzyme B activity in target cells loaded with a granzyme B substrate that fluoresces upon cleavage, degranulation of cytotoxic granules is also defective in the patients as indicated by the decreased percentage of NK cells exhibiting upregulation of the degranulation marker, CD107a (Figure 4-5D). Overall, the NKG2D defect in patient NK cells could lead to profound cytotoxicity defects against cancer lines and EBV transformed cells lacking HLA class I.

Like the NK cells, CTLs also exhibit defective NKG2D-mediated cytotoxicity. Unlike NK cells, CTL cytotoxicity requires stimulation of the TCR. Consistent with the costimulatory function of NKG2D, ULBP1 expression enhanced redirected lysis of OKT3 (anti-CD3) coated P815 cells by normal cells but not by patient cells. Because MagT1 is also required for TCR signaling, TCR-stimulated redirected lysis of non-ULBP1 expressing P815 cells by OKT3 is also mildly defective in the patients (Figure 4-6A). Consistent with these specific CTL cytotoxicity defects, expanded EBV-specific CTLs from the patients also do not kill autologous LCLs as well as those from normal controls (Figure 4-6B).

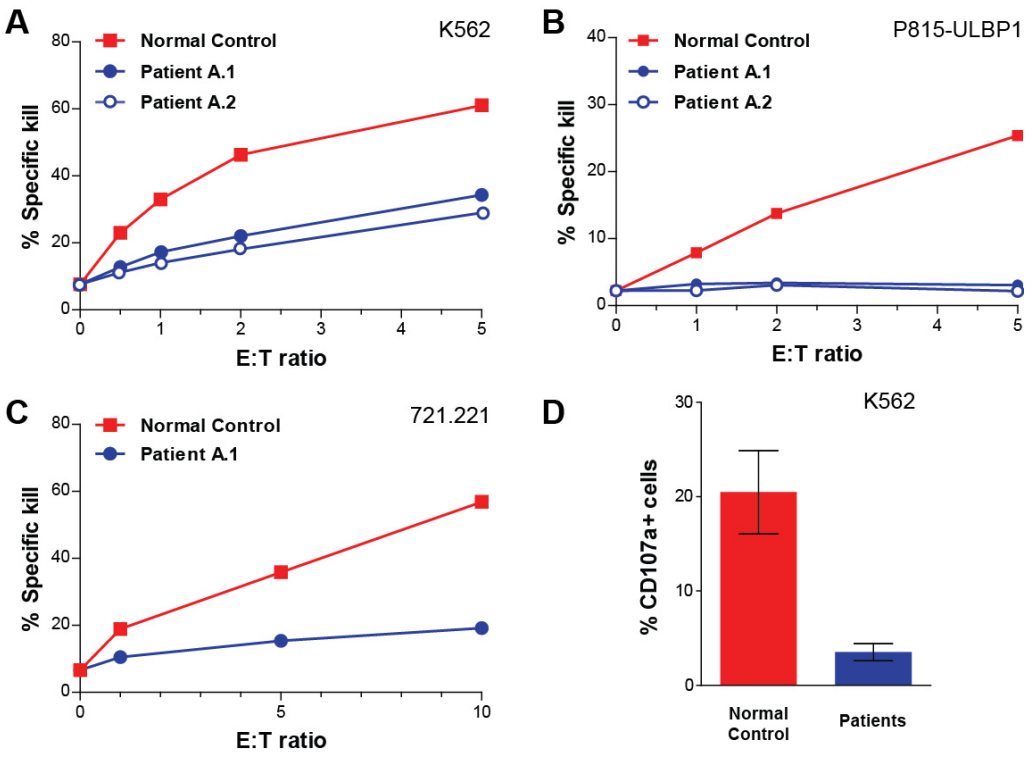

Figure 4-5: Cytotoxicity defects in patient NK cells

Cytotoxicity assay of normal or patient IL-2 activated NK cells on (**A**) K562 cells, (**B**) P815 mouse mast cell line overexpressing ULBP1, and (**C**) on 721.221 cell line. % specific kill = positive granzyme B activity; E:T = effector to target. (**D**) Degranulation of IL-2 activated NK cells from normal control and patients (A.1 and A.2) after 0.5 h incubation with K562 cells with 1:1 E:T ratio.

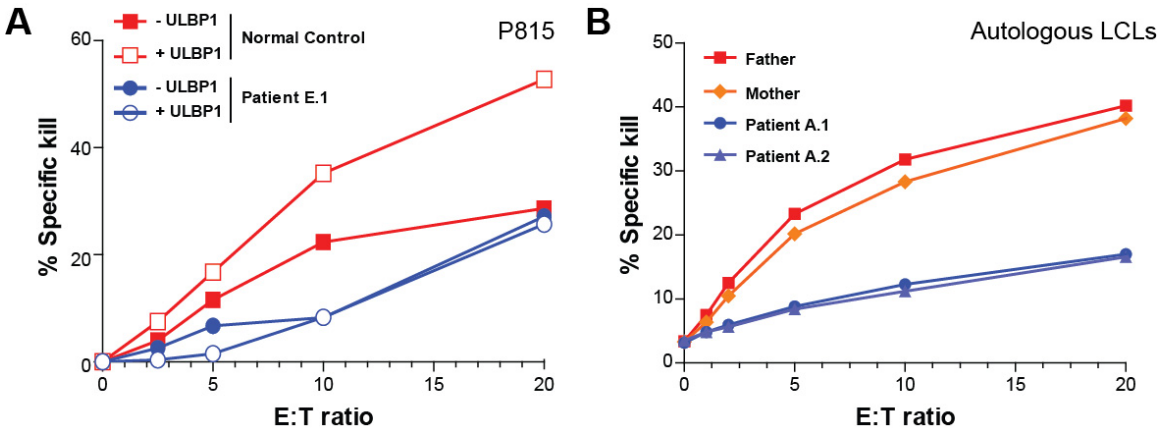

Figure 4-6: Cytotoxicity defects in patient CTLs

(**A**) Cytotoxicity assay of CTLs from normal controls and patient E.1 on P815 mouse mast cell line preincubated with OKT3 and overexpressing ULBP1 or not. (**B**) Cytotoxicity assay of EBV-specific CTLs from normal controls (father and mother) and patients (A.1 and A.2) on autologous LCLs. % specific kill = positive granzyme B activity; E:T = effector to target. Benjamin Chaigne-Delalande performed cytotoxicity assays in (**B**).

NKG2D expression is regulated by magnesium

The strict association between loss of MagT1 and downmodulation of NKG2D suggest that NKG2D may be regulated by the cellular magnesium level. Indeed, XMEN lymphocytes exhibit a lower basal level of free Mg^{2+} as detected by Magfluo4 loading (Figure 4-1). When we tried to mimic the loss of MagT1 in normal cells by depleting the Mg^{2+} in the culture media, we were able to see downmodulation of NKG2D correlated with a decreased basal level of cellular free Mg^{2+} (as indicated by the MagFluo4 loading relative to calibrator Fura Red staining) starting at 2 days after deprivation (Figure 4-7). Other receptors, such as CD8 and CD2, were not affected (data not shown). We also assessed whether extracellular Mg^{2+} supplementation in the culture media rescues NKG2D expression and cytotoxicity of the patients. We observed the percentage of patient cells exhibiting normal level of NKG2D expression starting to elevate at as low as 1 mM $MgSO_4$ supplementation to nearly complete restoration at 10 mM $MgSO_4$ supplementation (Figure 4-8A). This restoration is observed in both NK cells and CTLs. Expression of other NK activating receptors, such as NKp30, NKp44, NKp46, 2B4, DNAM-1, and CD122, were affected by the $MgSO_4$ supplementation (data not shown). Not only is the expression of

NKG2D specifically restored, its restoration is also correlated with an increase in the basal level of intracellular free Mg^{2+} (Figure 4-8B). This restoration of intracellular free Mg^{2+} is probably mediated by other non-specific Mg^{2+} channels like TRPM7, SLC41A1, MmgT1, and NIPA1, as their mRNA levels are elevated in the patient cells (Marshall Lukacs, personal communication). EBV-specific CTL killing of autologous LCLs is also nearly restored to normal levels after supplementation (Figure 4-8D). Thus, our data indicates that expression of NKG2D can be regulated by magnesium.

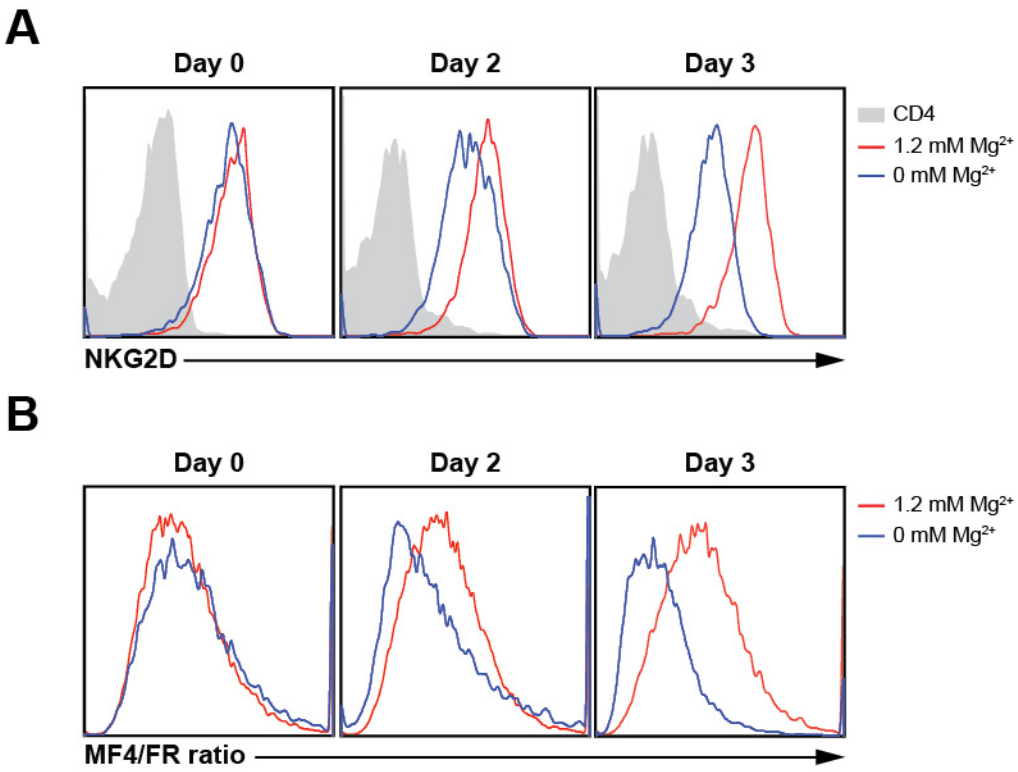

Figure 4-7: Magnesium deprivation leads to downmodulation of NKG2D on normal CTLs.

(**A**) Flow cytometry profile of NKG2D expression and (**B**) mean fluorescence intensity ratio of MagFluo4 (MF4) and Fura Red (FR) loading on $CD8^+$ T cells cultured in media with (red) or without (blue) Mg^{2+}. Normal control $CD4^+$ T cells (grey) are shown as reference for negative NKG2D expression. Performed by Benjamin Chaigne-Delalande.

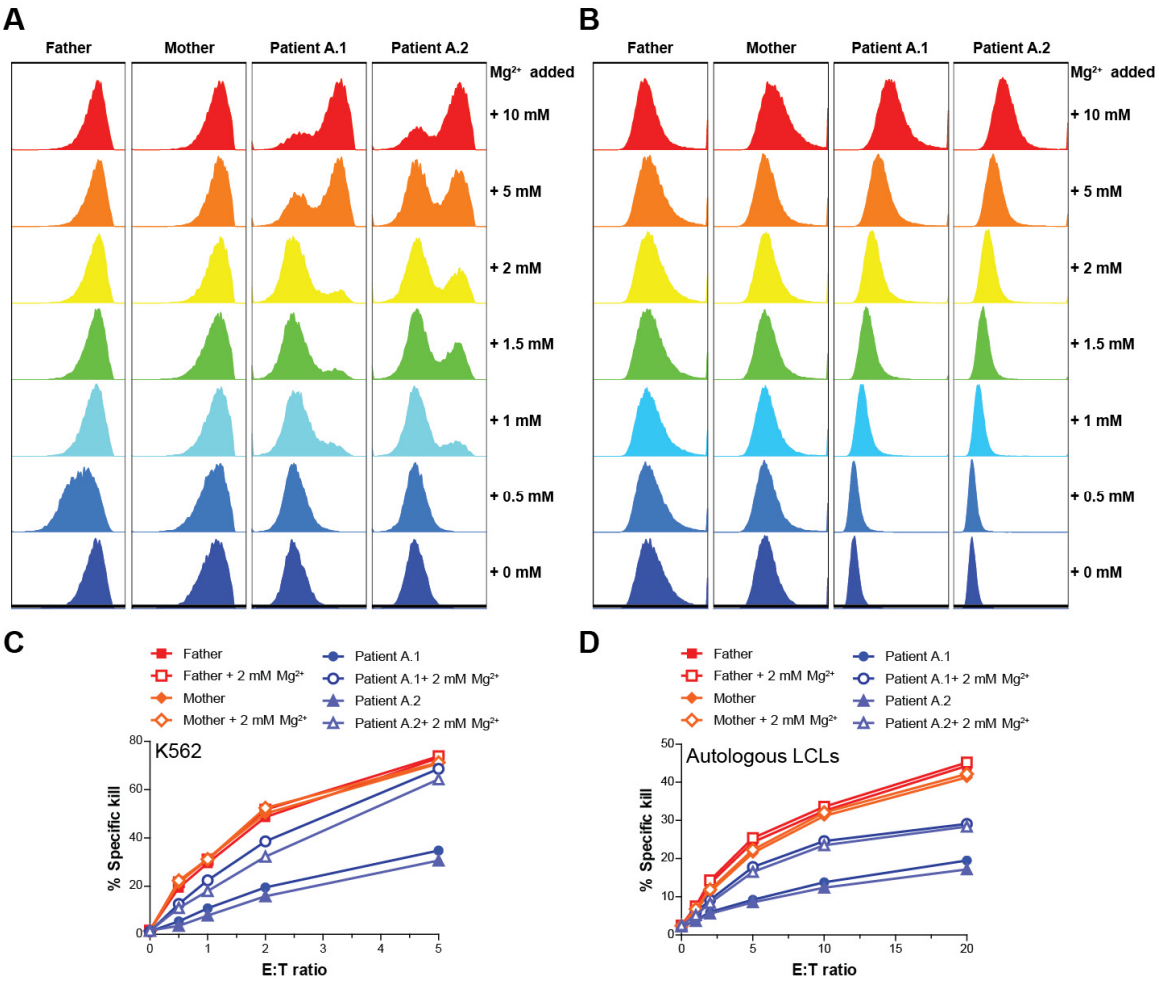

Figure 4-8: Magnesium supplementation restores NKG2D expression and function in patient cells

(**A**) Flow cytometry profile of NKG2D expression and (**B**) mean fluorescence intensity ratio of MagFluo4 (MF4) and Fura Red (FR) loading on normal control (father and mother) and patient CTLs cultured in 10% RPMI media supplemented with indicated amounts of Mg^{2+} for 4 days. (**C**) Cytotoxicity assay of normal or patient IL-2 activated NK cells after 4-day culture with or without Mg^{2+} supplementation on K562 cells. (**D**) Cytotoxicity assay of normal or patient EBV-specific CTLs after 4-day culture with or without Mg^{2+} supplementation on autologous LCLs. % specific kill = positive granzyme B activity; E:T = effector to target. Performed by Benjamin Chaigne-Delalande.

4.3 Discussion

XMEN disease exhibits unusual susceptibility to chronic EBV infections and EBV-associated lymphomas. Here, we found profoundly impaired cytotoxicity in XMEN patients particularly mediated by the NK cell activating receptor NKG2D due to loss of its expression. Cytotoxicity defects are also a key feature in SAP-deficient XLP, which also has susceptibility to chronic EBV infections and lymphoma. The unusual susceptibility to EBV in this disease has been attributed to the loss of 2B4 mediated cytotoxicity against EBV-infected B cells, which requires SAP-associated receptors for recognition[9–11,21]. NKG2D ligation can synergize with many NK activating receptors including 2B4[18]. Thus, loss of NKG2D in XMEN patients may debilitate 2B4-mediated recognition of EBV-infected cells, which may account for the susceptibility to EBV. In addition, EBV, unlike CMV, does not have extensive mechanisms of evading NKG2D recognition. Lytic induction in EBV infected cells can lead to downregulation of HLA class I and upregulation of ULBP1, allowing for NK recognition via NKG2D[16]. Thus, the profound killing defect of EBV cells lacking HLA class I or the autologous LCLs observed in XMEN patients suggests that their cytotoxicity defect may account for their inability to control EBV.

NKG2D has also been shown to promote cytotoxic NK and T cell responses against tumors both *in vitro* and in experimental mouse models[14]. In humans, NKG2D has only been observed to be downmodulated in some cancer patients[22]. However, 3 of our XMEN patients have not yet developed cancer, suggesting that their NKG2D downregulation could not be secondary to malignancy. Like in these patients, the loss of NKG2D in MagT1 deficient patients can lead to cytotoxicity

defects against tumor lines like K562 cells, which may explain for their susceptibility to lymphomas. Unlike these patients, however, the loss of NKG2D in XMEN patients appears to be an inborn defect secondary to MagT1 deficiency. The increased susceptibility to lymphomas in this disease suggests that NKG2D could play a role in tumor immunosurveillance in humans as well.

While MICA shedding from some patient cancer cells has been shown to be sufficient to decrease the surface expression of NKG2D[22], soluble MICA was not detected in supernatants of long term CTL cultures where the NKG2D remained suppressed. Expression of NKG2D ligands was also not elevated in lymphocytes, suggesting a cell intrinsic cause for the defect. The NKG2D defect is likely to due to the loss of MagT1-mediated regulation of cellular magnesium as Mg^{2+} supplementation is able to restore NKG2D expression on patient cells. As Mg^{2+} supplementation does not elicit a Mg^{2+} flux (Figure 3-3A) and total cellular magnesium content is not altered in patient cells (Figure 3-3B), the NKG2D expression is probably sensitive to the drop in intracellular free Mg^{2+} in MagT1 deficient cells. Likewise, absolute Mg^{2+} deprivation in normal cells can induce the loss of NKG2D expression specifically. But as little as 1 μM Mg^{2+} is sufficient to maintain almost normal NKG2D expression (data not shown), suggesting the cellular magnesium homeostasis is tightly regulated. Alternatively, this could suggest that NKG2D is extremely sensitive to a low threshold level of free Mg^{2+}. Interestingly, we also detected the loss of DAP10 protein expression but not its mRNA level in XMEN patient cells. Given the stability of DAP10 is affected by its association with NKG2D[20], the DAP10 defect could be a cause or consequence of the

NKG2D defect. Because NKG2D mRNA levels are also not diminished in the absence of MagT1, magnesium is probably required for a post-transcriptional effect, either the translation efficiency or stability of the NKG2D or DAP10 proteins. This may be determined by a pulse-chase experiment or by overexpression of NKG2D and Dap10 separately in the patient cells to check for rescue of expression of the other.

Earlier we found striking similarities between this disease and ITK deficiency given that loss of MagT1 leads to the abolition of a Mg^{2+} flux required for ITK activity in T cells. In NK cells, we only found that CD16 stimulation induces a Mg^{2+} flux, and its absence does not greatly impair the CD16-induced Ca^{2+} flux. However, ITK is expressed in NK cells and is required for CD16-mediated ADCC[23]. Thus, it remains to be determined whether there are cytotoxicity defects mediated by CD16 and other NK receptors in NK cells of XMEN patients as well. Interestingly, while MagT1 appears to regulate the NKG2D expression, NKG2D does not appear to signal to MagT1 to induce a Mg^{2+} flux like CD16 and the TCR. Although both CD16 and TCR contain ITAM-associated motifs, NKp46 also contain an ITAM motif but did not appear to induce a Mg^{2+} flux unless the flux was too weak to be detected. We have also found that other non-ITAM containing receptors such as epidermal growth factor receptor can induce a Mg^{2+} flux to regulate the Ca^{2+} flux (data not shown).

The loss of NKG2D expression in XMEN patients not only suggests the existence of a novel Mg^{2+} dependent mechanism for regulating NKG2D expression but also a novel pre-diagnostic screening test for XMEN disease by measuring the NKG2D expression in whole blood lymphocytes by flow cytometry. Moreover, our

findings suggest that Mg^{2+} supplementation may not only have therapeutic potential for this disease but perhaps for cancers that downmodulate NKG2D as well.

4.4 Materials and Methods

Cell purifications and culture

PBMCs purified from whole blood as described in Chapter 2 were subject to NK purification with CD56 microbreads (Miltenyi Biotech). T cells in the flow-through were activated with T cell activation/expansion kit (Miltenyi Biotech). After 3 days, activated T cells were washed and then cultured in complete RPMI-1640 medium supplemented with 100 U/ml rhIL-2 (R&D). Activated T cell subsets were separated using CD4 or CD8 microbeads (Miltenyi Biotech). Isolated NK cells were stimulated for 5 days with 200 U/mL rhIL-2 with 1:1 40 Gy γ-irradiated autologous PBMCs in Iscove modified Dulbecco medium (IMDM) supplemented with 10% human AB serum (CellBio), 1x non-essential amino acids (CellGro), 1 mM sodium pyruvate (CellGro), 2 mM glutamine, and penicillin and streptomycin (100 U/ml each, Invitrogen). These polyclonal IL-2-activated NK cells were continuously expanded with 100 U/mL rhIL-2 supplemented IMDM media in 96 well round bottom plates. Resting NK cells were resuspended in the same medium without IL-2 and were used within 1 to 4 days after isolation. The mouse mastocytoma cell line P815, the human erythroleukemia cell line K562 and the EBV+ *lymphoblastoid cell line (LCL 721.221)* HLA-class-I–deficient (ATCC) were maintained in RPMI 1640 medium (Lonza) containing 10% FBS, 2 mM glutamine, and penicillin and streptomycin (100 U/ml each, Invitrogen). The P815 cells overexpressing ULBP1 was a gift from E. Long and were selected with 0.8 μg/mL G418.

Generation of EBV-specific CTLs

Autologous LCLs were generated by incubating 10^7 freshly isolated PBMCs were incubated with 3 mL EBV-containing supernatant from the B95-8 cell line (ATCC) supplemented with 2 mL 20% RPMI for 2 h at 37° C before addition of 5 mL 20% RPMI containing 2 μg/mL of cyclosporin A. Cells were observed after 4-6 weeks for emergence of lymphoblasts. EBV-specific CTLs were generated from PBMCs as described previously[24,25]. Briefly, PBMCs depleted of NK cells by CD56 microbead selection (Miltenyi Biotech or STEM CELL Technologies) were cultured for 10 days with 40 Gy γ-irradiated autologous LCLs at a effector to stimulator (E:S) ratio of 20:1 in the presence of 10 ng/mL rhIL-7 (R&D) and 10 pg/mL rhIL-12 (PeproTech). After 10 days, 20 U/mL rIL-2 was added to the media. Repeated stimulations of EBV-CTL were performed every 7 days with irradiated γ-irradiated autologous EBV cells at a ratio of 4:1.

Flow cytometry

For phenotyping of NK cell receptors, whole blood or PBMCs were stained with the following antibodies: Anti-CD56 (clone HCD56) from Biolegend, CD3 (clone UCHT1), NKp46 (clone 9E2/NKp46), NKp30 (clone P30-15), NKp44 (clone P44-8.1), CD161 (clone DX12), NKG2D (Clone 1D11), CD122 (clone Mik-β3), 2B4 (clone 2-69) and DNAM-1 (clone DX11), all from BD biosciences. 100 μl of anticoagulant-treated blood was incubated with the appropriate mixture of mAb. Erythrocytes were lysed with an ammonium chloride solution, washed and the pelleted cells were analyzed with a LSRII flow cytometer (BD Biosciences). Remaining surface flow cytometry staining was performed as described in Chapter 2. CD2, CD3, CD4, CD8, CD25, CD56,

CD69, CD19, NKG2D, 2B4, CD16 antibodies were obtained from BD biosciences. For intracellular NKG2D staining, PBMCs were surface stained with CD3, CD4, CD8, CD56 and then treated with Cytofix/Cytoperm (BD biosciences) solutions before NKG2D staining for 30 min. Complete permeablization was verified by propidium iodide (SIGMA) staining. For granzyme B (Sigma) and perforin (Biolegend) staining, purified NK cells or CTLs were surface stained respectively with CD56 or CD8, fixed with 4% paraformaldehyde in PBS at 4^{o} C for 20 min, and then permeabilized with Saponin buffer (0.1% saponin, 0.1% BSA, 1 mM $CaCl_2$, 1 mM $MgSO_4$, 0.05% sodium azide, 10 mM HEPES pH 7.4) for staining in the same buffers. Cells were washed in PBS before acquisition. For NK cell activation, isolated NK cells were stimulated with or without 100 U/mL rhIL-2 or 10 ng/mL rhIL-15 and 10 ng/mL rhIL-18 (PeproTech). Cells were harvested on day 1, 4, and 6 for surface staining with NKG2D, CD56, CD69, and CD25 antibodies. For assessment of degranulation, IL-2 activated NK cells are incubated with K562 cells at 1:1 ratio with CD107 antibody (BD biosciences) and GolgiPlug (BD biosciences) for at least 30 min. at 37 ^{o}C before addition of CD56 antibody and acquisition on FACS Calibur flow cytometer. For NKG2D ligand staining, cells were first stained with or without 1:50 anti-MICA (AMO1 clone, Axxora) antibody or NKG2D-fc (R&D) for 30 min., washed, and then stained respectively with 1:400 goat anti-mouse Alexa 594 (Invitrogen) or mouse anti-human fc (Sigma).

Calcium and magnesium flux assays

Cells were loaded with 1 μM Magfluo4-AM (Invitrogen) or 1 μM Fluo3-AM (Invitrogen) and 1 μM Fura Red-AM (Invitrogen) for 20 min at 37 °C. Then cells

were washed in PBS and incubated with 10 μg/ml of anti-CD16, anti-NKp46, anti-NKG2D, anti-DNAM-1, anti-CD2 or anti-2B4 agonist antibodies (Biolegend) for 30 min on ice. Cells were washed and resuspended in Assay Buffer (AB: 120 mM N-methyl-D-glutamine, 20 mM HEPES, 4.7 mM KCl, 1.2 mM KH_2PO_4, 10 mM glucose, pH 7.4, 1.2 mM $CaCl_2$ and 1.2 mM $MgSO_4$). Calcium and magnesium flux were measured using a BD LSRII flow cytometer. Briefly, after acquiring 60 seconds for the baseline, 10 μg/ml of goat-anti-mouse antibody was added to crosslink the primary antibody and induce the flux. Kinetic analyses were done using FlowJo (TreeStar) with % responding cells defined as >95th percentile of unstimulated baseline. For the magnesium baseline measurement, cells were loaded with 1 μM Magfluo4-AM (Invitrogen) and 2 μM Fura Red-AM (Invitrogen) for 20 min at 37°C, and wash twice in PBS. Intracellular calcium and magnesium were measured using a BD LSRII flow cytometer.

Cytotoxicity assays

NK and CTL cytotoxicity were assessed using GranToxilux® Plus kit (OncoImmunin, Inc.) according to manufacturer instructions. Briefly, target cells were loaded with 1:5000 TFL4 dye for 20 min at 37°C, washed twice in PBS, and plated with effector cells in the provided Wash buffer. Cells were plated with E:T ratio from 0.5:1 to 20:1 in presence of the provided Granzyme B substrate (GS). After 30 min to 5 h incubation, cells were washed and cytotoxicity was measured in flow cytometry using a BD LSRII or FACS Calibur flow cytometer.

Immunoblotting

For NKG2D and DAP10 immunoblotting, cells were washed in PBS and immediately lysed in 1% Triton X-100, 1% NP40, 50 mM Tris-Cl pH 8, 150 mM NaCl, 20 mM EDTA, 1 mM Na_3VO_4, 1 mM NaF, phophatase inhibitor cocktail (Sigma) and complete protease inhibitor cocktail (Roche). Protein concentrations were quantitated by BCA assay (Pierce). 50 µg of cell lysates were separated by SDS-PAGE and transferred on nitrocellulose (Bio-Rad). Membrane was blocked with Odyssey blocking buffer (LI-COR Biosciences) for 1 h before incubating with anti-NKG2D (N20, Santa Cruz), DAP10 (Santa Cruz) or β–Tubulin (Upstate) antibodies overnight. Secondary Alexa Fluor 680-conjugated anti-Goat IgG (LI-COR Biosciences) and IRDye800-conjugated anti-Mouse IgG (LI-COR Biosciences) were incubated for 1h. Blots were imaged using an Odyssey Infrared Imaging System (LI-COR Biosciences).

Real-time PCR

NKG2D and *DAP10* mRNA levels were assessed using cDNA from ex vivo $CD8^+$ T cells and NK cells. Taqman Gene Expression Assays (IDT): Hs.PT.47.1578740 (NKG2D), and Hs.PT.47.18858195 (DAP10) were used to quantify target gene relative expression. Expression levels were normalized to simultaneous duplicate assessments of hypoxanthine-guanine phosphoribosyltransferase (*HPRT*) mRNA using Taqman Gene Expression Assay (ABI): Hs01003267. Reaction mixes were amplified for 40 cycles (95 ^oC for 15 s, 60 ^oC for 1 min) using PRISM 7900HT Sequence Detection System (Applied Biosystems).

Magnesium deprivation and supplementation.

For Mg^{2+} deprivation experiments, FBS supplemented with 20 mM glutamine was incubated with Chelex 100 resin (Bio-Rad) twice before pH was adjusted to 7.4.

RPMI without magnesium and calcium was supplemented with 10% resin-treated FBS and 1.2 mM $CaCl_2$ (Sigma) with 1 μM to 20 mM of $MgSO_4$ (Sigma). For Mg^{2+} supplementation, cells were cultured in their respective media supplemented with 100 U/mL of rhIL-2 and 0 to 10 mM $MgSO_4$. Cells were maintained in these custom-made media continuously, and samples were harvested for flow cytometric assessments of NKG2D, free Mg^{2+} baseline, and cytotoxicity as described above.

MICA ELISA

Soluble MICA levels in culture supernatant were assessed using MICA ELISA kit (Abcam) according to manufacturer instructions.

Statistical analysis

P values were calculated with the Students t-test using PRISM software (GraphPad Software), with a two-tailed distribution.

4.5 References

1. Brandstadter, J.D. & Yang, Y. Natural killer cell responses to viral infection. *Journal of innate immunity* **3**, 274-9 (2011).
2. Lodoen, M.B. & Lanier, L.L. Viral modulation of NK cell immunity. *Nature reviews. Microbiology* **3**, 59-69 (2005).
3. Groth, A., Klöss, S., von Strandmann, E.P., Koehl, U. & Koch, J. Mechanisms of tumor and viral immune escape from natural killer cell-mediated surveillance. *Journal of innate immunity* **3**, 344-54 (2011).

4. Groh, V. *et al.* Costimulation of CD8alphabeta T cells by NKG2D via engagement by MIC induced on virus-infected cells. *Nature immunology* **2**, 255-60 (2001).
5. Markiewicz, M. a *et al.* Costimulation through NKG2D enhances murine CD8+ CTL function: similarities and differences between NKG2D and CD28 costimulation. *Journal of immunology (Baltimore, Md. : 1950)* **175**, 2825-33 (2005).
6. Walsh, K.B., Lanier, L.L. & Lane, T.E. NKG2D receptor signaling enhances cytolytic activity by virus-specific CD8+ T cells: evidence for a protective role in virus-induced encephalitis. *Journal of virology* **82**, 3031-44 (2008).
7. Orange, J.S. Human natural killer cell deficiencies and susceptibility to infection. *Microbes and Infection* **4**, 1545-1558 (2002).
8. Dropulic, L.K. & Cohen, J.I. Severe viral infections and primary immunodeficiencies. *Clinical infectious diseases : an official publication of the Infectious Diseases Society of America* **53**, 897-909 (2011).
9. Nakajima, H. *et al.* Patients with X-linked lymphoproliferative disease have a defect in 2B4 receptor-mediated NK cell cytotoxicity. *European journal of immunology* **30**, 3309-18 (2000).
10. Parolini, S. *et al.* X-linked lymphoproliferative disease. 2B4 molecules displaying inhibitory rather than activating function are responsible for the inability of natural killer cells to kill Epstein-Barr virus-infected cells. *The Journal of experimental medicine* **192**, 337-46 (2000).

11. Sharifi, R. *et al.* SAP mediates specific cytotoxic T-cell functions in X-linked lymphoproliferative disease. *Blood* **103**, 3821-7 (2004).
12. Challa-Malladi, M. *et al.* Combined genetic inactivation of β2-Microglobulin and CD58 reveals frequent escape from immune recognition in diffuse large B cell lymphoma. *Cancer cell* **20**, 728-40 (2011).
13. Guerra, N. *et al.* NKG2D-deficient mice are defective in tumor surveillance in models of spontaneous malignancy. *Immunity* **28**, 571-80 (2008).
14. Hayakawa, Y. & Smyth, M.J. NKG2D and cytotoxic effector function in tumor immune surveillance. *Seminars in immunology* **18**, 176-85 (2006).
15. Ljunggren, H.-G. Cancer immunosurveillance: NKG2D breaks cover. *Immunity* **28**, 492-4 (2008).
16. Pappworth, I.Y., Wang, E.C. & Rowe, M. The switch from latent to productive infection in epstein-barr virus-infected B cells is associated with sensitization to NK cell killing. *Journal of virology* **81**, 474-82 (2007).
17. Zhang, B. *et al.* Immune Surveillance and Therapy of Lymphomas Driven by Epstein-Barr Virus Protein LMP1 in a Mouse Model. *Cell* **148**, 739-751 (2012).
18. Bryceson, Y.T., March, M.E., Ljunggren, H.-G. & Long, E.O. Synergy among receptors on resting NK cells for the activation of natural cytotoxicity and cytokine secretion. *Blood* **107**, 159-66 (2006).
19. March, M.E., Ljunggren, H.-gustaf & Long, E.O. Activation, coactivation, and costimulation of resting human natural killer cells. *Immunological Reviews* **214**, 73-91 (2006).

20. Park, Y.P. *et al.* Complex regulation of human NKG2D-DAP10 cell surface expression: opposing roles of the γc cytokines and TGF-β1. *Blood* **118**, 3019-27 (2011).

21. Palendira, U. *et al.* Molecular Pathogenesis of EBV Susceptibility in XLP as Revealed by Analysis of Female Carriers with Heterozygous Expression of SAP. *PLoS Biology* **9**, e1001187 (2011).

22. Groh, V., Wu, J., Yee, C. & Spies, T. Tumour-derived soluble MIC ligands impair expression of NKG2D and T-cell activation. *October* **419**, 2-6 (2002).

23. Khurana, D., Arneson, L.N., Schoon, R.A., Dick, C.J. & Leibson, P.J. Differential Regulation of Human NK Cell-Mediated Cytotoxicity by the Tyrosine Kinase Itk. *The Journal of Immunology* 3575-3582 (2007).

24. Savoldo, B. *et al.* Autologous Epstein-Barr virus (EBV)-specific cytotoxic T cells for the treatment of persistent active EBV infection. *Blood* **100**, 4059-66 (2002).

25. Comoli, P. *et al.* Successful in vitro priming of EBV-specific CD8+ T cells endowed with strong cytotoxic function from T cells of EBV-seronegative children. *American journal of transplantation : official journal of the American Society of Transplantation and the American Society of Transplant Surgeons* **6**, 2169-76 (2006).

Chapter 5 : Broader Implications for MagT1 and XMEN disease

5.1 Introduction

Our characterization of XMEN disease so far has revealed an unexpected role of Mg^{2+} in T cell signaling and in the regulation of NKG2D expression. Moreover, our analysis also revealed the significance of MagT1 for $CD4^+$ T cell development and for the fitness or survival of T cells. This led us to question the role of MagT1 for the development of other hematopoietic cell populations. This chapter will discuss our evidence to suggest a requirement of MagT1 for the development of several hematopoietic lineages as well as the therapeutic implications of our findings for XMEN disease.

5.2 Implications of MagT1 in hematopoietic cell development

Previously, our observation of skewed X-chromosome lyonization in activated cycling T cells from the mother of our proband suggested that MagT1-deficient T cells have decreased fitness relative to non-MagT1 deficient T cells (Figure 2-4). Similarly, we have observed completely skewed lyonization in mothers of other XMEN patients (Figure 5-1), indicating that this phenomenon is specific to the loss of MagT1. To better determine where this selection occurred during hematopoietic cell development, we performed the lyonization assay on various purified hematopoietic lineages. Not only did we find all T lineages (including $CD4^+$, $CD8^+$, and $\gamma\delta^+$ T cells) completely skewed in lyonization, we also found the same result in all lymphoid and myeloid lineages including B lymphocytes, NK cells, monocytes, eosinophils, neutrophils, etc. (Figure 5-2A-B). The selective pressure for this skewed lyonization appears to be specific to the hematopoietic

lineage cells as no skewing was observed for buccal swab cells (Figure 5-2C). Moreover, this skewing pattern is unlike the random age-related skewing observed in chronic granulomatous disease (CGD) where partial skewing of lyonization can be observed in both leukocytes and buccal swab cells from female carriers[1]. Thus, these results suggested that MagT1 specifically confers survival fitness either to all hematopoietic lineages sometime during their development or to an early common hematopoietic progenitor. However, the skewing was puzzling since it was observed in B lymphocytes, which have no apparent functional defect when deficient for MagT1. Hence, we favored the hypothesis that MagT1 was important for the fitness of an early hematopoietic progenitor in which skewed lyonization would first be imposed and then it would persist in all of the cellular progeny. Given that human hematopoietic stem cells (HSCs) are selectively marked by the expression of CD34 (a cell-surface sialomucin that serves to facilitate cell migration by blocking cell adhesion)[2], we assessed the latter hypothesis by purifying $CD34^+$ stem cells from maternal PBMCs, expanding them in culture, and separating the $CD34^+$ and $CD34^-$ cells for lyonization studies. Consistent with this hypothesis, we found both $CD34^+$ and $CD34^-$ cells from an XMEN carrier have completely skewed lyonization, whereas those from a female carrier of CGD exhibit incomplete skewing known to occur in this disease (Figure 5-3). Thus, MagT1 apparently confers a survival or growth advantage to the earliest hematopoietic stem cells or progenitors that precede the stage in which the CD34 marker is expressed. Consistent with this hypothesis, MagT1-deficient induced pluripotent stem cells or mouse embryonic stem cells did

not appear to proliferate as well as wildtype counterparts in culture (Randy Merling and Chryssa Kanellopoulou, personal communication).

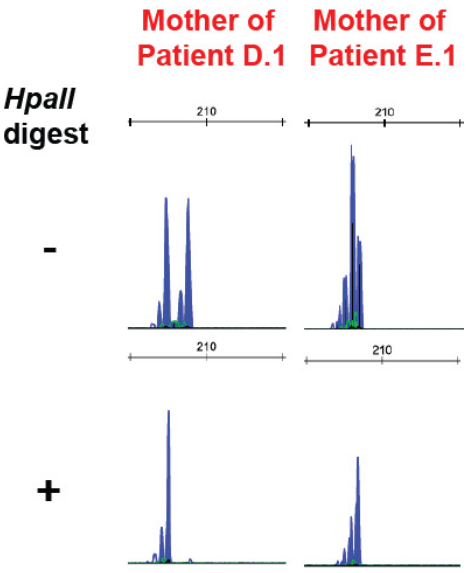

Figure 5-1: Skewed lyonization of T cells is present in other XMEN carriers.

X-chromosome inactivation pattern of the HUMARA locus in activated polyclonal T cells cycling with IL-2 from the mother of patient D.1 and E.1. Each set of peaks represents different alleles of each X-chromosome detected with (+) or without (-) digestion by methylation-sensitive enzyme *HpaII*. Mother of patient E.1 has overlapping allele peaks. .

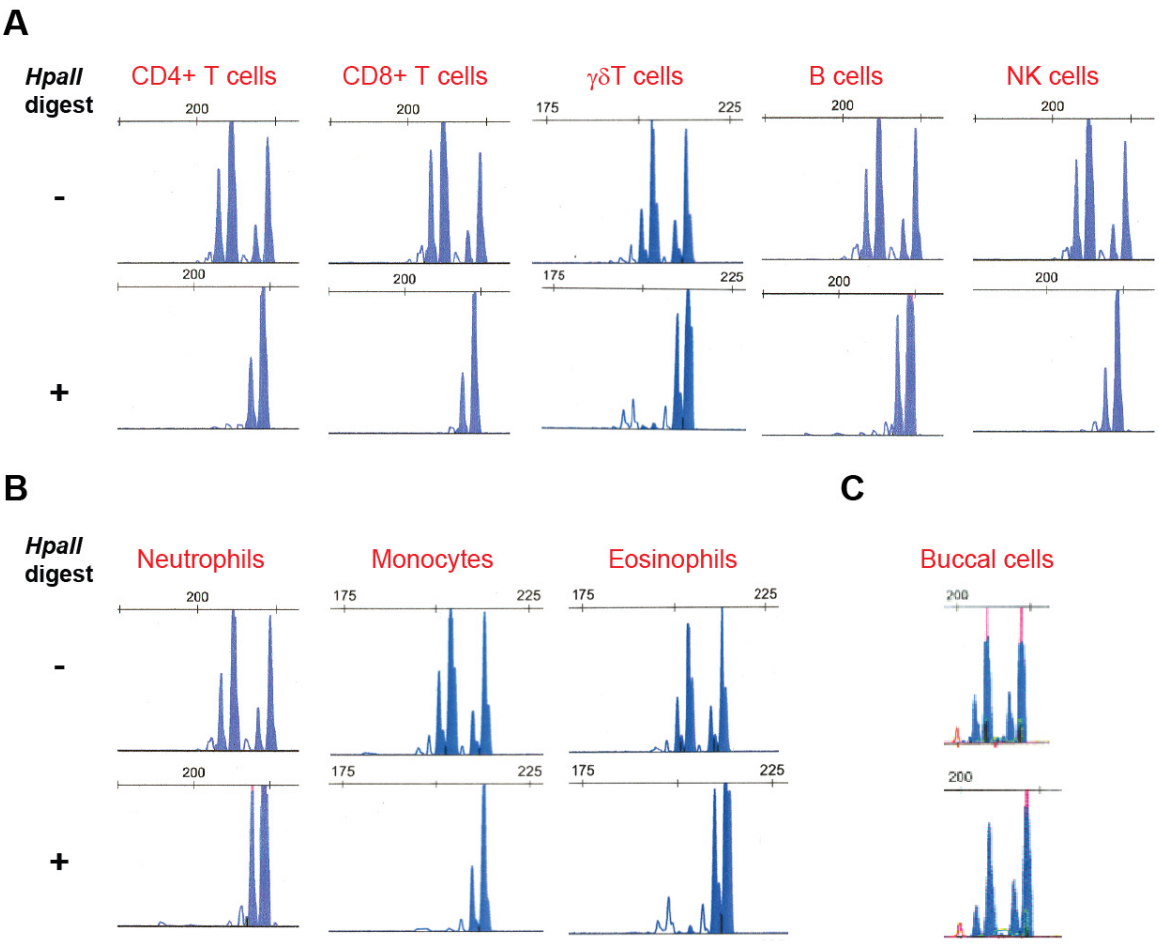

Figure 5-2: Preferential lyonization skewing in hematopoietic lineages from a XMEN carrier.

X-chromosome inactivation pattern of the HUMARA locus in various *ex vivo* (**A**) lymphoid and (**B**) myeloid lineage cells purified from PBMCs as well as (**C**) epithelial cells from a buccal swab of the mother of patient A.1 and A.2. Each set of peaks represents different alleles of each X-chromosome detected with (+) or without (-) digestion by methylation-sensitive enzyme *HpaII*.

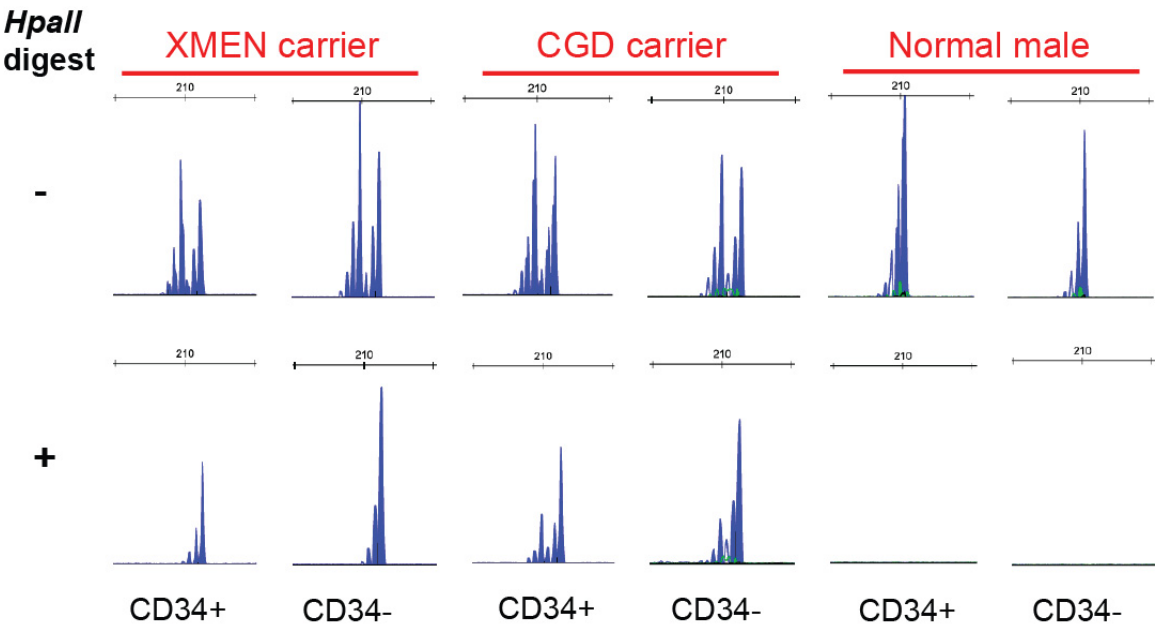

Figure 5-3: Skewed lyonization in peripheral hematopoietic stem cells of a XMEN carrier.

X-chromosome inactivation pattern of the HUMARA locus in *in vitro* expanded peripheral hematopoietic stem cells separated by CD34 expression from the mother of patient A.1 and A.2 (XMEN carrier), a CGD carrier, and a normal control male donor. Each set of peaks represents different alleles of each X-chromosome detected with (+) or without (-) digestion by methylation-sensitive enzyme *HpaII*. Hematopoietic stem cells were expanded and purified by Narda Theobald and Randy Merling.

The putative role of MagT1 in stem cell development raises the question whether this role depends on a Mg^{2+} flux or a threshold level of free basal Mg^{2+} level regulated by MagT1? To address the former hypothesis, one could assess Mg^{2+} fluxes in stem cells after stimulation with various stem cell growth factors such as stem cell factor, IL-6, granulocyte-macrophage colony-stimulating factor, and IL-3[3,4]. Alternatively, the latter hypothesis could be more likely if the growth defects in MagT1-deficient stem cells could be rescued by Mg^{2+} supplementation. If a MagT1

antibody can be developed for flow cytometry, one could co-stain MagT1 and stem cell developmental markers on XMEN carrier stem cells to determine the precise stages at which MagT1-deficient cells are present and absent in carrier stem cells. Completely skewed cell populations should have $MagT1^+$ staining on all cells whereas incompletely skewed populations should have $MagT1^-$ staining cells. Presumably, when the selective pressure is applied on the non-skewed stem cell population having $MagT1^+$ and $MagT1^-$ staining cells, MagT1-deficient cells can not survive as well as the MagT1-sufficient cells to the next stage so that only MagT1+ cells are present at that point.

The fact the XMEN patients appear to develop normally in the absence of MagT1 function suggests that MagT1 is not absolutely required for hematopoietic stem cell survival but instead is essential for their fitness in competition with wildtype cells. This conclusion is consistent with our findings that a lack of MagT1 only partially incapacitates T lymphocytes. Nonetheless, not all hematopoietic lineages appear to develop completely normally in the absence of MagT1. As we have shown earlier, thymic output of $CD4^+$ T cells appear to be impaired in XMEN patients. This observation is consistent with a potential role of MagT1 in regulating ITK activity, which is known to play a role in positive selection for $CD4^+$ T cells. Other imbalances of hematopoietic cell populations observed in XMEN patients include elevated B cells and borderline low neutrophils and NK cells (Figure 2-2-). While elevated B cells were also observed in ITK deficient mice, it is uncertain whether the low neutrophils relate to ITK function as well or other functions of MagT1 during their development. Alternatively, the mild neutropenia and elevated

B cells may be associated with the EBV infections in these patients as observed in other EBV infected patients[5,6]. Assessing these hematopoietic populations in the ITK deficient mice and the NKG2D deficient mice may explain these observations in XMEN patients.

Another hematopoietic subset that may be particularly affected by the loss of MagT1 is $CD8^+$ NK cells. The percentage of this population among NK cells in XMEN patients is lower than that in normal controls by a statistically significant amount (Figure 5-4). Although the function of this subset is still relatively uncharacterized, they have been shown to serve as better effectors for cytotoxicity and cytokine production than their $CD8^-$ counterparts[7,8] and may be selectively depleted during HIV infection[9]. Ligation of CD8 receptor on this subset has been shown to induce Ca^{2+} flux and promote their survival but not their cytotoxicity upon target cell conjugation[8]. Thus, it would be interesting to determine whether CD8 ligation on this subset would induce a MagT1-dependent Mg^{2+} flux to regulate the characteristic Ca^{2+} flux. Intriguingly, ITK deficient mice have abnormal hematopoietic lineage imbalances including a preferential outgrowth of a $CD8^+$ NKT-like cell population and a $\gamma\delta$ NKT cell population[10]. Although a large $\gamma\delta$ $CD4^-$ $CD8^-$ $CD56^-$ T cell population was found in one of our XMEN patients (A.1, data not shown) and the $CD8^+$ T cell population is usually borderline high in XMEN patients(Figure 2-2), similar abnormal cellular populations were not typically found in XMEN patients. Further understanding of the role of MagT1 in hematopoietic cell development may be achieved by direct functional and biochemical analyses of stem cells in MagT1 deficient mouse models.

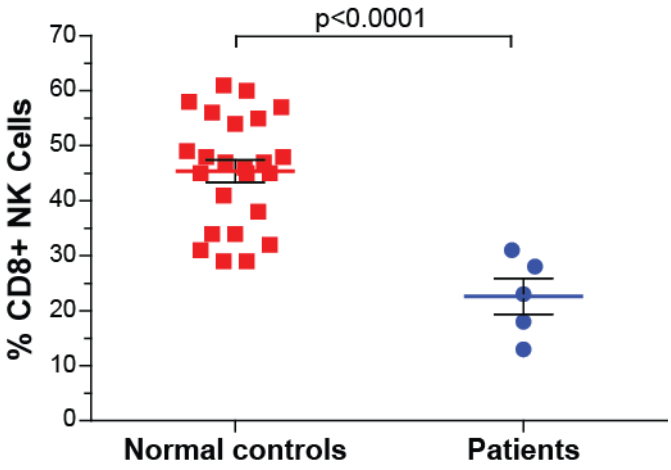

Figure 5-4: XMEN patients have decreased CD8+ NK cells

Percentage of NK cells with CD8 expression in normal controls and XMEN patients (represented patients include A.1, A.2, C.1, D.1, and E.1) as assessed by flow cytometry staining.

Consistent with the apparent role of MagT1 in the development of hematopoietic cells, MagT1 appears to be more highly expressed at the mRNA level in all hematopoietic lineages (Figure 5-5). Interestingly, MagT1 is also highly expressed in the thyroid, small intestine, colon, prostate, placenta, and pancreatic islets. Currently, we have not found any disease manifestations associated with these organs in our XMEN patients, but this may not rule out a function. While this may be explained by compensation by other Mg^{2+} channels expressed in these tissues, there may also be MagT1 functions in these tissues not sufficient to cause apparent disease phenotypes. For instance, MagT1 may have a role in the placenta for implantation as it was once named Implantation Associated Protein (IAP) because of its similarity to another protein associated with embryonic implantation. Notably, the mother of our proband family has reported 4 miscarriages. A function

for MagT1 in these tissues may also be uncovered by performing lyonization studies on these tissues from *MagT1*$^{+/-}$ female mice.

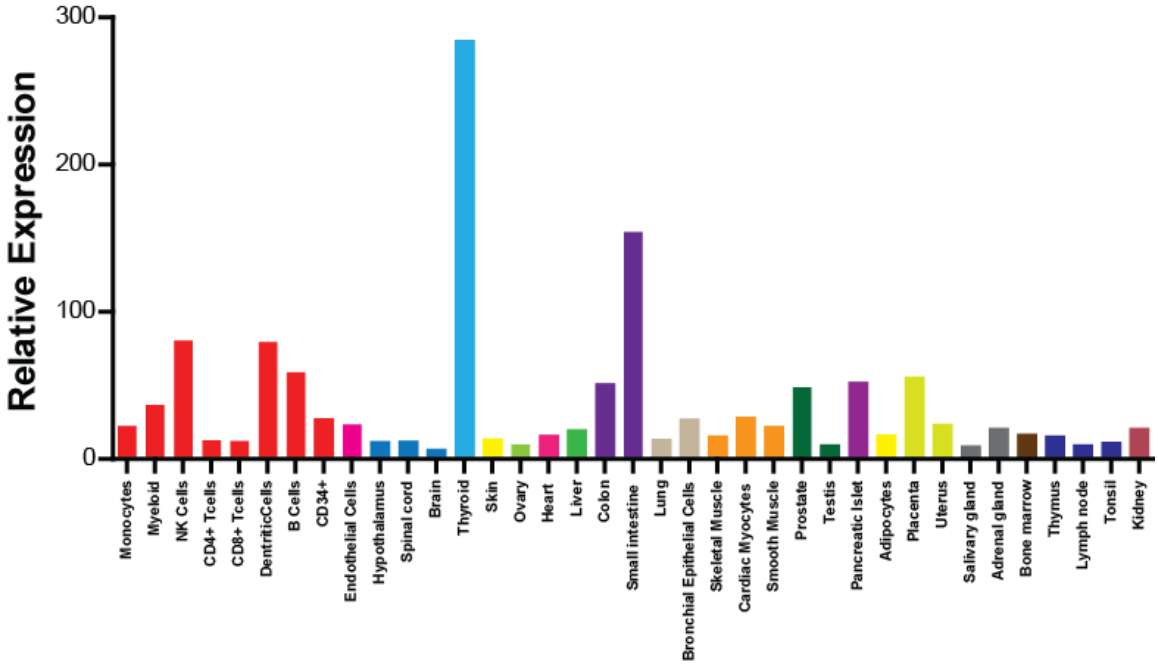

Figure 5-5: MagT1 is better expressed at the mRNA level in hematopoietic tissues and a few organs.

Microarray mRNA expression level of MAGT1 in various tissue types. Data adapted from the UCSC database (GeneAtlas U133A. gcmra 210596_at).

5.3 Therapeutic implications for XMEN disease

The conventional treatment for all PIDs is hematopoietic stem cell transplantation (HSCT). While success rates of HSCT can be as high as 90% with the most optimal conditions, survival rates for patients older than 5 years of age using unrelated donors can be as low as 30%. The 5-year disease-free survival rates post

HSCT for PIDs like HLH is about 60-70%. Although the development of high-resolution tissue typing and pre-transplant conditioning regimens have advanced HSCT significantly since its first use for treating PID in 1968, many challenges still remain, including inadequate B cell reconstitution requiring life-long intravenous immunoglobulin treatment and post-transplant complications such as graft versus host disease[11,12]. Given that diagnosis at an early age is key to the success of many HSCTs[11,13], newborn screening for XMEN disease by NKG2D staining in whole blood as a screening test may enhance HSCT success rates for this disease.

Because XMEN patients are often not diagnosed in early childhood due to their mild disease phenotype prior to the development of lymphoma, gene therapy may be a better alternative treatment for these patients than HSCT especially in the absence of a closely matched related donor. Moreover, the skewed lyonization of the hematopoietic stem cells also suggests that the cells corrected by gene therapy could eventually outgrow the non-corrected cells as observed for X-SCID. *Ex vivo* gene transfer into $CD34^+$ hematopoietic stem cells using retroviral vectors has been shown to be quite successful for treating X-SCID and ADA deficiency. For X-SCID, 17 out of 20 patients have survived the treatment with full restoration of T cell function without chemotherapy. The competitive advantage of gene corrected hematopoietic cells has been a key to the success of gene therapy restoring the common gamma chain in X-linked SCID[14]. However, the main complication associated with these gene therapy trials was cancer development due to nonspecific integration; five X-SCID patients developed an unusual form of leukemia with one being refractory to treatment[15]. Novel approaches to overcome this undesired insertion effect includes

using homing endonucleases or zinc finger nucleases to specifically induce double strand breaks at the mutation locus or a noncoding locus (safe harbor) and promote the insertion of the correct gene by homologous recombination with a repair matrix. However, the efficiency of delivery of these repair molecules needs further optimization[12].

While HSCT and gene therapy can be possible cures for XMEN disease, they both can have significant risks and limitations at the current time. Thus, another treatment that we have considered for these patients is magnesium supplementation. Intravenous magnesium has been safely used to treat patients in various clinical settings, including asthma and pre-eclampsia[16–18]. The basis for such a trial is that we showed that *in vitro* Mg^{2+} supplementation had a profound effect on restoration of NKG2D expression (Figure 4-8A). We have also assessed the T cell activation with Mg^{2+} supplementation *in vitro*, and we do not see a dosage dependent increase in CD69 upregulation upon TCR stimulation in the XMEN patients with Mg^{2+} supplementation (Figure 5-6), which is consistent with their lack of the MagT1-mediated transient Mg^{2+} flux required for TCR signaling. Nevertheless, this delayed T cell activation defect may not be sufficient to cause chronic elevation of EBV levels and development of lymphomas as we have detected a prominent central memory ($CCR7^+$ $CD45RA^-$) $CD8^+$ T cell population against at least one EBV lytic antigen (BZFL1) from two XMEN patients using tetramer staining (Figure. 5-7). Although the populations for other EBV lytic antigens (BMFL1, BRLF1), two EBV latent membrane proteins (LMP1 and LMP2), and two proteins derived from CMV (pp65) and influenza (matrix protein 6) are less prominent (Figure. 5-7), clonal

populations may be more evident for other antigenic epitopes, such as the EBV nuclear antigens EBNA3A, EBNA3B, and EBNA3C which are the dominant latent antigens recognized by CD8+ T cells[19]. Given that the $CD8^+$ T cell responses against BZFL1 in XMEN patients are within the range observed in normal healthy carriers (0.1-5.5%)[20], we presume the T cell activation defect does not prevent a memory CD8+ T cell response against EBV antigens from developing in XMEN patients. This is also supported by the fact that we were able to successfully grow out EBV-specific CTLs stimulated by irradiated autologous LCLs from XMEN patient PBMCs. The TCR signaling defect also does not seem to greatly impair CTL cytotoxicity stimulated by TCR engagement alone (Figure 4-6A). Thus, we believe the restoration of NKG2D expression by Mg^{2+} supplementation could be sufficient to control the EBV infection and limit tumor outgrowth as we have demonstrated *in vitro* (Figure 4-8D). Consequently, the clinical staff at the NIH Hatfield Clinical Research Center has been carrying out supplementation both orally and intravenously on patient A.1. Consistent with our *in vitro* data, these trials have shown promise in raising the intracellular free Mg^{2+} level, increasing the expression of NKG2D, and suppressing the cellular levels of EBV (data not shown).

The promising results in these two initial Mg^{2+} supplementation trials suggest that this should be considered as an alternative or temporary therapy for XMEN patients to suppress their EBV levels and decrease the potential for lymphoma development. Further trials will need to be completed to optimize the route and course of treatment. Problems associated with oral Mg^{2+} supplementation include limited bioavailability, increased urinary excretion, and continual diarrhea.

Intravenous Mg^{2+} infusion bypasses these problems and seems to be more effective therapeutically, but this route of administration may not be a suitable long-term solution for a child. Perhaps performing an undulated treatment course or co-treatment with imipramine (a tricyclic antidepressant capable of inhibiting the Na^{+}/Mg^{2+} antiporter[21]) to block Mg^{2+} cellular extrusion may enhance or prolong therapeutic effects. Other more bioavailable formulations of magnesium such as magnesium L-threonate[22] may provide better therapeutic effects. Another strategy would be to periodically use IV Mg^{2+} to try to reduce the EBV levels to below detection and monitor the EBV levels on a regular basis while keeping the patient on oral Mg^{2+} supplementation. One potential caveat with Mg^{2+} supplementation as a long-term treatment for XMEN disease is that it may not be sufficient to suppress long-term disease consequences due to its inability to overcome the T cell signaling defects, cellular developmental defects, or other yet uncharacterized defects. Nevertheless, a major challenge for treating XMEN patients with HSCT is that they are often diagnosed with high EBV titers or lymphoma, which may present difficulties during administration of immunosuppression required for HSCT. Pretreatment of XMEN patients with Mg^{2+} supplementation to suppress EBV levels may enhance the success rates of HSCT for this disease. Further clinical investigation will be necessary to establish an effective clinical approach. Nevertheless, our observations on the critical role of magnesium have provided an entirely new avenue of diagnosis and treatment for patients with this clinical condition. They may also shed light on other disorders involving EBV and lymphomagenesis.

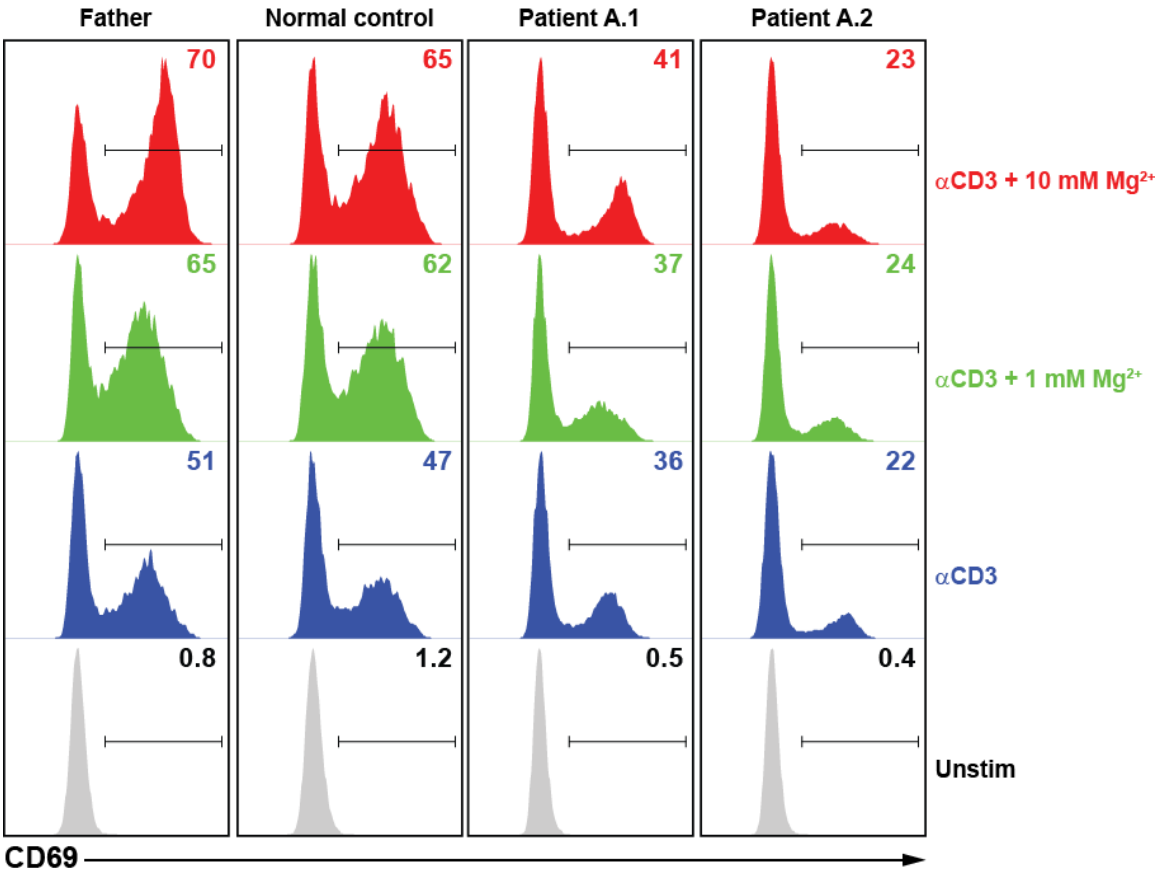

Figure 5-6: Mg^{2+} supplementation does not significantly increase T cell activation in a dosage dependent manner in XMEN patients.

Flow cytometry profiles of CD69 expression in $CD4^+$ T cells after 1 day of stimulation with or without OKT3 (αCD3) in the presence or absence of $MgCl_2$ (1 or 10 mM). Percentage of cells in the $CD69^+$ gate is shown.

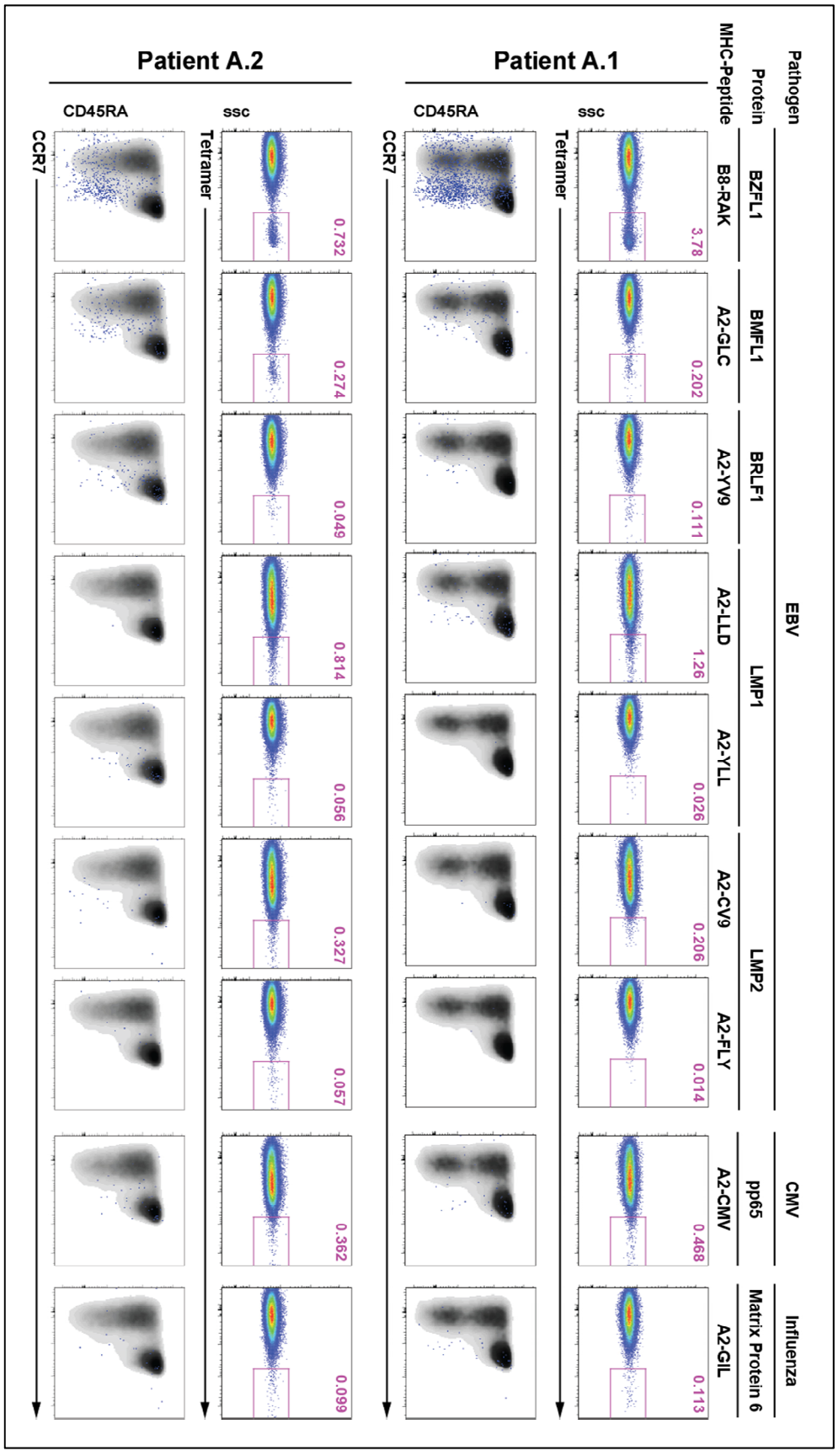
Pathogen
EBV
CMV
Influenza
Protein
BZFL1
BMFL1
BRLF1
LMP1
LMP2
pp65
Matrix Protein 6
MHC-Peptide
B8-RAK
A2-GLC
A2-YV9
A2-LLD
A2-YLL
A2-CV9
A2-FLY
A2-CMV
A2-GIL
Patient A.1
Patient A.2
ssc
Tetramer
CD45RA
CCR7
3.78
0.202
0.111
1.26
0.026
0.206
0.014
0.468
0.113
0.732
0.274
0.049
0.814
0.056
0.327
0.057
0.362
0.099

Figure 5-7: XMEN patients have a prominent central memory CD8+ T cell population specific for EBV lytic antigen BZFL1.

Flow cytometry pseudo-color plots for tetramer staining of $CD3^+$ $CD8^+$ gated T cells from patient A.1 and A.2. The MHC class restriction and antigen specificities of each tetramer are listed on top. Below each tetramer plot is a density plot of CCR7 and CD45RA staining on the gated $CD8^+$ T cell population overlaid with a blue dot plot of the tetramer+ gated cells. Peptide sequences for each epitope are listed in the Methods section. Maire Quigley performed tetramer conjugation and design of staining panel.

5.4 Concluding remarks

My journey through the characterization of this novel PID has made me appreciate that the investigation of rare Mendelian disorders presents both a moral obligation and an unusual opportunity. The moral obligation stems from the fact that these rare inborn diseases are a great burden to a few unfortunate families who have graciously provided a personal contribution to biomedical research often with only a remote chance of a personal therapeutic gain. Thus, as a scientist, this made me feel obligated to work hard to produce the most informative research on these patients with the hope of providing helpful diagnostic and/or therapeutic advances for their disease whenever possible. The unusual opportunity relates to the fact that these diseases are rare experiments of nature that can often provide novel insights about the molecular mechanisms of human physiology and may sometimes suggest novel therapeutic targets for more complex common human diseases[23]. We have been fortunate enough to fulfill both this obligation and this opportunity in the study of XMEN disease.

Our study of XMEN disease has provided an opportunity to gain insightful lessons into the role of a relatively uncharacterized magnesium transporter, MagT1, in human biology and has enhanced our appreciation for the regulatory roles of Mg^{2+} in biological processes. A requirement for Mg^{2+} to achieve optimal T cell activation was demonstrated more than 30 years ago, but the mechanism of its synergistic effect with Ca^{2+} in T cell activation had not been elucidated until our discovery. While Ca^{2+} has a well-recognized second messenger role in various signaling pathways, the signaling role of Mg^{2+} has been controversial over the last several decades. Our finding that MagT1 can mediate a transient Mg^{2+} flux to kinetically regulate the function of ITK upon TCR stimulation not only demonstrated that Mg^{2+} could fulfill Sutherland's criteria for second messengers but also explained how it could synergize with Ca^{2+} to regulate T cell activation[24]. By characterizing the cytotoxicity defects in this disease, we also learned that NKG2D expression is highly sensitive to the intracellular basal free Mg^{2+} level that is apparently regulated by MagT1. Lastly, the lyonization studies taught us that MagT1 might promote the fitness and survival of hematopoietic stem cells during development. These findings open up a broad horizon of possible future studies, which includes elucidating the protein directly responsive to the Mg^{2+} flux induced by TCR engagement, how TCR stimulation leads to opening of the MagT1 channel, how NKG2D/DAP10 expression is regulated by intracellular free Mg^{2+} level, and what are the ways by which MagT1 can influence the development of hematopoietic cells. The lack of B cell activation defects and the absence of disease phenotypes outside the immune system of XMEN patients also suggest great promise for investigations of MagT1 as a potential

extracellular therapeutic target for T and NK cell immunomodulation in autoimmune diseases or transplantation.

Not only have we been able to realize a great opportunity in scientific inquiry, our characterization of this disease has provided a rare opportunity to fulfill a morally gratifying obligation to the XMEN patients. Because we elucidated that XMEN disease is caused by loss of MagT1 function required for optimal T cell activation and NKG2D expression, XMEN families can now understand the etiology as well as the molecular pathogenesis of their disease. We further identified the common disease phenotypes characteristic of this PID and provided the natural history and the long-term prognosis of this disease by studying additional patients. By understanding that XMEN disease leads to decreased thymic output of $CD4^+$ T cells and chronic EBV infections that can ultimately result in the development of hematopoietic cancers, doctors and XMEN patients or families can now make better informed decisions about treatments for this disease. We also proposed an efficient way to screen for this disease and promote its early diagnosis by whole blood NKG2D flow cytometry staining, which may not only lead to early disease management but also better treatment outcomes for HSCT. Lastly, we showed the potential of this disease to be treated by Mg^{2+} supplementation either to decrease the chances for EBV-associated lymphoma development during HSCT or as a long-term or short-term treatment until better prospects for cure are available. Further research is necessary to understand the bypass mechanisms that allow Mg^{2+} supplementation to raise cellular free Mg^{2+}, how this Mg^{2+} level could be effectively maintained, and how it may affect other cellular processes or diseases. Nonetheless,

the work presented in this thesis illustrates the critical importance of understanding the fundamental molecular and physiological bases of disease as an engine for discovering new treatments, cures, and preventative measures. Hopefully, the findings in this thesis will not only lead to clinical benefits for XMEN patients but also suggest novel therapeutic strategies for other diseases as well.

5.5 Materials and Methods

Cell purifications and culture

PBMCs were purified from whole blood by Ficoll-Paque PLUS (GE Healthcare) density gradients, and T cells were activated and maintained in rhIL-2 as described chapter 3. $CD4^+$ T cells, $CD8^+$ T cells, γδ T cells, B cells, NK cells, monocytes, and eosinophils were purified from PBMCs using positive selection microbead kits (Miltenyi Biotec). Neutrophils were isolated from the blood pellets after red blood cell lysis with ACK lysis buffer (Quality Biological). $CD34^+$ hematopoietic stem cells were purified using the $CD34^+$ microbead kit (Miltenyi Biotec) and expanded using the NANEX $hCD34^+$ expansion system (Arteriocyte) for 6 days. Expanded cells were separated into $CD34^+$ and $CD34^-$ populations using $CD34^+$ microbead kit (Miltenyi Biotec). Purity of all purified populations was assessed by flow cytometry.

Lyonization studies

Lyonization assays and DNA preparations were performed as described in Chapter 2.

Flow cytometry

Assessment of T cell activation with and without the indicated amounts of $MgCl_2$ (Quality Biological) was performed as described in Chapter 3. Remaining flow cytometry studies were done as described in Chapter 4. Tetramer staining was performed on cryopreserved PBMCs by first staining with VIVID® dye (Invitrogen) for 10min. at room temperature, then staining with CCR7 and each tetramer at 37°C for 15 min., and finally followed by surface staining with CD3, CD4, CD8, CD14, CD45RA, CD27, CD57 antibodies for 15 min. at room temperature. All antibodies were gifts from Daniel Douek's lab.

Table 5.1: Tetramer epitopes

Epitope Name	Pathogen	Protein	Position	Sequence
RAK	EBV	BZLF1	190–197	RAKFQLL
GLC	EBV	BMLF1	280–288	GLCTLVAML
YV9	EBV	BRLF1	109–117	YVLDHLIVV
LLD	EBV	LMP1	167–175	LLVDLLWLL
YLL	EBV	LMP1	125–133	YLLEMLWRL
CV9	EBV	LMP2	426–434	CLGGLLTMV
FLY	EBV	LMP2	356–364	FLYALALLL
CMV	CMV	pp65	495–503	NLVPMVATV
GIL	Influenza	Matrix protein 6	58-66	GILGFVFTL

Statistical analysis

P values were calculated with the Students t-test using PRISM software (GraphPad Software), with a two-tailed distribution.

5.6 References

1. Köker, M.Y. *et al.* Skewing of X-chromosome inactivation in three generations of carriers with X-linked chronic granulomatous disease within one family. *European journal of clinical investigation* **36**, 257-64 (2006).

2. Nielsen, J.S. & McNagny, K.M. CD34 is a key regulator of hematopoietic stem cell trafficking to bone marrow and mast cell progenitor trafficking in the periphery. *Microcirculation (New York, N.Y. : 1994)* **16**, 487-96 (2009).

3. Olofsson, T.B. Growth regulation of hematopoietic cells. An overview. *Acta oncologica (Stockholm, Sweden)* **30**, 889-902 (1991).

4. Wognum, a W., de Jong, M.O. & Wagemaker, G. Differential expression of receptors for hemopoietic growth factors on subsets of CD34+ hemopoietic cells. *Leukemia & lymphoma* **24**, 11-25 (1996).

5. Hammond, W.P., Harlan, J.M. & Steinberg, S.E. Severe neutropenia in infectious mononucleosis. *The Western journal of medicine* **131**, 92-7 (1979).

6. Larcher, C. *et al.* Role of Epstein-Barr virus and soluble CD21 in persistent polyclonal B-cell lymphocytosis. *British journal of haematology* **90**, 532-40 (1995).

7. Rutjens, E. *et al.* CD8+ NK cells are predominant in chimpanzees, characterized by high NCR expression and cytokine production, and preserved in chronic HIV-1 infection. *European journal of immunology* **40**, 1440-50 (2010).

8. Addison, E.G. *et al.* Ligation of CD8alpha on human natural killer cells prevents activation-induced apoptosis and enhances cytolytic activity. *Immunology* **116**, 354-61 (2005).

9. Vuillier, F., Bianco, N.E., Montagnier, L. & Dighiero, G. Selective Depletion of Low-Density CD8 + CD16 Lymphocytes During HIV Infection. *Differentiation* **4**, (1988).

10. Andreotti, A.H., Schwartzberg, P.L., Joseph, R.E. & Berg, L.J. T-cell signaling regulated by the Tec family kinase, Itk. *Cold Spring Harbor perspectives in biology* **2**, a002287 (2010).

11. Filipovich, A. Hematopoietic cell transplantation for correction of primary immunodeficiencies. *Bone marrow transplantation* **42 Suppl 1**, S49-S52 (2008).

12. Pessach, I.M. & Notarangelo, L.D. Gene therapy for primary immunodeficiencies: looking ahead, toward gene correction. *The Journal of allergy and clinical immunology* **127**, 1344-50 (2011).

13. Savides, C. & Shaker, M. More than just infections: an update on primary immune deficiencies. *Current opinion in pediatrics* **22**, 647-54 (2010).

14. Bousso, P. *et al.* Diversity, functionality, and stability of the T cell repertoire derived in vivo from a single human T cell precursor. *Proceedings of the National Academy of Sciences of the United States of America* **97**, 274-8 (2000).

15. Fischer, A., Hacein-Bey-Abina, S., Cavazzana-Calvo, M. & Cavazanna-Calvo, M. Gene therapy for primary immunodeficiencies. *Immunology and allergy clinics of North America* **30**, 237-48 (2010).

16. McCarty, M.F. Magnesium taurate for the prevention and treatment of pre-eclampsia/eclampsia. *Medical hypotheses* **47**, 269-72 (1996).

17. Saris, N.E., Mervaala, E., Karppanen, H., Khawaja, J. a & Lewenstam, a Magnesium. An update on physiological, clinical and analytical aspects. *Clinica chimica acta; international journal of clinical chemistry* **294**, 1-26 (2000).

18. Beasley, R. & Aldington, S. Magnesium in the treatment of asthma. *Current opinion in allergy and clinical immunology* **7**, 107-10 (2007).

19. Steven, B.N.M., Leese, A.M., Annels, N.E., Lee, S.P. & Rickinson, A.B. Epitope Focusing in the Primary Cytotoxic T Cell Response to Epstein-Barr Virus and Its Relationship to T Cell Memory. *J Exp Med* **184**, (1996).

20. Tan, L.C. *et al.* A re-evaluation of the frequency of CD8+ T cells specific for EBV in healthy virus carriers. *Journal of immunology (Baltimore, Md.: 1950)* **162**, 1827-35 (1999).

21. Kolisek, M., Nestler, A., Vormann, J. & Schweigel-Röntgen, M. Human gene SLC41A1 encodes for the Na+/Mg^{2}+ exchanger. *American journal of physiology. Cell physiology* **302**, C318-26 (2012).

22. Slutsky, I. *et al.* Enhancement of learning and memory by elevating brain magnesium. *Neuron* **65**, 165-77 (2010).

23. Dietz, H.C. New therapeutic approaches to mendelian disorders. *The New England journal of medicine* **363**, 852-63 (2010).

24. Sutherland, E.W. Studies on the mechanism of hormone action. *Science (New York, N.Y.)* **177**, 401-8 (1972).

Publishing Agreement

It is the policy of the University to encourage the distribution of all theses, dissertations, and manuscripts. Copies of all UCSF theses, dissertations, and manuscripts will be routed to the library via the Graduate Division. The library will make all theses, dissertations, and manuscripts accessible to the public and will preserve these to the best of their abilities, in perpetuity.

I hereby grant permission to the Graduate Division of the University of California, San Francisco to release copies of my thesis, dissertation, or manuscript to the Campus Library to provide access and preservation, in whole or in part, in perpetuity.

Jeng-Yeu Fu
Author Signature

5/1/12
Date